



# Tissue miRNAs as a Tool to Predict and Improve Benefit From Trastuzumab

Student: **Giulia Cosentino**

OU personal identifier: J3920552

Director of studies: Dr Marilena V. Iorio

Supervisors: Dr Elda Tagliabue and Dr Elena Jachetti

Registered degree: Doctor of Philosophy

Sponsoring establishment: Fondazione IRCCS Istituto Nazionale dei Tumori, Milan, Italy

Date of submission for examination: January 2024

*Alle mie nonne*

*(To my grannies)*

**TABLE OF CONTENT**

## ABSTRACT

Trastuzumab has revolutionized the clinical management of HER2 positive breast cancers. Unfortunately, a consistent portion of patients is treatment resistant. Other anti-HER2 agents have already been tested. Still, predicting which patient will benefit from the therapy and design alternative strategies would prevent overtreatment and avoid unnecessary risks of side effects. MiRNAs, small non-coding RNAs involved in post-transcriptional gene regulation, have been described as promising biomarkers. Analyzing baseline tissue samples from the NeoALTTO trial, our group recently identified a 2 miRNA-based predictive signature comprising miR-31-3p and miR-382-3p, associated to response to neoadjuvant trastuzumab.

This PhD project aimed at exploring the functional role of miR-31-3p and miR-382-3p in HER2+ breast cancer cell models. Overexpression of miR-31-3p, which negatively associated to response in HER2 positive patients, in HER2-addicted SKBr3 cells was able to increase HER2 activity and cell number, in a 3D setting, of non-treated and trastuzumab-treated cells. HER2 non-addicted HCC1954 cells transfected with miR-31-3p inhibitor (LNA-31-3p), alone or in combination with miR-382-3p, showed a significantly increased response to trastuzumab. Moreover, LNA-31-3p was able to reduce viability of non-treated and trastuzumab-treated HCC1954 cells in a 3D setting. *In vivo* in SCID mice, the combination of LNA-31-3p administration and trastuzumab significantly reduced tumor weight compared to control group. Correlation analyses between the expression of the miRNAs in the NeoALTTO series and immune signatures and metagenes revealed

that tumors expressing higher levels of miR-31-3p are characterized by a downregulation of immune-related pathways.

Finally, RNAseq analyses performed on miR-31-3p modulated SKBr3 and HCC1954 cell lines suggest that the main pathways affected are TGF-β and mTOR signaling.

In conclusion, the results obtained demonstrate that predictive miR-31-3p indeed also plays a functional role in the responsiveness to anti-HER2 trastuzumab. In particular, the miRNA inhibition holds a promising potential as adjuvant tool to improve responsiveness to the anti-HER2 drug.

## ABBREVIATIONS

| | |
|---|---|
| ADC | Antibody–drug conjugate |
| ADCC | Antibody-dependent cell-mediated cytotoxicity |
| AGO | Argonaute RISC Component |
| AKT | Protein kinase B |
| APC | Antigen-presenting cells |
| AUC | Area Under the Curve |
| BRCA1/2 | Breast Cancer gene 1/2 |
| CCNE2 | Cyclin E2 |
| CDK | Cyclin-dependent kinase |
| CEP17 | Chromosome enumeration probe 17 |
| CI | Confidence interval |
| CREB1 | CAMP Responsive Element Binding Protein 1 |
| CTNNB1 | Catenin Beta 1 |
| DCIS | Ductal carcinomas in situ |
| DMSO | Dimethyl sulfoxide |
| EBP1 | ErbB3-binding protein 1 |
| EFS | Event-free survival |
| EMT | Epithelial-to-mesenchymal transition |
| ER/ESR1 | Estrogen receptor |
| ERBB/HER | Human epidermal growth factor receptor |
| ERBIN | ERBB2 interactive protein |
| EZH2 | Zeste homolog 2-gene |
| FcγRIII | Fcγ receptor III |
| FDA | Food and Drug Administration |
| FOXO3 | Forkhead Box O3 |
| HR | Homologous recombination |
| IBC | Inflammatory breast cancer |
| IDC | Invasive ductal carcinoma |
| IFN | Interferon |
| IGF1R | Insulin Like Growth Factor 1 Receptor |
| IGF2 | Insulin-like growth factor 2 |
| IHC | Immunohistochemistry |
| IRS1 | Insulin Receptor Substrate 1 |
| ISH | In situ hybridization |
| ITGB6 | Integrin Subunit Beta 6 |
| LCIS | Lobular carcinoma in situ |
| LNA | Locked nucleic acid |
| lncRNA | Long non-coding RNA |
| LPIN1 | Lipin 1 |
| MAPK | Mitogen-activated protein kinase |
| miRNA | microRNA |

| | |
|---|---|
| MSigDB | The Molecular Signatures Database |
| mTOR | Mechanistic target of rapamycin |
| mTORC | mTOR Complex |
| NF-κB | Nuclear factor-kappa B |
| NHEJ | Nonhomologous end-joining |
| NK | Natural killer |
| OR | Odds ratio |
| PAM50 | Prediction analysis of microarray 50 |
| PARP | Poly(ADP-Ribose) Polymerase |
| pCR | pathologic complete response |
| PDPK1/PDK1 | 3-Phosphoinositide-Dependent Protein Kinase-1 |
| PI3K | Phosphatidylinositol 3-kinase |
| PIP2 | Phosphatidylinositol 4,5-bisphosphate |
| PIP3 | Phosphatidylinositol 3,4,5-trisphosphate |
| PKA | Protein kinase A |
| PKC | Protein kinase C |
| PLC-γ | Phospholipase C-gamma |
| PP2A | Protein Phosphatase 2A |
| PR/PGR | Progesterone receptor |
| PRDM10 | PR/SET Domain 10 |
| PTEN | Phosphatase and tensin homolog |
| RAC1 | Rac Family Small GTPase 1 |
| RHOA | Ras Homolog Family Member A |
| ROCK1 | Rho Associated Coiled-Coil Containing Protein Kinase 1 |
| SCID | Severe combined immunodeficiency |
| T-DM1 | Ado-trastuzumab emtansine |
| T-Dxd | Trastuzumab deruxtecan |
| TFAP2C | Transcription Factor AP-2 Gamma |
| TGFBR1 | Transforming Growth Factor Beta Receptor 1 |
| TGF-β | Transforming growth factor β |
| TIL | Tumor infiltrating lymphocyte |
| TKI | Tyrosine kinase inhibitor |
| TNBC | Triple negative breast cancer |
| TNM | Tumor-Node-Metastasis |
| TP53 | Tumor Protein P53 |
| TRBP | Transactivation-responsive RNA-binding protein |
| IPA | Ingenuity Pathway Analysis |

# 1 INTRODUCTION

## 1.1 Breast cancer

### 1.1.1 Breast anatomy and physiology

The breast, an exocrine gland that is unique to mammals, is located within the anterior thoracic wall and mostly consists of adipose tissue, sustained by a complex scaffolding of fibrous tissue [1,2] (**Figure 1.1**). Several glandular structures called lobules are linked together to form a lobe. 15-20 lobes make up a single mammary gland. The development of the breast that starts at puberty as a result of the beginning of the menstrual cycle and changes in the body's hormone levels, is incomplete. The female breast will only fully mature during pregnancy [3]. Indeed, the breast primary function is milk production. Elevated concentration of progesterone induces lobular branching and enlargement in the breast. Increased concentration of estrogen mainly leads to ductal proliferation and elongation and to an increase in the proliferation of adipose tissue. The luminal epithelium of the lobule's functional units, known as alveoli, leans on a basal membrane, where mioepithelial cells are linked and aid milk passage through lactiferous ducts and secretion by the nipple. Mammary stem cells proliferate at a basal level and give rise to both progenitor and fully differentiated cells [4]. In addition to epithelial cells, breasts are made up of endothelial cells, fibroblasts, and immune cells [5]. Lymphocytes, eosinophils, and plasma cells gather inside the connective tissues when the breast expands in response to high hormone levels and release antibacterial substances into the alveoli. Progesterone rapidly declines after childbirth, whereas prolactin and oxytocin rise to favor

breastfeeding. When milk production stops as a result of a drop in prolactin, post-lactation involution takes place. The mammary gland experiences massive cell loss and apoptosis, and the breast tissue undergoes remodeling. The lobules' connective tissue changes from a loose to a dense structure. Acini lose their lining cells, and their basement membrane thickens [3]. Menopause is reached when the ovaries cease to produce estrogen and progesterone and the epithelial component of the breast is gradually substituted by stromal cells and adipose tissue [6].

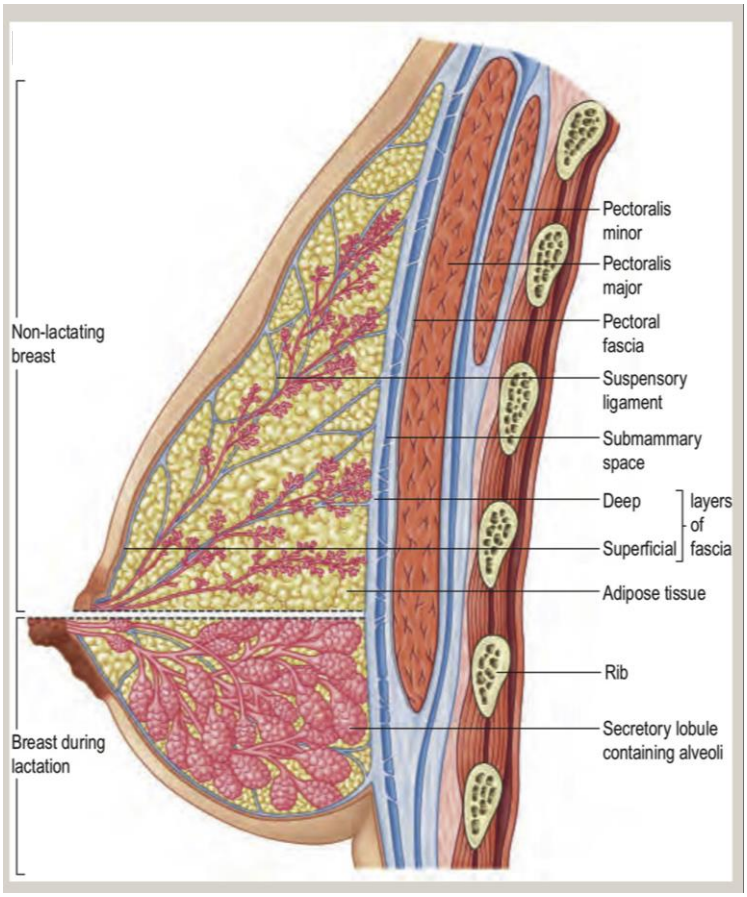


***Figure 1.1**. The structure of the breast and changes in breast structure during lactation. Adapted from Standring, S. Gray's anatomy, 41st edn, 2016. Edinburgh: Elsevier.*

### 1.1.2 Breast cancer epidemiology

Breast cancer affects 1 in 8 women in their lifetime and accounts for 2.3 million new cases overall in both sexes, currently displacing lung cancer as the most frequently diagnosed disease worldwide. It is the leading cause of death from any cancer in women, constituting 25% of all female cases, and its burden has been rising globally [7,8]. In 2020, breast cancer incidence rates were almost double in high-income countries compared to low and middle-income countries where, however, there is a 17% higher mortality rate, mainly due to late-stage diagnosis and poor access to high-quality care [9].

In 2019, a systematic review and meta-analysis estimated the overall 5-, and 10-year survival of women with breast cancer in the world; the results indicated that the pooled survival rates in 130 studies were 73%, and 61%, respectively [10].

Aging is one of the main risk factors of breast cancer [11]. 70% of all new cases and 81% of all deaths are observed in women aged 50 and above. Almost one-fourth of all breast cancer cases are related to family history or attributed to mutation of genes such as Breast Cancer gene 1/2 (BRCA1/2), involved in DNA repair pathways. Another important variable to be taken into account is mammographic breast density, calculated as the ratio between the amount of epithelial and stromal tissues, which respectively appear white (the epithelium) and dark, low-density fatty tissue (the stroma) at the radiologic examination. Women with dense breasts have both an increased risk of breast cancer and a lesser likelihood of a cancer being detected by mammographic screening [12]. Breast microcalcifications is a well-recognized risk factor; its value is elevated when combined

with breast density [13]. History of a benign breast disease also increases the probability to develop a malignant form within 15 years [14].

Reproductive factors such as early menarche, late menopause, and late age at first pregnancy constitute additional risk variables due to the role of estrogen in breast cell growth and the potential for genetic mutations to occur during the prolonged exposure to the hormone. Also lifestyle has to be taken into account [11,15]. For example, alcohol consumption can elevate the level of estrogen-related hormones in the blood and trigger the estrogen receptor pathways, while excessive intake of saturated fat contained in modern western diet is associated with poor prognosis in breast cancer patients. Moreover, women that start smoking at an early age have a higher risk of breast cancer occurrence [11]. Finally, expanding obesity epidemic occurring in many countries is linked to an increase in the incidence of estrogen receptor-positive malignancies in post-menopausal women and to a higher risk of pre-menopausal ER-negative and triple negative breast cancers [11,16–18].

The World Health Organization recommends organized mammographic screening every two years for women aged 50–69 years, an effective strategy that allows the detection of nodules when they are still too small to be palpable during an examination. For women who are not included in the age interval, and without specific germinal mutations, the benefit of the exam would not compensate the risks from radiation exposure and overdiagnosis [19,20].

### 1.1.3 Classification, staging and treatment

Breast cancer is a very heterogeneous disease, both morphologically and molecularly. The advancement of detection and high-throughput molecular technologies that have enormously increased the knowledge of breast cancer biology, resulted in an improved clinical management. Following the initial detection of a suspicious lump, a biopsy or aspirate is recommended, and histological, cytological, and molecular characterization is performed.

Depending on the site of origin and the spreading of the disease, breast tumors can be histologically categorized as either ductal or lobular, and non-invasive (or *in situ*) or invasive. Twenty percent of newly diagnosed tumors are ductal carcinomas in situ (DCIS) and can be graded based on the degree of differentiation and similarity to the normal breast tissue. Lobular carcinoma in situ (LCIS) is less frequent than DCIS and it is generally not thought to be a precursor of invasive cancer. It is also possible to find rare cases with characteristics of both types of carcinomas. Most breast cancers are invasive (or infiltrating) ductal carcinomas (IDCs), which mainly occur sporadically in women over 50 years of age and in those presenting BRCA1/2 germline mutations. Cell morphological properties subdivide IDCs into at least six subtypes with different prognosis, namely classical, apocrine, medullary, mucinous, papillary, and tubular ductal. The stage at diagnosis is a critical factor in determining the prognosis for all these subtypes but usually the apocrine subtype is associated to a very poor outcome [21]. Invasive lobular carcinomas account for 10% of invasive breast cancers; as for IDCs, the subtypes identified are classic, tubulolobular and histiocytoid. Among the rarest forms of invasive lesions,

inflammatory breast cancers (IBCs) stand out for their aggressiveness and fast growth. Indeed, in IBC, cancer cells invade and block the lymphatic vessels within the dermal layer of the skin. This leads to a buildup of lymphatic fluid and inflammation, which manifests as the red and swollen appearance of the breast [22].

The prognosis of invasive breast cancer is strongly influenced by the stage of the disease, which is defined according to the Tumor-Node-Metastasis (TNM) system. The TNM staging system classifies breast cancers on the basis of three important features of the tumor, i.e. size at the time of diagnosis, lymph node status and metastasization. There are therefore five possible stages, having stage 0 assigned to in situ carcinomas, stages I, II and III to tumor masses with different degrees of spreading in the breast surroundings and lymph node involvement, and stage IV corresponding to the presence of metastasis at distant sites.

A revision of the purely anatomical TNM system established the assessment of the status of the three main breast cancer biomarkers, estrogen receptor (ER), progesterone receptor (PR), and human epidermal growth factor receptor 2 (HER2), as essential parameter to be considered for prognosis and therapeutic evaluation [23]. Indeed, positivity for the three receptors is routinely assessed by immunohistochemical or in situ hybridization and significantly impacts on treatment decision and outcome. A tumor that lacks the expression of these markers is called triple negative breast cancer (TNBC). ER (ER$\alpha$ in particular) and PR are respectively encoded by *ESR1* (Ch 6q25.1-q25.2) and PGR (Ch 11q22) genes. Upon ligand binding, they translocate to the nucleus and act as transcription factors, activating cell growth, proliferation, and differentiation pathways. The receptor

HER2 is a transmembrane protein encoded on Ch 17q12 by *ERBB2* gene, it doesn't have a known ligand, forms homo- or heterodimers with the other members of the ERBB family to promote cell growth and proliferation. Being a central topic of this thesis, details on HER2 functions and oncogenic role can be found in chapter 1.2.

Complete molecular characterization of breast tumors integrated the information gained from receptor status and helped to obtain a better portray of the clinical complexity and heterogeneity of the disease. The five "intrinsic" molecular subtypes, luminal A, luminal B, HER2-enriched, basal, and normal-like, were defined based on the expression of a panel of 50 genes (prediction analysis of microarray 50, PAM50) [24,25]. The two Luminal subtypes are characterized by the expression of ER and/or PR associated genes. Luminal A is the most common breast cancer subtype, it is slow-growing (low expression of Ki-67, cellular marker of proliferation) and less aggressive than other subtypes and, thus, is associated with the most favorable prognosis [26,27]. Luminal B tumors tend to be of higher grade and are more aggressive (and have higher Ki-67 expression) than luminal A, due to frequent positivity for HER2 and TP53 mutations. [28,29]. ER positivity is the primary indicator of response to endocrine therapy (i.e. selective ER modulators like *tamoxifen*, ER down-regulators as *fulvestrant* and aromatase inhibitors). HER2-enriched malignancies are less differentiated, tend to grow and spread more aggressively than luminal subtypes. The widespread use of targeted therapies (for example the anti-HER2 antibody *trastuzumab*, in detail in chapter 1.2.3) has greatly improved the clinical outcome of this breast cancer subtype [30,31]. The Basal-like subtype shows the worst prognosis, being most of these malignancies TNBCs, with chemotherapy as standard treatment.

Recent efforts from the scientific community led to introduction of Poly(ADP-Ribose) Polymerase (PARP) inhibitors, antibody-drug conjugates and immune-checkpoint inhibitors as therapeutic options for this challenging disease [32], even though limited to specific subgroups of eligible patients.

Plasticity between the different subtypes, also favored by cues from the tumor microenvironment, is a known phenomenon and constitutes the basis of tumor progression and treatment resistance [33]. For example, luminal tumors with low ER expression have a higher tendency to gain basal-like traits compared to other luminal malignancies [34]. Patients with residual disease after neoadjuvant anti-HER2 targeted therapy can, instead, lose HER2-positivity and become resistant to the same drug in the adjuvant phase [35]. Loss of HER2-positivity is also frequently reported in metastasis of patients with primary HER2-positive breast cancer [36].

Finally, the disparity in outcomes between histological and molecular subtypes is nullified when the metastatic disease is considered. Indeed, in cases where cancer is confined to the breast alone or involves nearby lymph nodes, the 5-year survival rate is at least 86%; on the contrary, when cancer has metastasized to a distant area of the body, the survival rate drops to 28% [37].

## 1.2 HER2+ Breast cancer

### 1.2.1 HER2 signaling pathway

HER2 belongs to a family of type I transmembrane growth factor receptors, along with EGFR (or HER1), HER3, and HER4. The extracellular domain of HER2, which lacks a

known ligand, constitutively maintains an activated conformation. Conversely, when the other three members bind their respective ligands, they undergo a conformational change and can form homodimers or heterodimers. HER2 possesses the highest catalytic activity and, due to its constitutively activated conformation, is the preferred partner for dimerization [38]. Consequently, the transphosphorylation of the intracellular tyrosine kinase domains of these receptors initiates numerous signaling cascades, notably including the PI3K/AKT/mTOR (phosphatidylinositol 3-kinase/serine/threonine kinase, protein kinase B, mammalian target of rapamycin) and MAPK/ERK (mitogen-activated protein kinase, extracellular signal-regulated kinases) pathways [39]. In particular PI3K, directly activated by HER2, phosphorylates phosphatidylinositol 4,5-bisphosphate (PIP2) to form phosphatidylinositol 3,4,5-trisphosphate (PIP3); PIP3 serves as a second messenger that recruits AKT to the plasma membrane, where it is bound and partially activated. PTEN (Phosphatase And Tensin Homolog) antagonizes PIK3 activity by dephosphorylating PIP3 [40]. Full activation of AKT requires two critical phosphorylation events, the first being the phosphorylation at Thr308 carried out by PDPK1 (3-Phosphoinositide-Dependent Protein Kinase-1 or PDK1), which is recruited to the plasma membrane by PIP3. The additional phosphorylation step at Ser473 is typically carried out by mTOR Complex 2 (mTORC2), which further enhances AKT's activity. Physiologically, AKT signaling is rapidly turned back off to allow proper pathway function. Indeed, several downstream effectors, notably mTORC1, function as rheostats that both sense signaling within the pathway and control the pathway's activity [41]. As for MAPK pathway, upon HER receptor activation a protein called Ras, a small GTPase that serves as

a molecular switch, is activated. In turn, Ras recruits and activates a MAPKKK (MAP3K), often Raf, which starts the kinase cascade, starting from MAPKK (MAP2K), specifically MEK1/2, and finally ERK1/2. Once phosphorylated, activated ERK1/2 translocate from the cytoplasm to the nucleus to activate various transcription factors and regulatory proteins, modulating gene expression and affecting different cellular responses. The activated ERK1/2 can also trigger negative feedback mechanisms to regulate its own signaling and maintain cellular homeostasis [42].

As mentioned above, HER2 activates a plethora of other pathways: JAK-STAT (Janus kinase, signal transducer and activator of transcription) pathway impacts cell growth and survival regulating gene expression; PLC-γ/PKC (phospholipase C-gamma, protein kinase C) pathway contributes to increase cell proliferation, survival, and migration; nuclear factor-kappa B (NF-κB) is a transcription factor involved in inflammation and cell survival; Wnt/β-catenin pathway regulates cell proliferation and stem cell maintenance, together with Notch Pathway; Rho GTPase Pathway includes Ras Homolog Family Member A (RHOA), Rac Family Small GTPase 1 (RAC1), and Cdc42, which are involved in cell motility and cytoskeletal rearrangement [43,44]. Finally, HER2 activation can inhibit apoptosis and promote cell survival. The transcriptional programs involve proto-oncogenes like FOS, JUN, and MYC, but also a family of zinc-finger containing transcription factors that includes SP1 and EGR1. All these pathways are interconnected, and the specific response to HER2 activation can vary depending on the cellular context, the presence of other signaling molecules, and genetic factors. Additionally, HER2 engages in cross-talks with other transmembrane signaling pathways (such as Insulin and

insulin-like growth factor receptors), ultimately promoting growth, proliferation, and survival of epithelial cells [45,46]. Lastly, it has been also demonstrated that HER2 signaling, through the modulation of chemokine production, regulates the recruitment and activation of tumor infiltrating immune cells [47].

Breast cancer cells can present up to 25-50 copies of the HER2 gene and up to 40-100 fold increase in HER2 protein expression resulting in up to 2 million receptors expressed at the tumor cell surface [48]. Thus, the overexpression of HER2 can profoundly alter the composition of HER family dimers, resulting in a notable increase in HER2-containing hetero and homodimers. These heterodimers are characterized by a prolonged activity and evasion of negative feedbacks, leading to an enhanced signaling potency. For example, EGFR undergoes endocytic degradation following activation through ligands and homodimerization, in contrast with the other family members that are recycled to the membrane. Similarly, EGFR-HER2 heterodimers also avoid endocytic degradation, favouring the recycling pathway. Consequently, HER2 overexpression leads to an elevation in EGFR membrane expression and activity [49]. Considering the HER2-HER3 complex, its primary oncogenic function is activating the PI3K/Akt pathway. Unlike HER3, HER2 lacks binding sites for PI3K's p85 subunit. Growth factor-triggered PI3K and Akt activation by HER2 occurs through HER3 phosphorylation. Overexpressed HER2 leads to increased HER3 phosphorylation and PI3K/Akt signaling activation, contributing to cell transformation [46,50].

### 1.2.2 Diagnosis, prognosis and treatment

HER2 overexpression, amplification, or both is detected in 20% of primary invasive breast cancer cases. To assess HER2 positivity, two primary methods are generally used: immunohistochemistry (IHC) and in situ hybridization (ISH). IHC is employed as the initial test and consists in evaluating levels of HER2 protein, assigning scores of 3+ (HER2 positive), 2+ (HER2 equivocal), and 1+/0 (HER2 negative) based on the intensity of staining, the percentage of cancer cells stained, and completeness of membrane staining. Accordingly, a 1+/0 score is assigned when the signal is absent or weak and incomplete, 2+ score corresponds to a moderate and complete membrane staining in more than 10% of tumor cells or strong and complete membrane staining in less than 10% of tumor cells, and 3+ scored tumors have more than 10% of cells with a strong, complete membrane staining. In cases where the IHC score is 2+, further analysis with ISH is typically required. ISH examines the HER2/CEP17 ratio and HER2 copy number to definitively determine whether the cancer is HER2-positive or negative. CEP17, which stands for *chromosome enumeration probe 17*, is used as a control probe to assess the number of chromosome 17 copies. Cancers with more than one chromosome 17 often have increased copies of the HER2 gene, which is located on chromosome 17, indicating chromosomal instability in the cancer. CEP17 plays a crucial role in correcting for chromosome aneuploidy during HER2-positive cancer testing, enabling the detection of HER2 gene copies in relation to centromere 17 copies per nucleus [48,51,52] (**Figure 1.2**).

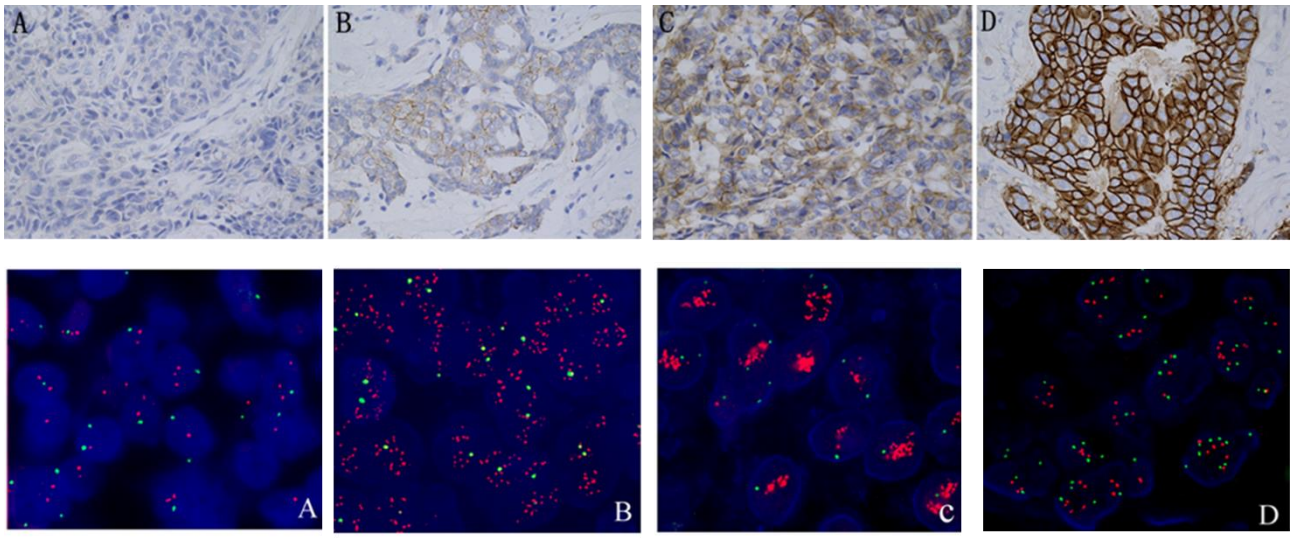


***Figure 1.2*** *HER2 protein expression detected by IHC. (×400) A: Negative (score 0). B: Negative (score 1+). C: Equivocal (score 2+). D: Positive (score 3+). HER2 gene status identified by FISH. Red signals represent HER2 gene, green signals represent CEP17 (×600). A: HER2 gene negative case; B:HER2 gene positive case, HER2/CEP17 ratio of higher than 2.0; C: HER2 gene positive case, HER2 signals are clustered; D: HER2 gene with CEP17 gain, average CEP17 copy number 3.76 to 6. Adapted from Ji H et al PLOS ONE 2015*

In the past, HER2 positivity was linked to unfavourable outcomes and higher mortality rates compared to other subtypes [53]. However, thanks to the development of HER2-targeting therapies, this disease is now manageable, and patient outcomes have significantly improved, with survival rates that can surpass 90%, depending on tumor stage.

In particular, here are the currently available therapeutic options for HER2+ breast cancer patients:

- Humanized monoclonal antibodies: *trastuzumab* is the first anti-HER2 agent developed, it binds extracellular domain IV of the receptor. *Pertuzumab*, instead, targets extracellular domain II of HER2 and is often used in combination with trastuzumab and chemotherapy [54,55]. Since trastuzumab is one of the main topics of this thesis, thorough information is included in Section 1.2.3.

- Tyrosine kinase inhibitors (TKIs): *lapatinib* is a small molecule that acts as a reversible inhibitor of EGFR and HER2. In contrast, *neratinib* is an irreversible pan-HER TKI that targets EGFR, HER2 and HER4. *Tucatinib* is a HER2-specific TKI with >1,000-fold greater potency for HER2 than EGFR [56–58].
- Antibody–drug conjugates (ADCs): created to channel chemotherapy's toxic effects specifically to tumor cells. They consist of a tumor-targeting antibody linked to a cytotoxic drug via a synthetic linker. *Ado-trastuzumab emtansine* (T-DM1), the first anti-HER2 ADC developed, couples trastuzumab and DM1, a maytansine derivative which causes mitotic disruption [59]. *Trastuzumab deruxtecan* (T-Dxd) comprises a humanized HER2 antibody with the same sequence as trastuzumab conjugated to deruxtecan (DXd), a topoisomerase I inhibitor. DXd linker is selectively cleaved by cathepsins, which are upregulated in tumors [60]. The membrane-permeable payload is thus able to diffuse in the extracellular compartment and exert its anti-tumor activity on neighboring heterogeneous cells; this phenomenon is known as ‘‘bystander’’ effect [61].
- Chemotherapy: various chemotherapy regimens may be used in combination with HER2-targeted therapies. Common chemotherapy drugs used include taxanes like docetaxel or paclitaxel, and anthracyclines [62]. When combining trastuzumab and anthracyclines it is important to consider patient’s cardiac conditions because the two drugs are both cardiotoxins and could synergize and increase the likelihood of heart problems [63].
- Adjuvant Therapy: In early-stage HER2-positive breast cancer, adjuvant therapy with trastuzumab is recommended to reduce the risk of recurrence after surgery [64].

- Hormone Therapy: if an HER2-positive breast cancer is also hormone receptor-positive, hormone therapy drugs like tamoxifen or aromatase inhibitors are used in combination with HER2-targeted therapies, depending on patient's menopausal status [65].
- Radiotherapy: is used after non radical surgery to reduce the risk of local recurrence [66].

Currently, the ASCO Guidelines for systemic therapy of advanced disease recommend combination of trastuzumab, pertuzumab, and a taxane for first-line treatment [67]. If tumors are also positive for ER/PR, endocrine therapies can be given alone (in selected cases) or in combination with anti-HER2 antibodies. The regimen at second-line has been recently updated: if a patient's HER2-positive advanced breast cancer has progressed during or after first-line HER2-targeted therapy (and the patient has not received T-Dxd), clinicians should recommend T-Dxd as a second-line treatment, instead of T-DM1. Indeed, in the DESTINY-Breast03 trial comparing the two ADCs in metastatic patients that had progressed during or after first-line treatment, T-Dxd group had a remarkable 12-month progression-free survival of 75.8% versus 34.1% of T-DM1 group [68]. It is important to note that T-Dxd has also shown a notable efficacy in HER2-low patients, opening the discussion regarding the definition of HER2 status and the necessity to consider HER2-low tumors an independent clinical subgroup from the HER2 negative [69,70]. Indeed, patients with tumors scored by IHC analysis as 0, 1+ or 2+ without gene amplification, have been so far all diagnosed as HER2-negative and considered unresponsive to conventional anti-HER2 treatments [71]. Increasing evidence underlines instead how HER2 1+ or 2+ with no amplification (the so called HER2low tumors) can benefit from

anti-HER2 drugs. Finally, the remaining therapeutic options mentioned above are then available for third-line treatment and the decision-making process takes into consideration therapy schedules, routes, and toxicities [72].

### 1.3 Focus on trastuzumab

Trastuzumab (commercially named Herceptin) was the first recombinant humanized IgG1 monoclonal antibody designed to specifically target the oncogene HER2. Scientist noticed early on that antibodies against HER2 were shown to reverse the transformed appearance of cells expressing the tumor antigen and selectively inhibit their growth [73]. Then, the antibody 4D5 was selected for its ability to specifically bind HER2 versus EGFR, but it was not feasible to test in patients due to the rodent origin and consequent immunogenicity. Thus, 4D5 was humanized by replacing the mouse-specific amino acid sequences in the variable regions with equivalent human sequences while maintaining the binding specificity for HER2, resulting in the clinical antibody Herceptin, approved by the U.S. Food and Drug Administration (FDA) in 1998 for the treatment of HER2-positive metastatic breast cancer [74,75]. In 2006, the FDA expanded the approval of the drug to include its use as an adjuvant therapy for early-stage HER2-positive breast cancer. This decision was based on clinical trials, the HERA trial for example, showing that adjuvant trastuzumab could help achieve a remarkable 50% decrease in risk of relapse and a 33% decrease in risk of death [75–77]. In 2010, Luca Gianni et al published the results of the NOAH trial which supported, for the first time, the addition of neoadjuvant trastuzumab to neoadjuvant chemotherapy to improve patient's prognosis [78]. Thanks to these

successes, trastuzumab rapidly became the treatment of choice, revolutionizing the management of the disease, significantly improving patient lives. Importantly, trastuzumab example paved the way for the development of numerous targeted therapies in the field of oncology.

### 1.3.1 Mechanism of action

Despite its wide implementation in the clinical practice, trastuzumab holds a multifaceted mechanism of action that has been described almost completely only in recent years. For example, it exerts a cytostatic effect associated with cell cycle arrest in G1, due to the upregulation of the cyclin-dependent kinase (Cdk) inhibitor p27 [79]. When overexpressed, HER2 undergoes proteolytic cleavage, the extracellular domain is released in the serum but the membrane-bound truncated form (p95) constitutively retains its oncogenic activity [80]. Trastuzumab, by binding extracellular domain IV of the HER2, interferes by steric hindrance both with its shedding and with its dimerization, inhibiting the signaling cascade described in section 1.2.1. [81,82]. It also promotes HER2 endocytosis and degradation [83]. However, a substantial part of trastuzumab efficacy is probably due to its ability to trigger the so called antibody-dependent cell-mediated cytotoxicity (ADCC) [84]. Indeed, the constant Fc portion of the antibody, not being implicated in antigen binding, is exposed to the extracellular compartment and it is recognized by Fcγ receptor III (FcγRIII) expressed on the surface of natural killer (NK) cells, macrophages, neutrophils and eosinophils, inducing activation and release of cytotoxic molecules [85]. Subsequently, antigen-presenting cells (APCs), especially dendritic cells, identify tumor-immune complexes using FcγRIII and initiate the activation of CD4+ T-helper

lymphocytes through MHC-II molecules. The cytokines produced by T-helper cells amplify the CD8+ cytotoxic T cell response. CD8+ T cells become active upon exposure to antigens presented by MHC-I molecules expressed on both APCs and tumor cells [86]. Finally, trastuzumab also induces the normalization and regression of the altered tumor vasculature by modulating the effects of different pro- and anti-angiogenic factors [87].

### 1.3.2 Mechanisms of resistance

Trastuzumab has undoubtedly positively impacted cancer treatment, reaching way beyond HER2 positive breast malignancies. Still, a significant portion of patients unfortunately does not benefit from this treatment. Indeed, these patients present intrinsic or acquired mechanisms of resistance, which can be grouped into 4 main categories: failure of HER2 binding, upregulation of HER2 downstream pathways, signaling through an alternative receptor and failure to trigger ADCC (**Figure 1.3**).

*Failure of HER2 binding*

The presence of p95HER2 reduces the number of trastuzumab molecules on cell surface, impairing treatment efficacy [88]. Similarly, alternative initiation of HER2 translation may generate truncated isoforms without proteolysis [89]. Shifting the therapeutic regimen to a TKI like lapatinib can overcome this event and promote tumor regression. Epitope masking can also impede trastuzumab binding. In fact, highly glycosylated membrane-associated proteins, for example mucin-4, expressed in the vicinity of HER2 can hide the target region, decreasing antibody-binding capacity. Knockdown of the protein of interest can restore treatment response [90].

*Upregulation of HER2 downstream pathways*

Given the amplitude of HER2 signaling cascade, there are multiple escape pathways that the tumor can exploit to survive trastuzumab activity. Recently, a study that compared alterations associated with either intrinsic or acquired resistance, observed a PKC-mediated MEK/ERK pathway activation in an acquired trastuzumab-resistant cellular model. Conversely, intrinsic resistant cells were mainly characterized by PI3K/Akt and RAS/RAF/MEK/ERK activation, stabilization of β-catenin and cell cycle inhibition [91]. In general, around 30% of HER2+ breast cancers present somatic mutations in the PI3K/Akt pathway, especially PI3K gain-of-function alterations [92,93]. Loss of PTEN is a very frequent event in cancers and coincides with a reduced sensitivity to trastuzumab due to sustained Akt activity *in vitro* and *in vivo* [94].

*Signaling through an alternative receptor*

Other tyrosine kinase receptors can compensate HER2 inhibition. For example, increased levels of Insulin Like Growth Factor 1 Receptor (IGF1R) interfere with trastuzumab activity, maintaining the stimulation of proliferation pathways [95] . c-MET belongs to the family of hepatocyte growth factor receptors. It is frequently overexpressed along with HER2 and confers resistance to trastuzumab by preventing the induction of p27, thus sustaining cell growth [96]. Within the HER family, EGFR is the main alternative member that is found overexpressed in HER2+ malignancies and associates with poor treatment response [97,98].

ER upmodulation is another escape mechanism used by tumor cells to overcome HER2 blockade. Indeed, upon activation, ER acts as transcription factor for proliferation and survival genes. Additionally, it has been demonstrated that ER/HER2 crosstalk promotes proliferation also by inducing an increase in MYC-mediated glutamine metabolism. Combination of HER2 and ER targeting can be an effective strategy in this scenario [99].

*Failure to trigger ADCC*

On this regard, both tumor and host characteristics have to be considered. The type of single nucleotide polymorphism present in Fcγ receptor III coding genes determines a different affinity for trastuzumab Fc portion [100,101]. The number and lytic efficiency of effector lymphocytes (NK and T cells) influences ADCC intensity and, thus, response to treatment [102,103]. Chemotherapy can reduce the number and activity of NK cells, compromising the efficacy of combination settings [104,105]. ADCC triggering can also fail due to tumor release of immunosuppressive factors like TGF-β and IL-10 [106,107].

Expanding knowledge of the disease and therapy mechanism of action has recently led to the discovery of multiple additional ways that the tumor exploits to survive and progress, which include metabolism modulation, cellular plasticity and stemness, and deregulation of non-coding RNAs.

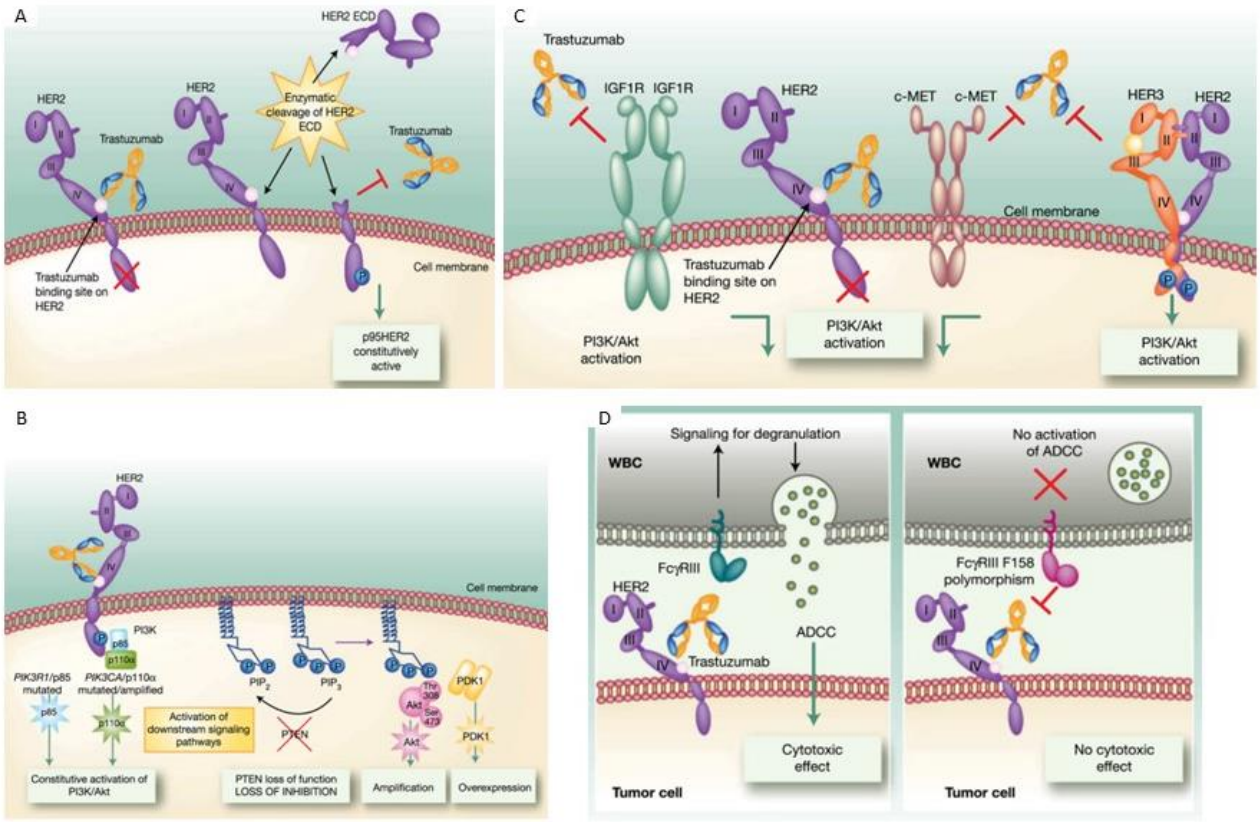


***Figure 1.3*** *Mechanisms of resistance to trastuzumab: failure of HER2 binding (A), upregulation of HER2 downstream pathways (B), signaling through an alternative receptor (C), and failure to trigger ADCC (D). Adapted from Pohlmann PR et al, Clin Cancer Res 2009 [79].*

### 1.3.3 Predictive biomarkers of response

HER2 expression is, intuitively, the first indicator of trastuzumab response but, unfortunately, it is not sufficient to explain the heterogeneity of clinical responses to the treatment [108]. Nevertheless, tumors that are categorized as HER2 enriched by the PAM50 classifier are those that benefit the most from this treatment, especially in the neoadjuvant setting [109,110]. Data from different clinical trials support ERBB2 and ESR1 mRNA levels as superior in predicting HER2 activity and tumor-addiction than the standard IHC tests [110–112]. PTEN status and PI3K pathway were initially thought to be able to predict response due to the resistance mechanisms they are involved in. However,

they recently failed to be associated with pathologic complete response (pCR) in the NeoALTTO trial, in any given arm of treatment [110].

As mentioned before, the contribution of the immune system to trastuzumab activity is essential to efficiently fight the tumor. Accordingly, in the last decade, researchers focused on identifying the best immunological profile associated to a higher benefit from this treatment. Some key findings include the development of a genomic signature that predicts the benefit of trastuzumab in tumor enriched with immune-related genes [113]. In the neoadjuvant setting, the expression of immune genes, metagenes and the percentage of tumor-infiltrating lymphocytes (TILs) significantly correlated with pCR [114,115]. A recently identified signature, known as the 41-gene classifier TRAR, highlights the importance of the combined evaluation of ERBB2 and ESR1 mRNA levels and immune-related genes to identify trastuzumab responsive patients [116,117].

## 1.4 MicroRNAs and HER2+ Breast Cancer

### 1.4.1 MicroRNAs: biogenesis and mechanism of action

MicroRNAs, also known as miRNAs or miRs, are short, single-stranded RNAs consisting of 19-25 nucleotides. They play a crucial role in post-transcriptional gene regulation. The discovery of miRNAs dates back to 1993 when researchers identified in Caenorhabditis elegans a small regulatory RNA called lin-4, which was involved in larval development by regulating lin-14 translation through an antisense RNA-RNA interaction [118]. In 2000, another regulatory RNA, let-7, was found to regulate the same target, not only in annelids and molluscs but also in their adult stages [119]. This discovery sparked significant

research interest in miRNAs, revealing their involvement in various biological processes [120–122]. MiRNAs are initially encoded as long primary transcripts called pri-miRs. These pri-miRs undergo a two-step processing, starting in the nucleus and finishing in the cytoplasm. They exhibit a hairpin structure with a terminal loop and an approximately 30-base pair stem with single-stranded ends. RNA polymerase II transcribes these pri-miRs, and they are cleaved by a multi-protein complex called the Microprocessor, consisting of DROSHA and its essential cofactor DGCR8 [123,124]. This cleavage produces ~60-nucleotide-long molecules known as pre-miRs, characterized by a hairpin structure with a 3' overhang. Pre-miRs are then specifically recognized and exported to the cytoplasm through the nuclear export machinery, which includes Exportin-5 and Ran-GTPase. In the cytoplasm, pre-miRs are further processed by the enzyme DICER, which cleaves the double-stranded RNA stem near the terminal loop, generating the mature nucleotide duplex. During this process, the transactivation-responsive RNA-binding protein (TRBP) facilitates the assembly of the miRNA-induced silencing complex (miRISC) by connecting DICER with Argonaute proteins (AGO1, AGO2, AGO3, or AGO4) [125]. MiRISC selects and retains one of the two strands (the mature miRNA), while the other strand is usually released and degraded [126]. Once the miRISC complex is assembled, the mature miRNA guides its interaction with target mRNA. Specifically, the "seed" region of the miRNA, comprising nucleotides 2-8 at the 5' end, recognizes complementary sequences within the 3'UTR, 5'UTR, or coding DNA sequence of the target mRNA [127,128]. This complementarity is often partial, allowing miRNAs to bind and modulate multiple transcripts. Depending on the degree of miRNA-mRNA base pairing, miRISC can induce

various mechanisms to inhibit target translation. Perfect pairing leads to mRNA degradation, while miRNA binding can also prevent the mRNA from being translated (**Figure 1.4**). The exact mechanism of this repression is not fully understood, but it is believed that miRISC interferes with the assembly of translation initiation machinery, blocking the eIF4F cap-binding complex [129,130]. Intriguingly, some evidence suggests that miRNAs might also stimulate mRNA translation under certain conditions, depending on the extent of base complementarity and the cellular context in which the modulation occurs [131,132].

MiRNA strand selection was initially thought to be guided only by 5′ nucleotide identity and relative duplex-end stability, determining a unique dominant mature miRNA [133]. Instead, numerous evidence demonstrates that both strands can be alternatively or simultaneously functional; this process, often referred to as miRNA "arm switching" is highly dynamic and tissue specific [134,135]. Among the factors that could influence the ratio of the two strands there are mRNA target availability, duplex sequence alteration, AGOs and AGO-interacting proteins [136]. Intuitively, a dysregulated miRNA strand selection can occur in cancer [133]. In breast cancer, for example, it has been shown that tumor cells deficient for homologous recombination (HR)-associated proteins can escape therapy-induced synthetic lethality by promoting the downmodulation of miR-223-3p, a suppressor of nonhomologous end-joining (NHEJ) components, in favor of the 5p mature strand [137].

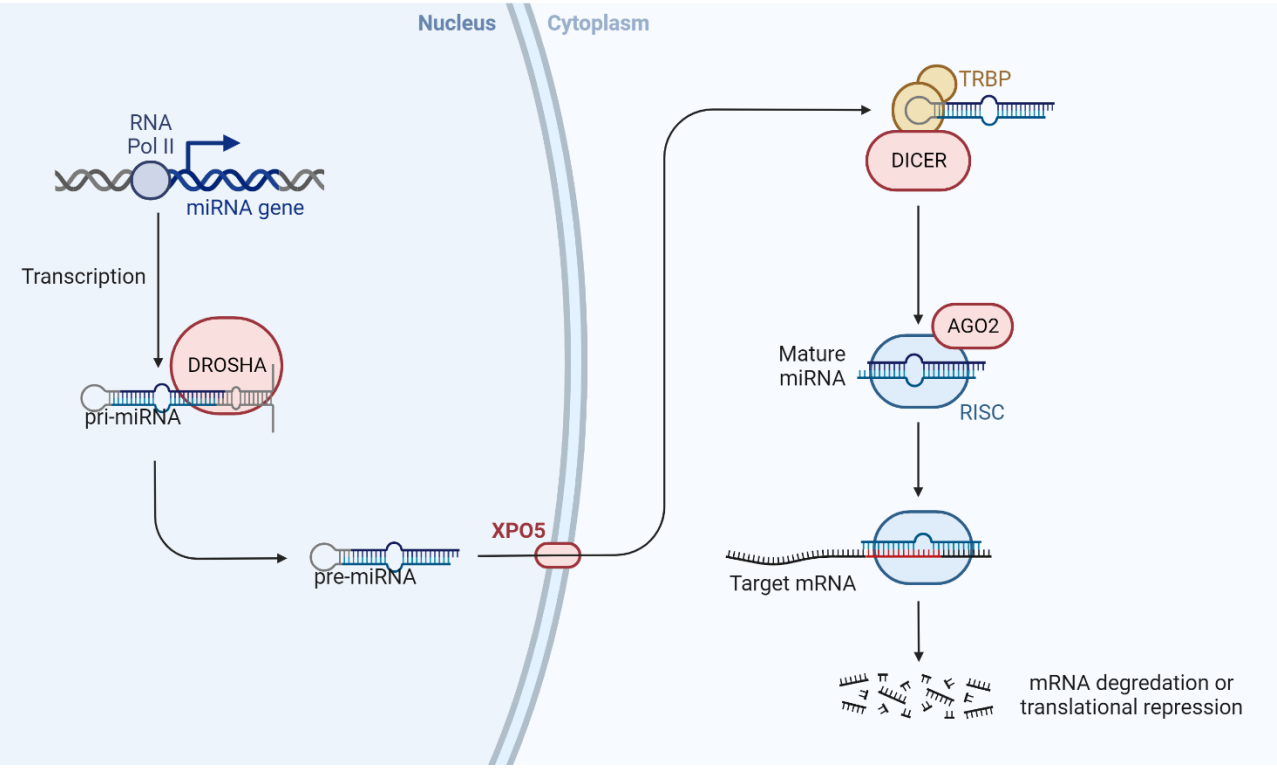


***Figure 1.4*** *MicroRNA biogenesis. Created with BioRender.com.*

### 1.4.2 Deregulation of miRNAs in cancer

In 2002, Dr. Croce's laboratory made a groundbreaking discovery concerning the involvement of miRNAs in cancer. Their research revealed a connection between the loss of two miRNA genes, miR-15a and miR-16-1, and the onset of chronic lymphocytic leukemia [138]. Subsequently, numerous other human miRNA-coding genes were identified within fragile sites and regions with genetic alterations in various cancer types, suggesting a significant role for these small molecules in the development of human cancer [139]. The dysregulation of miRNA expression in cancer can be attributed to various mechanisms, including structural genetic changes, deficiencies in miRNA biogenesis machinery, and abnormal epigenetic modifications [140–144]. MiRNAs are classified as either oncogenes (oncomiRNAs) or tumor suppressors (tsmiRNAs)

depending on their target function. OncomiRNAs target tumor suppressor molecules and, when up-regulated, can promote the initiation of tumors, whereas ts-miRNAs modulate oncogenes and, when downregulated, can contribute to malignant progression [145,146]. Additionally, some miRNAs, referred to as metastamiRNAs, influence tumor progression at later stages by regulating malignant cell migration, invasion, and metastasis. For instance, in non-metastatic breast cancer cells the overexpression of miR-10b promotes invasion and metastasis, while the downregulation of the proto-oncogene MET by miR-34a inhibits migration and invasion in human hepatocellular carcinoma cells [147,148]. Given the widespread involvement of miRNAs in cancer, various platforms have been developed to comprehensively assess genome-wide miRNA expression in different types of tumors, aiming to identify specific miRNA signatures associated with malignant tissues [149–153]. In the context of breast cancer, the first miRNA expression profile was described by Iorio et al. in 2005. Their study compared 76 human breast cancers with 10 normal samples, identifying 29 miRNAs that exhibited significant deregulation between normal and cancerous tissues, with 15 showing the ability to accurately distinguish between the two categories. Notably, miR-10b, miR-125b, and miR-145 were the most robust predictors among the downregulated miRNAs, while miR-21 and miR-155 were prominent among the upregulated ones. Furthermore, the researchers identified miRNAs whose expression correlated with specific breast cancer pathological features, such as estrogen and progesterone receptor status, lymph node metastasis, vascular invasion, proliferation index, and p53 immunohistochemical detection [154]. In conclusion, miRNAs

make a substantial contribution to the pathogenesis of cancer and hold significant potential as clinical biomarkers and targets for therapies.

### 1.4.3 Deregulation of miRNAs in HER2 positive breast cancer

Numerous are the examples of miRNAs that are involved in any of the phases of tumor progression, even in HER2+ malignances. Back in 2013, Leivonen et al, by using miRNA gain-of-function assays and reverse-phase protein array technique, identified miRNAs that modulate HER2 and its downstream pathways. In this study, 38 miRNAs were identified as inhibitors of HER2 signaling and cell growth, with the most effective ones being miR-491-5p, miR-634, miR-637, and miR-342-5p. Additionally, seven novel miRNAs (miR-552, miR-541, miR-193a-5p, miR-453, miR-134, miR-498, and miR-331-3p) were found to directly regulate the HER2 3'UTR. The clinical significance of these miRNAs was demonstrated, and it was noted that miR-342-5p and miR-744* were significantly downregulated in HER2-positive breast tumors compared to HER2-negative tumors in two separate cohorts of breast cancer patients (101 and 1302 cases). Interestingly, miR-342-5p specifically inhibited the growth of HER2-positive cells while having no effect on HER2-negative control cells *in vitro*. Furthermore, higher expression of miR-342-5p was associated with improved survival in both cohorts of breast cancer patients [155]. In 2019, Pattanayak and coworkers investigated the role of miR-33b in primary HER2+ breast cancers. Their findings revealed a significant reduction in miR-33b levels in both patient-derived samples and cancer cell lines. MiR-33b ectopic expression resulted in a notable reduction in EMT, proliferation, invasion, and migration, while simultaneously promoting apoptosis. Subsequent investigation unveiled that miR-33b acts as a tumor suppressor by

targeting MYC, a known binder of the EZH2 (zeste homolog 2-gene) promoter [156]. Further research by Gorbatenko et al. aimed to identify distinctions in miRNA expression profiles induced by HER2 and its truncated variant, p95HER2, in HER2-/p95HER2-overexpressing MCF-7 breast cancer cells. Their investigations disclosed discernible shifts in the expression profile, indicating a transition toward a pattern characteristic of the basal breast cancer subtype upon p95HER2 overexpression. Among the markedly altered miRNAs, miR-221, miR-222, and miR-503 were identified. These particular miRNAs downregulated the expression of ER$\alpha$ in p95HER2-overexpressing cells, thereby compromising their response to anti-hormonal therapy. Additionally, the upregulation of miR-221/222 and -503 amplified cell mobility, collectively suggesting that altered miRNA expression played a contributory role in the heightened aggressiveness of the p95HER2 tumor subtype [157]. Recently, Shabaninejad et al. discovered an intronic miRNA within the ERBB2 gene, named HER2-miR1. This novel miRNA was confirmed in various human cell lines. Overexpression of HER2-miR1 downmodulated the Wnt signaling pathway, indicating an oncosuppressive role [158].

### 1.4.4 MiRNA-based prognostic and predictive signatures

Clinical trials investigating the potential of miRNAs as biomarkers for diagnosis, prognosis, and therapy effectiveness are numerous. Several studies are testing miRNAs in blood or tissue samples from cancer patients to diagnose different cancer types, such as bladder cancer, breast cancer, non-Hodgkin's lymphoma, acute leukemia, thyroid cancer, and colorectal cancer [159]. The recent interest of the scientific community in the

microbiota and cancer crosstalk also led to miRNA analysis in fecal samples for colorectal cancer screening [160].

In HER2+ breast cancer, Li and colleagues identified in serum of metastatic patients a four-miRNA signature of response to trastuzumab. The four miRNAs, miR-451a, miR-16-5p, miR-17-3p, and miR-940, were found to be involved in resistance mechanisms through the targeting of PTEN, IGF1R, and SRC [161]. In the NeoALTTO trial, miRNA profiling was done in plasma samples collected at baseline (T0) and after two weeks of trastuzumab (T1). Four miRNA signatures were identified as predictive of pCR. Among these, circulating (ct) miR-140-5p was also associated with event-free survival (EFS) in the trastuzumab arm (HR 0.43; 95% CI, 0.22–0.84). Additional analysis focusing on early changes of circulating miRNA levels revealed that increased levels of ct-miR-148a-3p and ct-miR-374a-5p were significantly associated with pCR [162,163]. In HER2+ and TNBC breast cancer patients, Stevic et al. investigated miRNAs in plasma-derived exosomes. They found differences in miRNA expression patterns based on tumor biology. Exosomal miR-27b was higher in HER2+ patients and predicted pCR, while miR-422a was downregulated in HER2+ breast cancer and upregulated in TNBC exosomes [164]. MiR-16, miR-328, and miR-660 in exosomes were associated with lymph node status in HER2+ patients. In serum samples from early HER2+ breast cancer patients receiving neoadjuvant chemotherapy with trastuzumab, miR-21 was significantly reduced in responding patients, and changes in its levels were associated with overall survival and disease-free survival. This suggests potential as a predictive and prognostic marker [165]. Additionally, Zhang's group found that higher baseline levels of serum-miR-222-3p were linked to an

inferior pCR rate in HER2+ breast cancer patients receiving neoadjuvant chemotherapy with trastuzumab. Lower serum-miR-222-3p expression correlated with better disease-free survival and overall survival [166]. Moreover, miRNA and lncRNA (long non-coding RNA) interactions were explored. Indeed, miRNAs were shown to regulate lncRNA expression; lncRNAs, on the other end, are able to act as molecular sponges or decoys for miRNAs. Moreover, in some cases, miRNAs and lncRNAs can work together to cooperatively regulate gene expression [167]. Müller and colleagues investigated the biological role of functionally or physically interacting couples of lncRNA and miRNAs that were found deregulated together in plasma samples of HER2+ breast cancer patients compared to other breast cancer subgroups. In particular, they focused on H19 and miR-675, which is transcribed from H19 first exon and NEAT1/miR-204, which co-repress each other through the binding of complementary regions. In vitro functional studies showed that the modulation of H19/miR-675 and NEAT/miR-204 affected breast cancer cell proliferation and apoptosis [168].

### 1.4.5 MiRNAs involved in trastuzumab resistance

As pointed out before, trastuzumab is widely used in the clinic but resistance cases are frequent. Over the last decade or so, researchers examined the possibility to identify miRNAs involved in resistance to trastuzumab and eventually exploit them as target or tools to restore treatment sensitivity. In 2012, Ichikawa et al performed a microarray-based miRNA profiling and identified a subset of trastuzumab responsive miRNAs, including miR-26a and miR-30b. The authors identified CCNE2 (Cyclin E2) as target of miR-30b [169]. Few years later, Tormo et al demonstrated that, indeed, CCNE2 targeting reduced

trastuzumab resistance in HER2+ breast cancer cells [170]. Rezaei and colleagues identified other dysregulated miRNAs in trastuzumab-resistant cell lines. In BT-474 cells seven candidate miRNAs were evaluated. MiR-23b-3p, miR-195-5p, miR-656-5p, and miR-340-5p were significantly dysregulated in the resistant cell lines. Using different online softwares of prediction, several putative targets associated with drug resistance pathways (i.e foxO signaling pathways, the response to MAPK and PI3K-AKT pathways) were identified [171]. In a recent Nature Communication paper, Luo et al. unveiled that, in HER2+ breast cancer cell models sensitive to trastuzumab, there exists a negative feedback loop governed by two IRS1(Insulin Receptor Substrate 1)-targeting miRNAs, miR-128-3p and miR-30a, as well as an IGF2 (Insulin-like growth factor 2)-targeting miRNA, miR-193-5p, which keeps IGF2/IGF-1R/IRS1 oncogenic signaling in check. FOXO3a, activated by IGF2 levels, induces the expression of these three miRNAs. However, in resistant cells, this negative feedback loop breaks down, resulting in upregulated IGF2 and IRS1 [172]. Another interesting work by Zhou et al. focused on the intronic miRNA-4728, which originates from an excised intron of the HER2 pre-mRNA. Both mature forms, miR-4728-5p and miR-4728-3p, are functional and significantly upregulated in HER2+ breast cancer patients. The authors found out that miR-4728 promotes cell survival and reduces sensitivity to hormonal therapy through ESR1 downmodulation, and that it also enhances the response to anti-HER2 therapy by directly targeting ErbB3-binding protein 1 (EBP1) [173]. Normann et al. recently identified eight miRNAs that sensitized KPL4 and SUM190PT cell lines to treatment with trastuzumab or lapatinib. Notably, higher miR-101-5p expression levels were associated with better breast cancer-specific survival and overall

survival [174]. Subsequently, another article from the same group focused exclusively on the role of miR-101-5p in HER2+ breast cancer. Analysis from the TCGA and METABRIC datasets confirmed the downregulation of miR-101-5p in HER2+ patients. *In vitro* experiments with KPL4 cells showed an improved response to trastuzumab upon miR-101-5p overexpression. The combination of miR-101-5p transfection with anti-HER2 treatment led to several changes in the proteomic landscape of KPL4 cells, including alterations in PI3K-Akt, mTOR, and ErbB signaling [175].

### 1.4.6 MiRNA-based therapeutic approaches

MiRNA dysregulation in the context of tumor biology is a widely accepted notion in cancer research. What remains a subject of ongoing debate is the practicality of using miRNAs as therapeutic tools. Over the years, miRNA mimics and inhibitors have been proposed for clinical applications, but only a few trials have advanced to the phase II stage [176]. There are indeed numerous challenges that researchers must overcome to achieve this goal [177]. First, naked miRNAs are unstable when exposed to extracellular environments, rapidly degraded by nucleases within seconds. In biological systems, miRNAs are mainly transported to other cells or districts shielded within lipoprotein complexes or enclosed in lipid microvesicles, often referred to as exosomes [178–181]. Consequently, for miRNAs to be administered as drugs either into the bloodstream or directly at the tumor site, they need to undergo chemical modifications or to be encapsulated into nanoparticles. This latter approach may also help address other issues, such as the presence of leaky blood vessels in tumors, leading to insufficient miRNA delivery to the target tissue due to poor blood flow. Moreover, once miRNAs enter cells,

they pass from early to late endosomes and ultimately reach lysosomes, which contain an acidic environment and nucleases [182]. One of the primary drawbacks of employing miRNA-based therapies is that it inadvertently capitalizes on one of their strengths: the capacity to regulate multiple targets simultaneously. Naturally, the mechanism of action of miRNAs is meticulously fine-tuned and often cell- and tissue-specific. This precision may not be preserved once miRNAs are introduced artificially into the system, potentially resulting in unintended gene silencing, known as the off-target effect [183]. Recently, a potential solution was proposed, involving the administration of low doses of cooperating miRNAs to mitigate such phenomena [184]. Furthermore, the delivery of exogenous molecules, whether double-stranded RNA or their carriers, holds the risk of triggering an adverse immune response as they can be perceived as pathogens [185,186]. Developing carriers capable of capitalizing on or bypassing all these features could facilitate efficient cargo delivery, reduce required dosages, and minimize side effects [187–189]. A recent review by Silva-Cázares et al. summarizes the selection of delivery systems employed over the years for testing in breast cancer treatment [190]. In the context of HER2+ metastatic breast cancer, the delivery of miR-125a-5p in lipid nanoparticles coated with hyaluronic acid reduced HER2 levels and suppressed cell proliferation and migration via the PI3K/AKT and MAPK signaling pathways [191].

### 1.5 Tissue miRNA-based signatures in the NeoALTTO study

In 2022, my research group, in collaboration with the Unit of Bioinformatics and Biostatistics of our Institute, published results of an investigation of tissue miRNA-based

signatures aimed at predicting response and prognosis upon neoadjuvant trastuzumab [192]. We had access to tumor tissue samples from the phase III NeoALTTO clinical trial, aimed at evaluating the efficacy of neoadjuvant HER2 dual blockade with trastuzumab + Lapatinib vs single blocking, in concomitance with chemotherapy (Paclitaxel), in HER2+ breast cancer patients. The primary and secondary endpoints of the study were pCR and EFS, respectively. Focusing on the Trastuzumab arm, a predictive and a prognostic signature were identified. In details, from the univariate analysis, 8 miRNAs were significantly associated with pCR in the training set. By combining these miRNAs into multivariate models, and after their confirmation in the testing set, a final signature of two miRNAs, miR-31-3p and miR-382-3p, was selected as best model in the overall study population (hsa-miR-31-3p, OR 0.70, 95% CI: 0.53-0.92, and hsa-miR-382-3p, OR: 1.39, 95% CI: 1.01-1.91, **Figure 1.5**).

TABLE 4 Results of the univariate logistic model-training set

| miRNAs | OR | 95% CI |
|---|---|---|
| hsa-miR-132-3p | 0.410 | 0.169; 0.991 |
| hsa-miR-23b-5p | 0.520 | 0.316; 0.856 |
| hsa-miR-31-3p | 0.566 | 0.351; 0.912 |
| hsa-miR-31-5p | 0.508 | 0.291; 0.887 |
| hsa-miR-330-3p | 0.501 | 0.251; 0.999 |
| hsa-miR-34b-3p | 0.673 | 0.474; 0.956 |
| hsa-miR-382-3p | 1.392 | 1.006; 1.925[a] |
| hsa-miR-548j-5p | 1.702 | 1.090; 2.658[a] |

Abbreviations: CI, confidence interval; OR, odds ratio.
[a]MicroRNAs retained its statistical significance (at 10%) also when normalized for the overall mean.

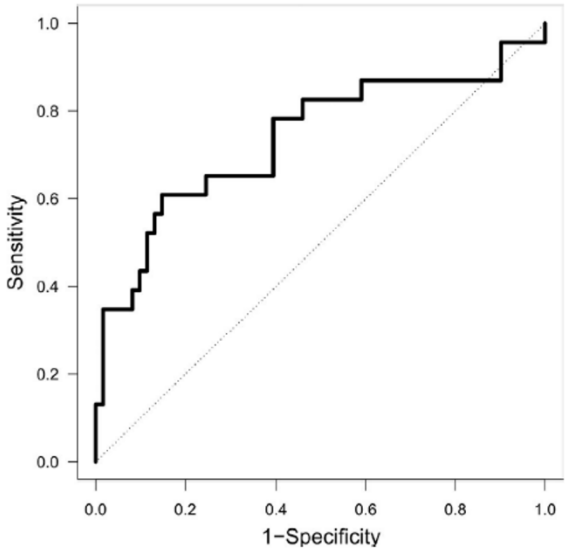


FIGURE 2 Receiver operating characteristic (ROC) curve of the final signature of miR-31-3p and miR-382-3p

***Figure 1.5**. MiRNAs significantly associated with pCR and predictive signature ROC curve. Adapted from Pizzamiglio S, Cosentino G et al, Cancer Med. 2022.*

Moreover, in the training set, 23 miRNAs were significantly associated with EFS by univariate analysis. By combining these miRNAs into a multivariate model, and after its confirmation in the testing set, a final signature of two miRNAs, miR-153-3p and miR-219a-5p, was selected as best model in the overall study cohort (hsa-miR-153-3p, HR 1.831, 95% CI: 1.34-2.50 and hsa-miR-219a-5p, HR 0.629, 95% CI: 0.50-0.78) [192]. For both signatures, no statistically significant relationships were observed between miRNAs expression level and the available clinico-pathological variables (i.e. ER status, lymph nodal status, tumor size and age). Finally, we also found two miRNAs (miR-215-5p and miR-30c-2-3p) with a statistically significant interaction term with pCR (p.interaction: 0.017 and 0.038, respectively), meaning that the expression analysis of only two miRNAs can predict a different outcome depending on whether the patient achieved pCR or not. This information is particularly useful to guide patient clinical management after neoadjuvant treatment.

Thus, our data support the idea that analysing miRNAs in primary tumor tissue could be a useful strategy to ameliorate the clinical management of HER2+ breast cancer patients treated with neoadjuvant trastuzumab.

This scenario could be improved even more considering that miRNAs, besides being biomarkers, could also be biologically active in mechanisms of resistance to trastuzumab.

Focus of my PhD project was, indeed, investigating the biological function of the two miRNAs identifying the predictive signature, miR-31-3p and miR-382-3p, exploring the

possibility to use them as therapeutic tools to restore responsiveness to trastuzumab in resistant patients.

Concerning miR-31-3p, the few studies found in the literature explore its potential as biomarker in anti-EGFR-treated metastatic colorectal cancer. Specifically, this miRNA was found significantly upmodulated in the progressive disease vs stable disease and in non-responders vs responders, negatively associated with progression-free survival and time to progression, thus resulting as promising predictive biomarker of selection for anti-EGFR antibodies [193–197]. Moreover, a more recent publication linked miR-31-3p to c-MYC, defined as key driver of resistance to EGFR inhibitors in the same tumor model [198]. Being EGFR another member of the ERBB family, the literature encouraged miR-31-3p investigation.

As for miR-382-3p, information gathered from the literature loosely pertains to the focus of this project. Nevertheless, miR-382-3p is described as an oncosuppressor in most models. For example, in ovarian cancer it inhibits metastasis-related gene Rho Associated Coiled-Coil Containing Protein Kinase 1 (ROCK1) and, in pancreatic and head and neck cancers, it was shown to inhibit PD-L1, reducing cancer progression [199–201]. In 2022, miR-382-3p downregulation was demonstrated to promote carcinogenesis of lung adenocarcinoma [202]. In breast cancer, miR-382-3p expression level was higher in serum from patients compared to healthy donors [203].

Overall, the literature published to these days concerning the two miRNAs is not exhaustive, especially in the breast cancer context. The data included in this PhD thesis

aims to fill this gap of knowledge and provide useful information for future research on HER2+ breast cancer malignancies.

# 2 AIM OF THE PROJECT

The anti-HER2 humanized monoclonal antibody trastuzumab is the standard-of-care treatment for HER2 positive breast cancers patients, but the percentage of resistant cases is high. Although researchers and clinicians have already tested other anti-HER2 agents, predicting benefit from trastuzumab monotherapy and design alternative strategies would prevent overtreatment and avoid unnecessary risks of side effects. Our group has recently identified a predictive signature of response to neoadjuvant trastuzumab composed of 2 miRNAs, miR-31-3p and miR-382-3p, in baseline tissue samples from the phase III NeoALTTO clinical trial. Evidence from the literature concerning the biological activity of the two miRNAs is currently limited.

Thus, this PhD project aimed at exploring whether miR-31-3p and miR-382-3p, besides being promising biomarkers, could also be functionally involved in the mechanism of resistance to trastuzumab in HER2+ breast cancer cells, with the ultimate goal of exploiting them in the clinics as targets or tools to restore response in resistant patients.

# 3 MATERIALS AND METHODS

## 3.1 Cellular biology

### 3.1.1 Human and murine breast cancer cell lines and treatments

Human SKBr3 and HCC1954, and murine N202.1A and TUBO HER2+ breast cancer cell lines were cultured in GIBCO RPMI 1610-medium (Thermo Fisher Scientific, Waltham MA, USA) with 10% fetal bovine serum (FBS) (Thermo Fisher Scientific); BT474 and MDAMB361 human luminal B cell lines were cultured in GIBCO DMEM with 10% FBS. All cells were maintained at 37 °C under 5% CO2. All human cell lines were purchased from ATCC (Manassas, Virginia, USA). The TUBO cell line derived from spontaneous lobular mammary tumour developed in BALB/c mice transgenic for the transforming rat neu gene [204]. For the blocking of HER2 signals, trastuzumab (Roche, Basel, Switzerland) was given to all the cell lines at a concentration of 10 μg/ml, while 250 nM and 0.9 μM of lapatinib (LC Laboratories, Woburn, MA, USA) were administered respectively to SKBr3 and HCC1954 cells. Since lapatinib is resuspended in dimethyl sulfoxide (DMSO), non-treated cells were given DMSO as control. 7.16.4 monoclonal antibody was, instead, used to target rat HER2 expressed in N202.1A and TUBO cell lines.

### 3.1.2 MiRNA, LNA and siRNA transfection

MiR-31-3p, miR-382-3p, miR-31-5p and miRNA mimic negative control (with random sequence that produce no identifiable effects), were purchased as Pre-miR precursor molecules (Thermo Fisher Scientific). Locked nucleic acid (LNA) against miR-31-3p and miR-31-5p and the corresponding control were purchased from QIAGEN (Hilden,

Germany). ERBIN silencer (Silencer® Select) was purchased at Thermo Fisher Scientific. HER2+ breast cancer cells were seeded in 6-well and, when at 80% confluency, transfected for 24 hours with 50 nM of oligos using Lipofectamine 2000 (Thermo Fisher Scientific) according to the manufacturer's instruction.

#### 3.1.3 3D assay

SKBr3 ($7x10^5$ cells/well) and HCC1954 ($5x10^5$ cells/well) cells were seeded on day 1 in the afternoon in 6-well plates and transfected after 24h with miRNA mimics or inhibitors (50 nM) for 24h. The cells were then transferred on Geltrex LDEV-Free, hESC-Qualified, Reduced Growth Factor Basement Membrane Matrix (Thermo Fisher Scientific) in a 96-wells plate ($5x10^4$ cells/well, 50 uL of Geltrex/well, 10 wells/condition) and treated (or not) with trastuzumab (10 ug/mL) the following morning. Images of the cells were captured at T0 and after 3, 5 and 7 days of treatment and, subsequently, quantified with ImageJ software. The quantification obtained was normalized on the initial number of cells seeded on the matrix.

### 3.2 Molecular biology

#### 3.2.1 RNA extraction and quantitative real-time PCR

The cells were harvested after Trypsin-EDTA (Corning, Corning, New York, USA) incubation and centrifuged at 1500 rpm for 5 minutes. Total RNA was isolated using QIAzolLysis Reagent (Qiagen) according to the manufacturer's instruction. The purified RNA was subjected to reverse transcription reactions using Taqman microRNA reverse trascription kit (Thermo Fisher Scientific) for miRNA analysis and High-Capacity RNA-to-

cDNA™ Kit (Thermo Fisher Scientific) for gene analysis. qRT-PCR was performed using TaqMan™ Fast Universal PCR Master Mix (2X), no AmpErase™ UNG (Thermo Fisher Scientific). RNU44 and GAPDH were used as internal control for miRNAs and genes respectively [205,206]. MiRNAs and genes' TaqMan™ probes were all purchased from Thermo Fisher Scientific (**Table 3.1**). All qRT-PCR assays were performed in StepONEPlus Real-Time PCR system (Thermo Fisher Scientific) and the relative expression was calculated using the comparative 2-ΔCt method.

***Table 3.1.*** *TaqMan™ probes*

| Probe | Catalog # | Assay ID |
|---|---|---|
| Hsa-miR-31-3p | 4427975 | 002113 |
| Hsa-miR-382-3p | 4427975 | 000572 |
| Hsa-miR-31-5p | 4427975 | 002279 |
| ERBB2 | 4448892 | Hs01007077_m1 |
| ERBIN | 4331182 | Hs01049966_m1 |
| TFAP2C | 4448892 | Hs00231476_m1 |
| SLC25A17 | 4448892 | Hs00697095_m1 |
| PRDM10 | 4448892 | Hs00999748_m1 |
| ASXL2 | 4448892 | Hs00827052_m1 |
| RAB10 | 4448892 | Hs00794658_m1 |
| LPIN1 | 4448892 | Hs00299515_m1 |
| PDPK1 | 4448892 | Hs00928927_m1 |

### 3.2.2 Luciferase reporter assay

3 x $10^5$ HEK293 cells were seeded in 12-well plates and co-transfected with 500 ng of Human ERBB2IP 3′UTR miRNA Target Clone in vector pEZX-MT06 (BioCat GmbH, Heidelberg, Germany) and 50 nM of miR-31-3p precursor or negative control, using Lipofectamine 3000 transfection reagent (Thermo Fisher Scientific). Cell lysates were collected 24h post transfection and Firefly and Renilla luciferase activities were quantified by Dual-Luciferase Reporter Assay System (Promega, Madison, WI, USA) on a GLOMAX

20/20 luminometer (Promega). Firefly luciferase was normalized on Renilla luciferase, and the reporter activity was finally expressed as relative activity between cells silenced for miR-31-3p and the corresponding control. Three biological replicates were performed.

### 3.2.3 RNA-seq

RNA-seq analysis was performed on four biological replicates of SKBr3 cells overexpressing miR-31-3p or control and treated or not with trastuzumab for 24h (2D assay protocol), and three biological replicates of HCC1954 cells transfected with either miR-31-3p or LNA-31-3p (or controls) and treated or not with trastuzumab for 24h. In collaboration with the Genomics Unit, RNA was isolated using miRNEasy Micro Kit (QIAGEN), following the manufacturer's instructions. mRNA seq library was prepared using QuantSeq 3‘mRNA-Seq Library Prep Kit for Illumina (Lexogen, Vienna, Austria), according to the manufacturer’s instruction. The libraries were then sequenced by collaborators at the Biology Department of the University of Padua and analyzed by bioinformaticians of the Genomic Unit. Pathway enrichment analysis was performed using the Enrichr software (https://maayanlab.cloud/Enrichr/) and considering the pathway significantly modulated based on The Molecular Signatures Database (MSigDB) hallmark gene set collection [207]. This analysis was performed considering genes with an absolute value of LogFC of at least 0.30. Ingenuity pathway analysis (IPA) was carried out using QIAGEN IPA application (https://digitalinsights.qiagen.com/products-overview/discovery-insights-portfolio/analysis-and-visualization/qiagen-ipa/) ; no gene LogFC cut off was applied for this analysis.

## 3.3 Biochemistry

### 3.3.1 Protein extraction and Western Blot analysis

Whole cell lysates and total exosomal proteins were prepared using NTG buffer (Tris HCl 50mM, NaCl 150mM, NaF 100mM, Sodiopirofosfato 10mM, Glicerolo 10%) with the addition of one cOmplete Mini protease inhibitor cocktail tablet (Roche), Triton X-100 (1:100; sigma-aldrich, St. Louis, Missouri, USA) and activated, at the time of use, with sodium orthovanadate 100 mM (pH 10). Bradford assay with CoomassiePlus Protein Assay Reagent (Thermo Fisher Scientific) was used to quantify the total proteins at Ultrospec 2100 pro (GE Healthcare Life Sciences, Marlborough, MA, USA) spectrophotometer. 30 μg total proteins were electrophoretically separated on NuPAGE 4-12% Bis-Tris Gel (Thermo Fisher Scientific). Western blot analyses were performed with primary antibodies listed in **Table 3.2**. The secondary antibodies were anti-mouse and anti-rabbit peroxidase-linked (1:5000 and 1:10 000, respectively, Merck). The signals were visualized by Pierce™ ECL and ECL Plus Western Blotting Substrate and SuperSignal™ West Pico PLUS Chemiluminescent Substrate and Femto Maximum intensity substrate (Thermo Fisher Scientific). The quantification of proteins bands was performed by Quantity One 1-D Analysis (Bio-Rad Laboratories, Hercules, CA, USA).

***Table 3.2*** *Primary antibodies*

| Target | Brand | ID | Dilution |
|---|---|---|---|
| Phospho-HER2/ErbB2 (Tyr1221/1222) (6B12) | Cell signaling technology* | #2243 | 1:1000 |
| HER2/ErbB2 (D8F12) XP | Cell signaling technology | #4290 | 1:1000 |
| Phospho-AKT (Ser473) (D9E) XP | Cell signaling technology | #4060 | 1:1000 |

| | | | |
|---|---|---|---|
| AKT (Pan) (C67E7) | Cell signaling technology | #4691 | 1:1000 |
| Phospho-p44/42 MAPK (Erk1/2) (Thr202/Tyr204) (D13.14.4E) XP | Cell signaling technology | #4370 | 1:1000 |
| p44/42 MAPK (Erk1/2) (137F5) | Cell signaling technology | #4695 | 1:1000 |
| Phospho-PDK1 (Ser241) (C49H2) | Cell signaling technology | #3438 | 1:1000 |
| PDK1 (D4Q4D) | Cell signaling technology | #13037 | 1:1000 |
| ERBIN | Abcam** | ab247081 | 1:1000 |
| Phospho-HER3/ErbB3 (Tyr1289) (D1B5) | Cell signaling technology | #2842 | 1:1000 |
| HER3/ErbB3 (D22C5) XP | Cell signaling technology | #12708 | 1:1000 |
| FOXO3A (7508) | Cell signaling technology | #2497 | 1:1000 |
| Beta-catenin (D10A8) XP | Cell signaling technology | #8480 | 1:1000 |
| p-CREB-1 (Ser 133) | ***Santa Cruz Biotechnology | sc-101663 | 1:200 |
| CREB-1 (C-21) | Santa Cruz Biotechnology | sc-186 | 1:200 |

(*Cell signaling technology, Danvers, MA, USA; **Abcam, Cambridge, UK; Santa Cruz Biotechnology, Dallas, TX, USA)

#### 3.3.2 Flow Cytometry Analyses

HER2 expression on SKBr3 and HCC1954 cell membranes was detected by Flow Cytometry using PE anti-human CD340 (erbB2/HER-2, 24D2 clone) antibody (BioLegend, San Diego, CA, USA).

### 3.4 *In vivo* experiments

Mice were maintained in laminar-flow rooms at constant temperature and humidity, with food and water given ad libitum. Experimental protocols used for animal studies were approved by the Ethics Committee for Animal Experimentation (OPBA) of Fondazione IRCCS Istituto Nazionale dei Tumori of Milan and by the Italian Ministry of Health in accordance with institutional guidelines (project # INT_10_2023).

### 3.4.1 SKBr3 and HCC1954 growth and treatment test (TEST experiment)

$2.5x10^6$ and $5x10^6$ SKBr3 cells were injected respectively into the right and left mammary fat pad of 8-week-old female SCID mice (n=10) (Charles Rivers Laboratories, Calco, Italy) and tumor growth was monitored for two weeks. $1.5x10^6$ HCC1954 cells were injected in the mammary fat pad of 8-week-old female SCID mice (4/5 mice per group). At palpable tumors, the mice were treated twice a week with either 6, 10 or 20 mg/kg of trastuzumab, administered via intra peritoneal injection (i.p.), for 2.5 weeks. Every 3-4 days, the tumor volume was calculated as $0.5 \times d1^2 \times d2$, where d1 and d2 are the smaller and larger diameters. Statistical significance was analyzed by the two-tailed Student's t-test and a P-value of less than 0.05 was considered significant.

### 3.4.2 COMBO and SINGLE experiments

$1.5x10^6$ HCC1954 cells were injected in the mammary fat pad of 8-week-old female SCID mice (5 mice per group). At palpable tumors, the mice were treated twice a week with 10mg/kg, of trastuzumab, administered via intra peritoneal injection (i.p.), for 3 weeks.

LNA-31-3p, miR-382-3p, or controls were given peritumor five times (20 ug/injection), two injections per week. Cel-miR-67 was used as control oligo for miR-382-3p due to its minimal sequence homology with mouse, rat, and human miRNAs ([208]) For the SINGLE/2 experiment, mice received two additional LNA-31-3p or control injections before starting trastuzumab administration.

### 3.4.3 Tumor sample homogenization

To perform miR-31-3p expression analysis, the frozen tumor tissues were homogenized using RETSCH MM 200 Model Mixer Mill (Thermo Fisher Scientific). Briefly, tumor samples stored at -80°C were first transferred in liquid nitrogen, then cut into smaller fragments, and then transferred into 1.5 mL pre-cooled vials containing a 2.4 mm metal beads. Qiazol was added for RNA extraction. The vials were inserted in pre-cooled plastic tubes and loaded into the mixer mill where they were shaken two times for 2 min (30 movements/s). The samples were then centrifuged at 1500 rpm for 5 min at 4 °C and the supernatants collected in new tubes.

## 3.5 *In silico* analyses

### 3.5.1 Correlation analysis in the NeoALTTO study

A first correlation analysis between the predictive signature composed of the two miRNAs (miR-31-3p and miR-382-3p) and the expression levels of genes obtained from the gene profile of the NeoALTTO series, was performed. The resulting list of genes correlated with the signature was, consequently, matched with the lists of miR-31-3p and miR-382-3p putative targets predicted by at least three online tools, specifically miRwalk (http://mirwalk.umm.uni-heidelberg.de/), TargetScan (https://www.targetscan.org/vert_72/), and miRTarBase (https://mirtarbase.cuhk.edu.cn/~miRTarBase/miRTarBase_2022/php/index.php) [209–211]. Next, a second correlation analysis was performed between the selected putative targets and the expression of the two miRNAs in the NeoALTTO series. The most

promising genes, in terms of statistical significance of the correlation and biological role, were analyzed by qRT-PCR in miRNA-overexpressing cell line models. A third correlation analysis was carried out between the expression levels of the two miRNAs, considered independently, and the gene expression performed on the NeoALTTO series. The strength of the association between expression of genes and miRNAs of interest was assessed by the Spearman correlation coefficient (rs) and its 95% confidence interval (95% CI). A value of Spearman correlation coefficient > 0.4 in absolute value was considered as relevant for evaluate the relationship in subsequent analysis. Finally, correlation analysis between miRNA expression and both the immune infiltrate in the NeoALTTO study and 60 immune-related metagenes was performed by considering Spearman Corr. coeff. >0.30 in absolute value. In particular, 28 immuno signature by Charoentong et al., 13 by Safonov et al., 14 tumor-infiltrating immune cells population by CIBERSORT and immune-related metagenes 5 by Rody et al, were used in this analysis [212–215].

### 3.6 Statistical analyses

Analyses of *in vitro* and *in vivo* experiments were performed using GraphPad Prism 5 (GraphPad software Inc, CA, USA). Differences between groups were determined by two-tailed unpaired Student's t-test if datasets passed Shapiro-Wilk normality test, otherwise Mann-Whitney non-parametric test was applied. $p<0.05$ was considered statistically significant.

# 4 RESULTS

## 4.1 MiR-31-3p increases HER2 level and activation in non-treated and trastuzumab-treated SKBr3 cells

The main aim of my PhD project was investigating the biological meaning of the differential expression of two miRNAs in association with responsiveness to trastuzumab in HER2+ breast cancer patients. In particular, my research group has recently identified a two-miRNA signature, comprising miR-31-3p and miR-382-3p, associated to pCR in the trastuzumab arm of the NeoALTTO study, as thoroughly described in Chapter 1.5 of the introduction section. Thus, as first step of my research plan, I evaluated the expression of the two miRNAs in four HER2+ breast cancer cell lines, specifically SKBr3, BT474, MDAMB361 and HCC1954. According to the literature, the first two cell lines are described as HER2-addicted, thus sensitive to HER2-inhibiting drugs as trastuzumab. On the contrary, the other two models are resistant (MDAMB361) or only partially sensitive (HCC1954) [216].

**Figure 4.1A-B** illustrates miRNA basal expression in HER2+ breast cancer cell lines, evaluated by qRT-PCR. Both miRNAs displayed a wide range of expression among the different models, a feature that I exploited to select the most appropriate cell line for miRNA modulation. Indeed, I selected SKBr3 as "sensitive" model and HCC1954 as "resistant" model, on the basis of both their sensitivity to HER2-targeted therapy and the basal expression of the two miRNAs.

In order to assess the biological effect of miR-31-3p and miR-382-3p upmodulation upon treatment with trastuzumab *in vitro*, I used two different approaches:

1. 2D assay: Evaluation of HER2 signaling pathway modulation, by western blot assay
2. 3D assay: Evaluation of cell viability in a 3D setting.

Starting from the 2D assay, in order to design the protocol, I had to consider that each cell line has a different growth rate and attachment speed to cell culture plastics; moreover, HER2 signalling is influenced by cell confluence. Accordingly, I first defined the appropriate number of cells to have approximately the same confluence (60-70%) at the time of treatment for both cell lines. Subsequently, I tested three different time points (1h, 9h and 24h). Besides HER2, I checked phosphorylated and total protein levels of AKT and MAPK (ERK1/2), which are the two main downstream effectors of HER2 signaling. Usually, HER2 pathway inhibition by anti-HER2 agents is a fast event. In SKBr3 cells, which are HER2-addicted, the downmodulation is still maintained at 24h, whereas, at the same point, in the non-addicted HCC1954 cells HER2 activation is already restored and even slightly higher compared to the non-treated counterpart (**Figure 4.1C**).

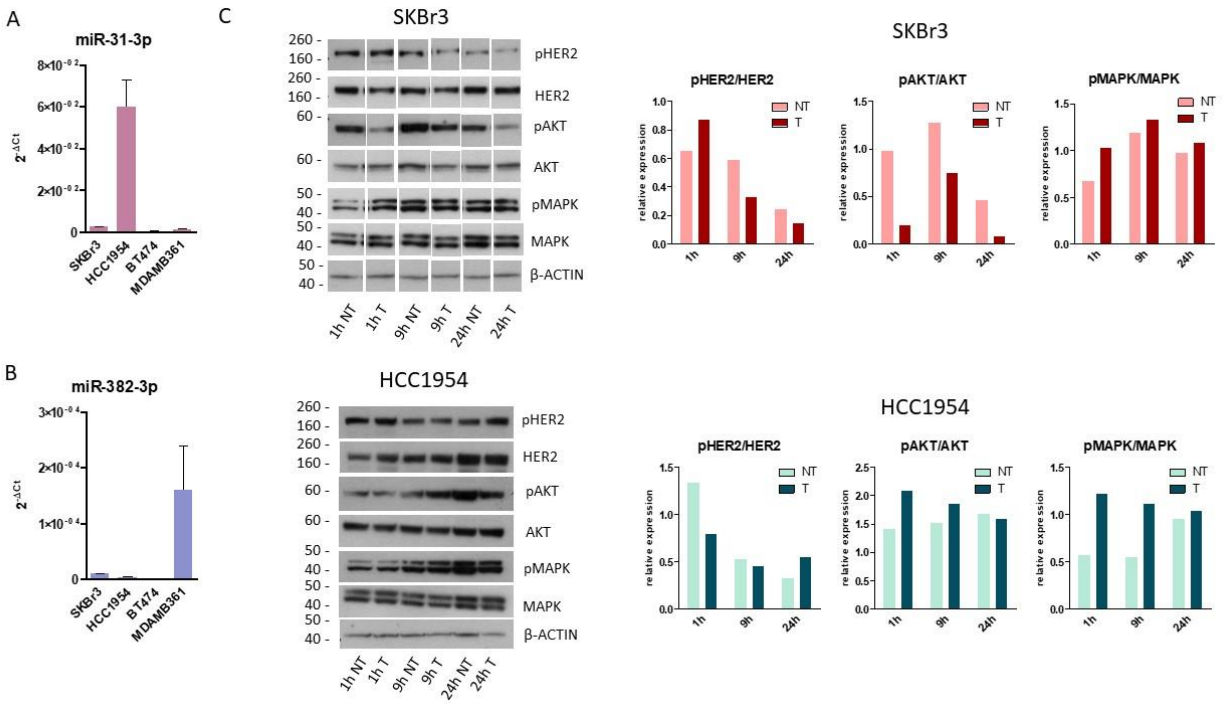


***Figure 4.1.*** *qRT-PCR analysis evaluating miR-31-3p (A) and miR-382-3p (B) basal expression in SKBr3, HCC1954, BT474 and MDAMB361 HER2+ breast cancer cell lines. The bar plots show mean expression values of three replicates (±SD). Western blot for total and phosphorylated (p) protein levels of HER2, AKT and MAPK in SKBr3 and HCC1954 cells treated or not with trastuzumab for 1h, 9h or 24h. Quantification was done normalizing on total protein signal. β-ACTIN signal was used as loading control. Images and quantifications are representative of three biological replicates (C).*

Since my goal was assessing whether miR-31-3p and miR-382-3p induce a change in cell response to trastuzumab, according to the previous analysis I concluded that the more appropriate time point was 24h. Concerning trastuzumab concentration, according to previous experience with the same HER2+ breast cancer cell line models acquired over time in my laboratory, I was advised to use 10 ug/mL.

Given that high miR-31-3p levels negatively correlated with pCR in the NeoALTTO study, I decided to overexpress it in SKBr3 cells to appreciate a possible gain of resistance to trastuzumab; conversely, as high miR-382-3p levels positively correlated with pCR, this miRNA was overexpressed in HCC1954 cells.

For this experiment SKBr3 and HCC1954 cells were seeded on day 1 in 6-well plates and, the following day, the cells were transfected with miRNA mimics (50 nM) for 24h. Then, the cells were treated (or not) with trastuzumab (10 ug/mL). After other 24h the cells were collected for RNA and protein isolation (**Figure 4.2**).

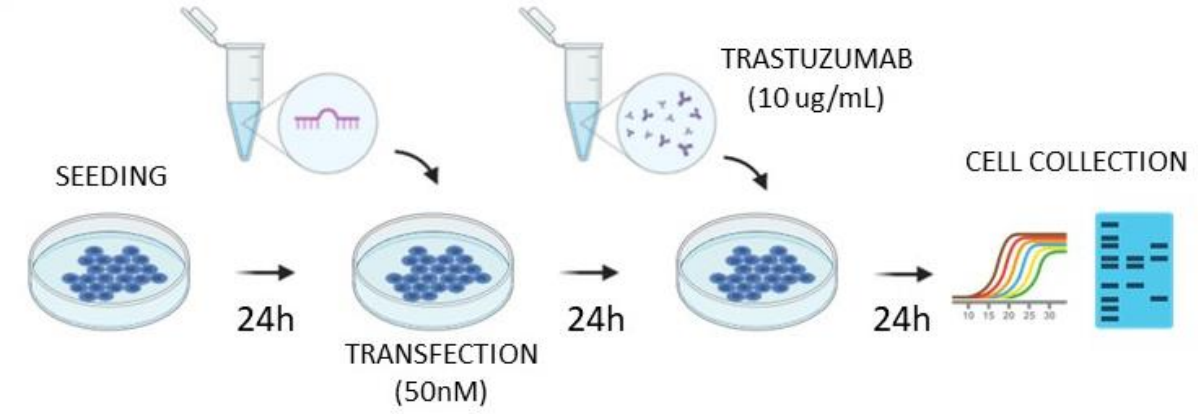


***Figure 4.2.*** *2D assay protocol (Created with BioRender.com).*

Expression levels upon transfection are reported in **Figure 4.3A** and **4.3C** for miR-31-3p/SKBr3 and miR-382-3p/HCC1954, respectively. **Figure 4.3B** and **Figure 4.3D** show a representative western blot analysis, comparing the expression of HER2, AKT, MAPK and their phosphorylated forms in SKBr3 (4B) and HCC1954 (4D) cells, respectively transfected with miR-31-3p and miR-382-3p, or with miRNA mimic negative control (miR-NEG) with random sequence that produce no identifiable effects, and treated or not with trastuzumab for 24h. In SKBr3 cells, I detected higher levels of pHER2 and HER2 in miR-31-3p overexpressing cells vs their controls, regardless of trastuzumab treatment. However, this increase is paralleled by a higher activation of MAPK only in the treated condition. AKT, on the contrary, is downmodulated upon miR-31-3p upregulation in both non-treated and

treated cells. Thus, these results suggest that miR-31-3p upregulation of HER2 activity only partially induces a higher activation of the downstream pathways.

Concerning HCC1954 cells, miR-382-3p overexpression slightly reduced pHER2 but this modulation was not mirrored downstream. This result may not be surprising, being HCC1954 a HER2 non-addicted cell line. Indeed, AKT levels did not change upon miRNA transfection, while MAPK activity increased in both non-treated and treated miR-382-3p overexpressing cells, indicating a possible counteractive mechanism to miRNA action (**Figure 4.3D**).

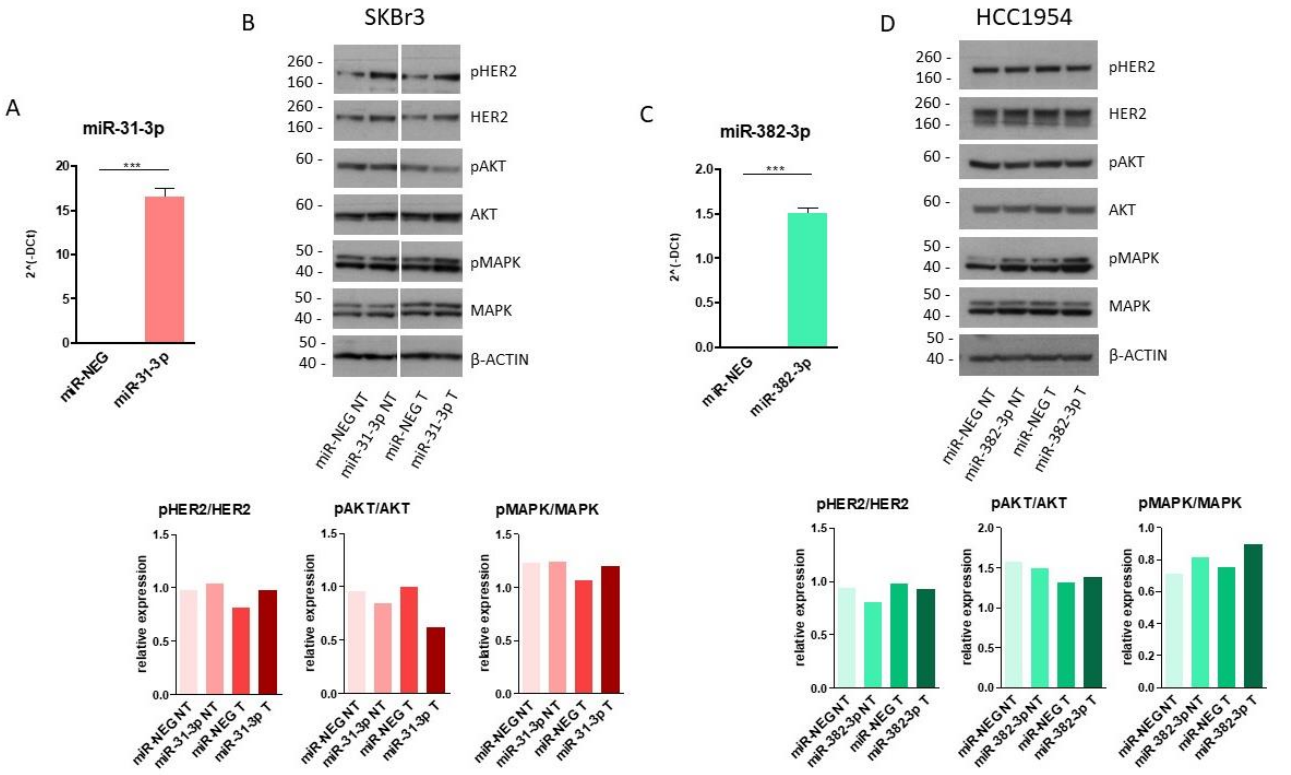


***Figure 4.3**. qRT-PCR analysis evaluating miR-31-3p expression level upon miRNA mimic transfection in SKBr3 cells (A) and miR-382-3p in HCC1954 (C) (mean expression of three replicates ±SD, ***p<0.001). Western blot analysis evaluating HER2, AKT, MAPK and their phosphorylated (p) forms in SKBR3 cells transfected or not with miR-31-3p and treated or not with trastuzumab (B), and in HCC1954 cells transfected or not with miR-382-3p and treated or not with trastuzumab (D). β-ACTIN signal was used as loading control. The bar plots below the western blots quantify the expression of the activated forms normalized on their respective total protein. Images and quantifications are representative of three biological replicates.*

### 4.2 MiR-31-3p inhibition alone or in combination with miR-382-3p overexpression reduces HCC1954 viability upon trastuzumab treatment

Since miR-382-3p did not have a significant impact on HER2 downstream signaling, I decided to change strategy and test the effect of the combination (COMBO) of a miR-31-3p inhibitor (LNA-31-3p) and miR-382-3p up-modulation on trastuzumab sensitivity of HCC1954 cells. LNA-31-3p transfection efficiency was assessed by analyzing miR-31-3p levels (**Figure 4.4A**). **Figure 4.4B** shows, instead, miR-382-3p transfection efficiency.

I conducted the 2D assay to evaluate whether the COMBO modulates HER2 signaling pathway. I also surprisingly observed in the 2D assay a reduced viability of trastuzumab-treated HCC1954 cells transfected with either LNA-31-3p alone or in combination with miR-382-3p. This observation was confirmed by cell count: there was a significant decrease of cell number in the two cited experimental conditions, compared to negative treated control (NEG T) (**Figure 4.4B**).

The related western blot analysis was instead puzzling due to the modulation of HER2 pathway. Indeed, in treated cells transfected with LNA-31-3p, the pathway was more activated then in the controls. One theory could be that, given the cell count result, the surviving cells are trying to upregulate HER2 pathway, especially through MAPK activity.

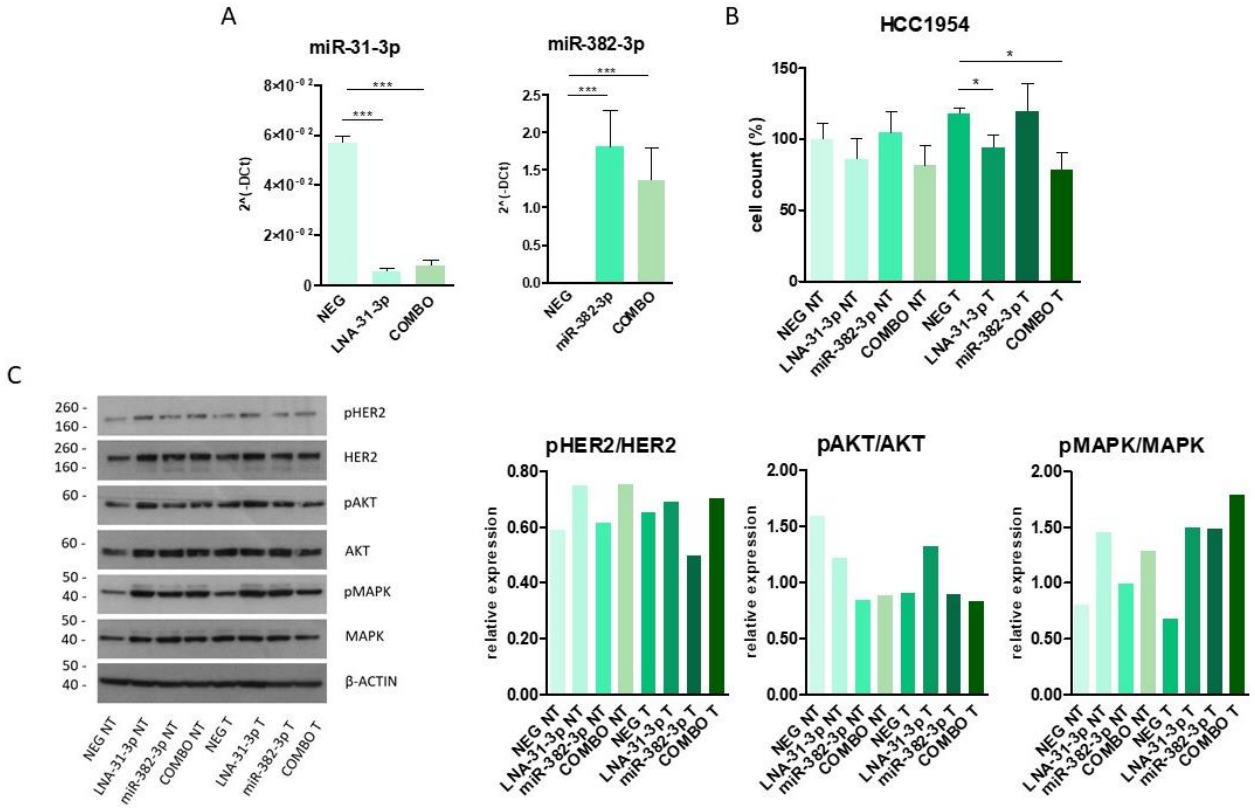


***Figure 4.4.*** *qRT-PCR analysis evaluating miR-31-3p expression level upon inhibition with LNA-31-3p and miR-382-3p expression level upon miRNA mimic transfection in HCC1954 cells (A, ***p<0.001). Cell counts shown as mean percentage of three biological replicates (±SEM, *p<0.05) calculated considering the non-treated negative control mean as 100% (B). Western blot analysis evaluating HER2, AKT, MAPK and their phosphorylated (p) forms in HCC1954 cells transfected or not with LNA-31-3p, miR-382-3p or the combination of the two (COMBO) and treated or not with trastuzumab. β-ACTIN signal was used as loading control. Images and relative quantifications are representative of three biological replicates; the expression of the activated forms is normalized on the respective total protein expression and quantified in the bar plots on the right (C).*

Following the suggestion of my colleagues, I assessed HER2 pathway and treatment response in SKBr3 and HCC1954 upon miR-31-3p modulation in concomitance with administration of lapatinib, another anti-HER2 drug, instead of trastuzumab. The main reason supporting this strategy is the possibility to better appreciate miRNA effect in 2D assays due to different mechanism of action of the two compounds. Indeed, even though both drugs downmodulate HER2 pathway, they bind two different domains of the

receptor, one extracellular (trastuzumab-domain IV), the other intracellular (lapatinib-tyrosine-kinase domain), which could imply alternative resistance mechanisms, which are the focus of my thesis. Moreover, lapatinib, differently from trastuzumab, is known to affect cell viability in 2D. Once I established IC50 concentrations of lapatinib for both cell lines at 72h (timing suggested by colleagues to evaluate cell response), I repeated all the 2D assays described before, adjusting the initial number of seeded cell to the longer timing of treatment (72h instead of 24h). The results obtained confirmed what I already established with the experiments with trastuzumab in SKBr3 cells (see Figure 4.3B). Indeed, the upregulation of miR-31-3p increased HER2 activation. Instead, I was able to detect, for the first time, a reduction of pHER2 levels by western blot analysis upon miR-31-3p inhibition in treated HCC1954 cells, accompanied by a reduced cell viability already seen upon trastuzumab treatment (**Figure 4.5B**). It is possible that, in the first 24h upon treatment, HCC1954 cells tried to counteract LNA-31-3p onco-suppressive activity, but at 72h the combination of miRNA inhibition and HER2 targeting overcame cell resistance.

Given the results obtained at 72h in the lapatinib experiment, I wondered whether I had never been able to appreciate HER2 downmodulation by LNA-31-3p in HCC1954 cells due to a too short exposure time to trastuzumab. Thus, I repeated the 2D assay with trastuzumab, modifying the protocol accordingly. Firstly, in this setting, I appreciated that overexpression of miR-31-3p is able to increase pHER2 and HER2 levels also in HCC1954 cells, despite the high basal levels of the miRNA in this cell line (**Figure 4.5A-B**). Moreover, as hypothesized, HCC1954 cells transfected with LNA-31-3p and treated or not with trastuzumab at 72h showed a reduced expression of pHER2 and total HER2 (**Figure**

**4.5C**). In conclusion, inhibition of miR-31-3p efficiently reduces HER2 activation only after 72h of trastuzumab treatment, even though its biological effect on cell viability is already evident at 24h, even in a 2D assay. I could speculate that miR-31-3p has a broader range of action than the HER2 signaling and affects HCC1954 response to trastuzumab by modulating alternative pathways.

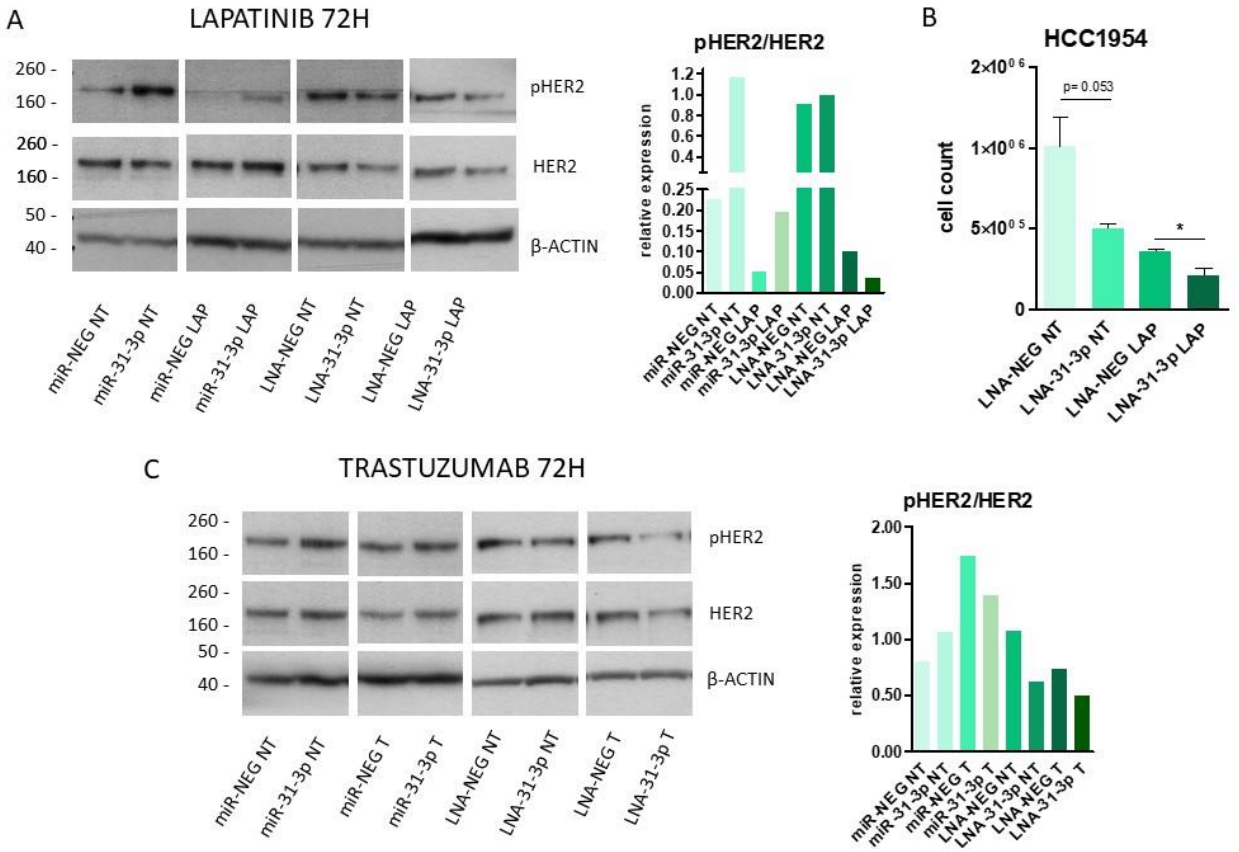


***Figure 4.5.*** *Western blot analysis showing pHER2 and HER2 expression in HCC1954 cell transfected or not with miR-31-3p or LNA-31-3p and treated or not with lapatinib (A) or trastuzumab (C) for 72h. Images and quantifications are representative of three biological replicates, and the expression of the activated form is normalized on the total protein and quantified in the bar plots on the right. β-ACTIN signal was used as loading control. HCC1954 mean cell counts (three biological replicates) upon LNA-31-3p transfection alone or combined with trastuzumab treatment (B, ±SEM, *p<0.05).*

### 4.3 MiR-31-3p modulation affects SKBr3 and HCC1954 3D cell growth and responsiveness to trastuzumab

According to the literature and to the experience of my colleagues, cell viability upon treatment with trastuzumab has to be assessed in a 3D setting [217]. For the seeding and transfection steps, I set the same experimental conditions as in the 2D assay. Then, 24h later, the cells were transferred on Geltrex matrix in the afternoon. The morning after, images of the cells were captured at T0, followed by treatment with trastuzumab (10 ug/mL). In particular, trastuzumab-containing fresh medium (50 uL/well) was added to the already present medium (100 uL/well) aliquoted at the time of cell seeding on the matrix; thus, since the final total volume was 150 uL, trastuzumab in the fresh medium had a concentration of 30 ug/mL. Cell growth was then monitored for 7 days. Images of the cells were captured again after 3, 5 and 7 days of treatment and, subsequently, quantified with ImageJ software. The quantification obtained was normalized on the initial number of cells seeded on the matrix (T0 quantifications) (**Figure 4.6**).

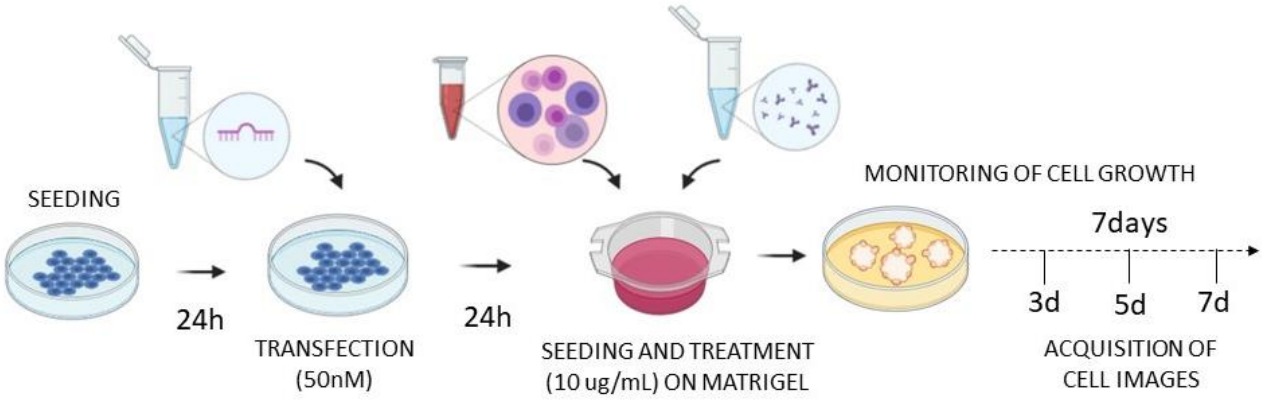


***Figure 4.6.*** *3D assay protocol (Created with BioRender.com).*

**Figure 4.7** displays the results of the 3D assay. Representative images were selected to show cell viability of SKBr3 and HCC1954 cells in each experimental condition. MiR-31-3p overexpression in SKBr3 cells was able to significantly increase cell number in comparison with control cells transfected with miR-NEG. This effect is consistent with the HER2 upmodulation observed in the 2D setting, suggesting a possible involvement of this miRNA in proliferation pathways, sustained by a persistent HER2 signaling (**Figure 4.7A**). In addition, whereas a significant decrease of cell growth upon 5 days of treatment with trastuzumab was observed as expected in control cells, miR-31-3p overexpression was able to partially counteract the effect of the drug. Indeed, cell growth in miR-31-3p-overexpressing SKBr3 cells is significantly higher than control cells also in treatment condition. Trastuzumab and miR-382-3p combination, instead, did not affect cell number (**Figure 4.7B**). Since LNA-31-3p alone was able to increase HCC1954 cell response to trastuzumab, even in a 2D setting, I decided to test its effect also by 3D assay. This analysis confirmed that inhibiting miR-31-3p significantly reduces cell viability in non-treated and treated cells compared to controls, also in a 3D setting, regardless of trastuzumab administration (**Figure 4.7C**).

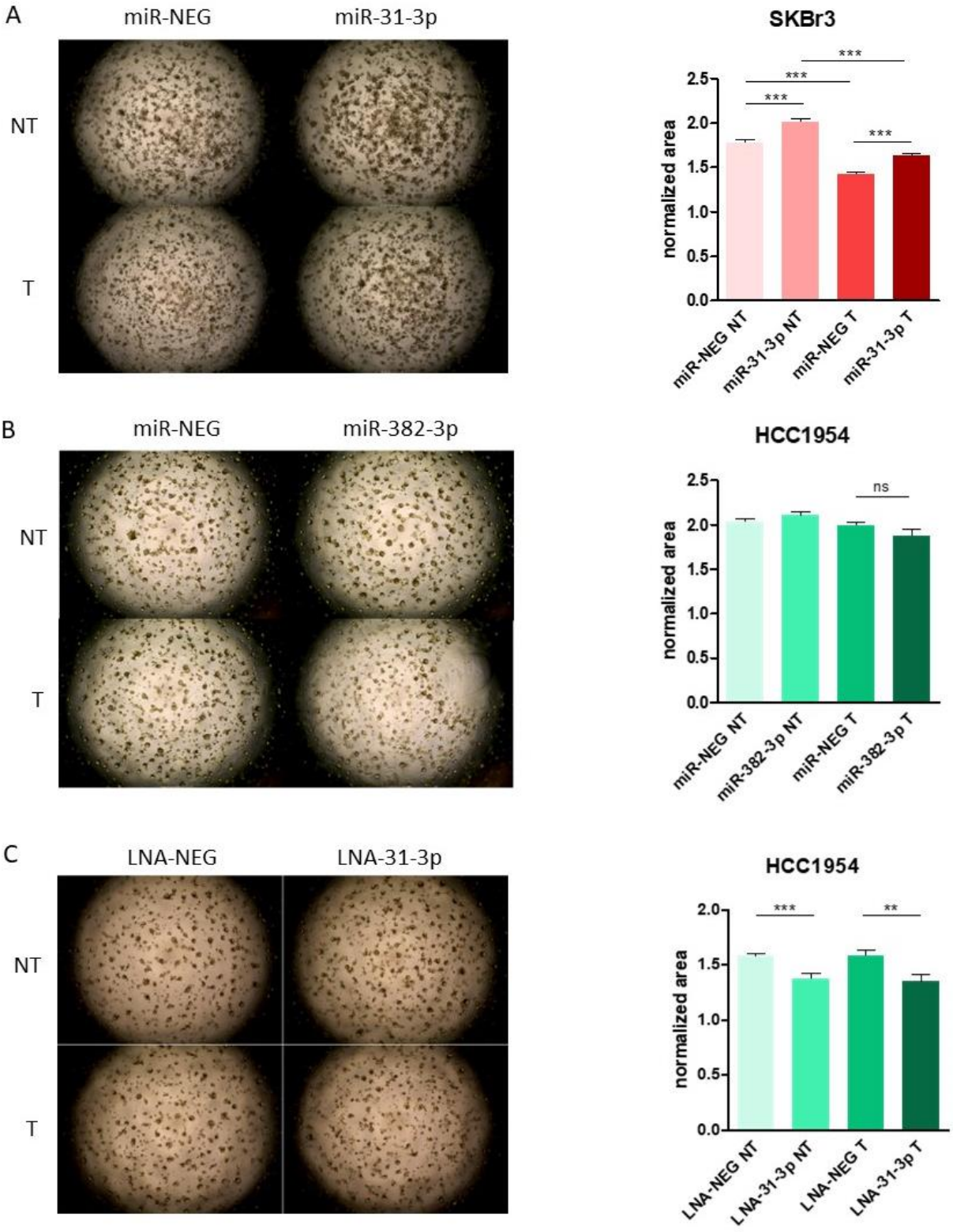


***Figure 4.7**. 3D assays evaluating cell growth and viability of SKBr3 overexpressing or not miR-31-3p and treated or not with trastuzumab (A), of HCC1954 overexpressing miR-382-3p (B) or transfected with LNA-31-3p (C) and treated or not with trastuzumab, compared to controls. Images are representative of three biological replicates. The bar plots show the mean normalized area occupied by cell colonies at day 5 of treatment (± SEM, **p<0.01, ***p<0.001, ns=not significative).*

### 4.4 MiR-31-5p overexpressing SKBr3 cells show a similar in vitro behavior than miR-31-3p overexpressing cells

*MIR31*, miR-31-3p gene on human chromosome 9 (9p21.3), encodes for another mature miRNA, miR-31-5p, the miR-31-3p complementary strand, which was found as well negatively associated with pCR in the NeoALTTO series [192]. Indeed, the miRNA predictive signature obtained from analysis of NeoALTTO series, originally included miR-31-5p together with miR-31-3p and miR-382-3p; it was then reduced to a two-miRNA signature because it retained the same predictive power. The 5p strand of miR-31 is more expressed in tissues than the 3p and it is known to act as an oncogene [195]. Due to these intriguing reasons, I decided to explore also the effect of miR-31-5p modulation, repeating the 2D and 3D assays. First, I checked the miRNA basal expression in a panel of HER2+ breast cancer cell lines. All the experiments were performed keeping miR-31-3p as control in order to compare the results obtained with the two strands. MiR-31-5p is indeed almost 10 times more expressed than its "brother" strand but has the same trend among the different cell lines, being HCC1954 cells the higher expressing model (**Figure 4.8A**). Mirroring what I previously did with miR-31-3p, I transfected miR-31-5p into SKBr3 cells. Western Blot analysis suggested that miR-31-5p has similar but not equal impact on the HER2 signaling pathway. Indeed, as shown in **Figure 4.8B**, miR-31-5p is able to increase pHER2 and HER2 levels in non-treated cells, but this effect was lost after 24h of treatment with trastuzumab. Given this result, I presumed the 3D assay would mirror such HER2 modulation. Instead, miR-31-5p overexpression increases the number of both untreated and trastuzumab treated SKBr3 cells grown in 3D (**Figure 4.8C**). A possible explanation

could have been that the 5p strand "behaves" differently in 2D and 3D settings; a second hypothesis was that miR-31-5p needed more time to restore HER2 expression and activity upon trastuzumab treatment. Thus, I decided to repeat the 2D assay, collecting the cells after 48h of treatment. **Figure 4.8D** shows the western blot that supports the second hypothesis: indeed, whereas at 24 h only miR-31-3p is able to sustain HER2 activation, at 48h both miRNAs counteract trastuzumab-induce p-HER2 downregulation. In conclusion, both miRNAs encoded by *MIR31* are able to increase HER2 activity and the number of non-treated and treated SKBr3 cells in the 3D setting, but the different timing may reflect an alternative or only partially overlapping molecular mechanism.

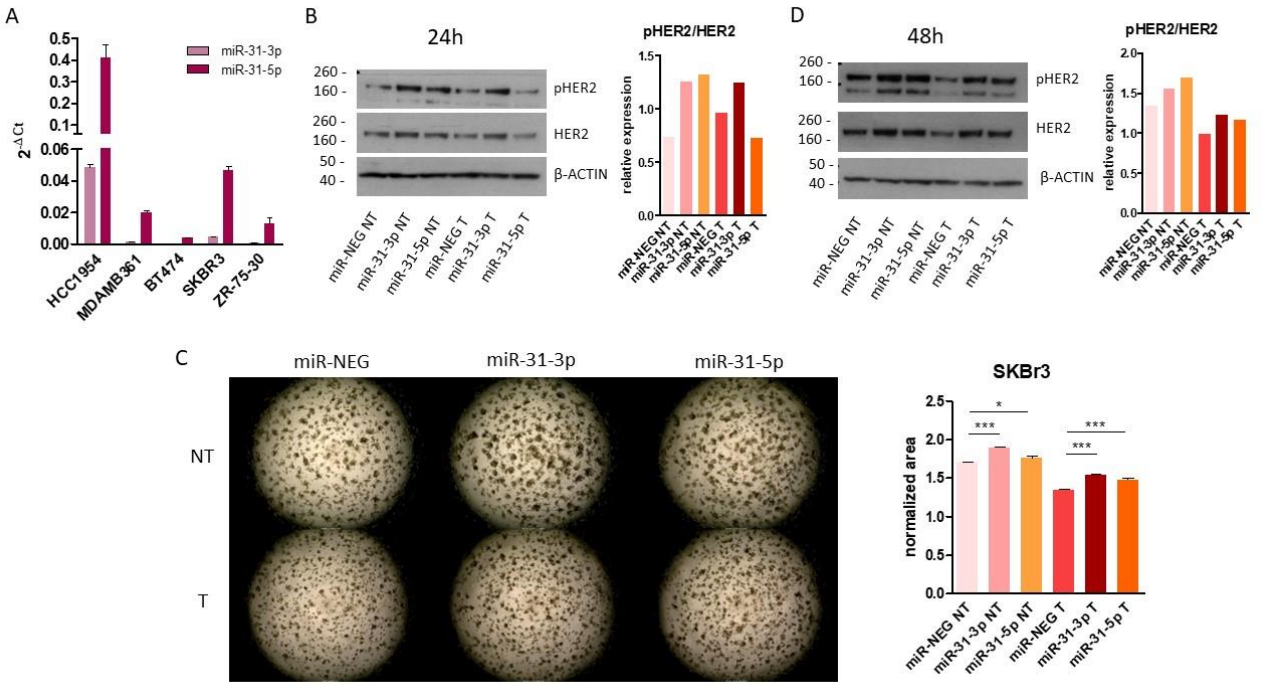


***Figure 4.8**. qRT-PCR evaluating miR-31-3p and miR-31-5p expression in panel of HER2+ breast cancer cell lines (A). Western blot analysis showing pHER2 and HER2 expression in SKBr3 cells transfected or not with miR-31-3p or miR-31-5p and treated or not with trastuzumab for 24h (B) or 48h (D). Images and quantifications are representative of three biological replicates, and the expression of the activated form is normalized on the total protein and quantified in the bar plots on the right. β-ACTIN signal was used as loading control. 3D assays evaluating cell growth and viability of SKBr3 overexpressing or not miR-31-3p or miR-31-5p and treated or not with trastuzumab. Images are representative of three biological replicates.*

*The bar plot shows the mean normalized area occupied by cell colonies at day 5 of treatment (± SEM, *p<0.05, ***p<0.001).*

## 4.5 Inhibition of miR-31-3p reduces HCC1954 tumor growth and increases responsiveness to trastuzumab in vivo

### 4.5.1 HER2-addicted models: SKBr3, N202.1A, TUBO

Having obtained encouraging results by modulating miR-31-3p in the HER2-addicted cell line SKBr3 and aiming at translating *in vitro* analysis to an *in vivo* setting, SKBr3 cell growth was tested in SCID mice. Unfortunately, the cells did not form tumors after injection. As alternative strategy, we decided to switch to a murine cell line, able to efficiently grow in the immune-competent FVB murine strain. I thus tested the rat HER2 expressing mouse mammary carcinoma cell line N202.1A, repeating 2D and 3D experiments, focusing on miR-31-3p. As substitute for trastuzumab, I used 7.16.4 monoclonal antibody, which binds rat HER2. As shown in **Figure 4.9A**, in this model we could detect a similar pHER2 upmodulation upon miR-31-3p overexpression in treated cells as seen in the SKBr3 model. However, the result of the 3D assay was not consistent with what we observed with the human cell line since cell growth on the matrix was comparable in all the experimental conditions (**Figure 4.9B**). The other murine model I tested, the TUBO cell line, instead, showed an increased HER2 activation in non-treated miR-31-3p overexpressing cells compared to control; however, a too strong receptor inhibition upon 7.16.4 treatment did not allow any evaluation of expression differences between miRNA-transfected cells and control (**Figure 4.9C**). Considering the 3D assay, miR-31-3p combination with anti-HER2 treatment reduced cell number, rather than

increasing it as suggested by western blot analysis, when compared to its control (**Figure 4.9D**). These results suggest that miR-31-3p effect on TUBO cell line do not recapitulate data observed in SKBr3 human cell line. In conclusion, none of the tested HER2-addicted models revealed to be suitable to assess miR-31-3p effect *in vivo*.

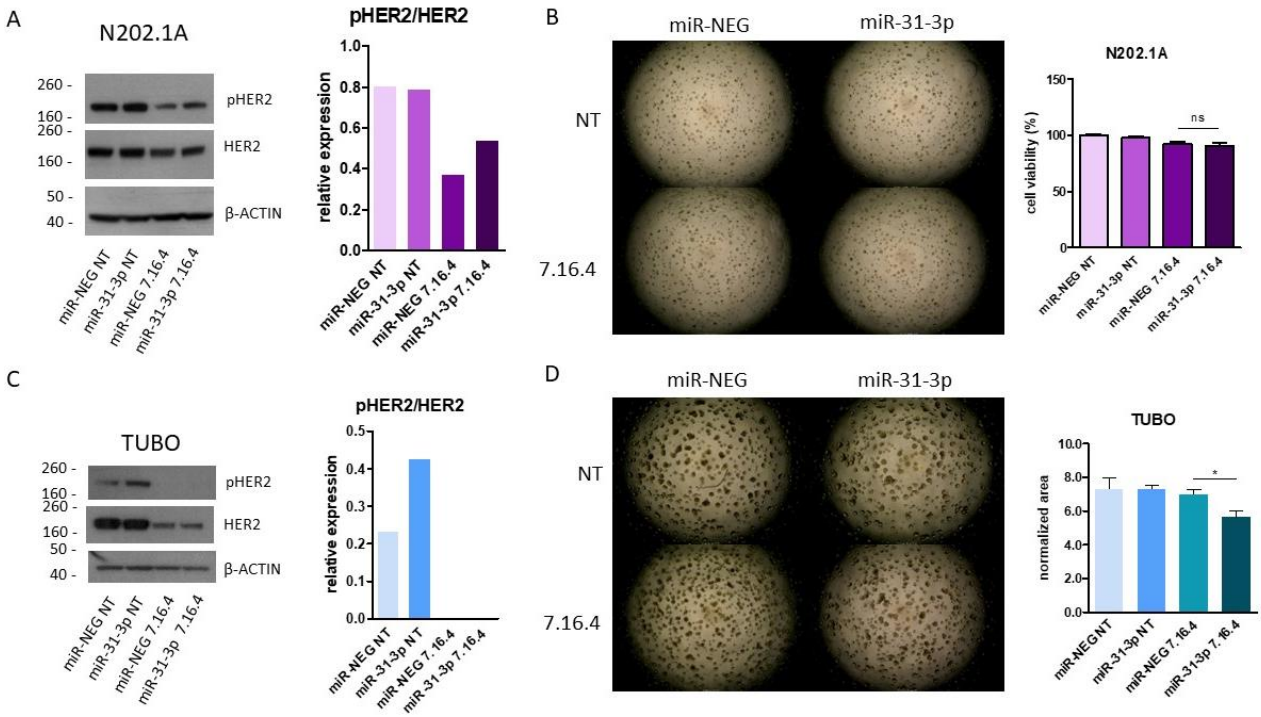


***Figure 4.9**. Western blot analysis showing pHER2 and HER2 expression in N202.1A (A) or TUBO (C) cells transfected or not with miR-31-3p and treated or not with 7.16.4 antibody. Images and quantification are representative, the bar blot shows quantification of pHER2 signal normalized on total protein. β-ACTIN signal was used as loading control. 3D assays evaluating cell growth and viability of N202.1A (B) or TUBO (D) cells overexpressing miR-31-3p or control and treated or not with 7.16.4 antibody. Images are representative of three biological replicates. The bar plot shows the mean normalized area (as percentage for N202.1A, miR-NEG NT as 100%) occupied by cell colonies at day 5 of treatment (± SEM, ns=not significative, *p<0.05).*

### 4.5.2 HER2- non addicted model: HCC1954

As described in the previous paragraph, the HER2-addicted models were not suitable for *in vivo* experiments. Consequently, encouraged by the results obtained by inhibiting miR-31-3p in both 2D and 3D assays, HCC1954 cell growth and sensitivity to trastuzumab were

tested *in vivo* in SCID mice, upon injection in the mammary fat pad (TEST experiment). These and the following in vivo experiments were performed with the help of my colleagues. At palpable tumors, mice were treated with 6, 10 or 20 mg/kg trastuzumab five times, two times per week. As expected, we did not detect any response to the treatment, even at the highest concentration. (**Figure 4.10A**). I checked HER2 tumor expression, the loss of which could have explained the lack of response to trastuzumab. However, both non-treated and trastuzumab-treated (10mg/kg treated group only) tumors did express HER2 at the end of the experiment (**Figure 4.10B**).

The HER2+ breast cancer cell line HCC1954 thus proved to be the most suitable one for *in vivo* experiments, in order to appreciate a gain of sensibility by modulating miRNA expression. We concomitantly delivered miR-31-3p inhibitor (LNA) and miR-382-3p mimic to evaluate a possible increase of response to trastuzumab (COMBO exp). Cel-miR-67 was used as control oligo for miR-382-3p (**Figure 4.10C**). In details, LNA-31-3p, miR-382-3p or controls were given peritumor five times (20 ug/injection), two injections per week. Each oligo delivery was followed by systemic treatment with trastuzumab (i.v., 10 mg/kg) the day after. Tumor growth was monitored every 3-4 days. In parallel we also performed a pilot *in vivo* study to test the effect of LNA-31-3p alone (SINGLE exp) (**Figure 4.10D**). This decision was supported by both 2D and 3D assays but, more importantly, it took into consideration the possible use of the inhibitor as therapeutic tool. Indeed, it would be more feasible to propose the delivery of a single agent than a combo, thus reducing potential off targets effects, and of a miRNA inhibitor rather than a mimic, since it does not necessarily require a carrier. In both experiments, we detected no statistically

significant differences in tumor volumes between the experimental groups (**Figures 4.10C-D**).

Considering the *in vivo* data described in the previous paragraph, we repeated the SINGLE experiment adjusting the protocol to better appreciate the effect of miR-31-3p inhibition alone (SINGLE /2). Therefore, we pre-administered the oligo and its control alone twice before starting the usual schedule of oligo injection followed by trastuzumab. Unfortunately, also in this experiment we obtained no statistically significant results (**Figure 4.10E**). We reasoned that miR-31-3p inhibition once the tumor is already formed is probably not sufficient to revert treatment resistance in this cell model. Thus, to appreciate miRNA functional role, we decided to recapitulate the low basal level observed in responsive patients by inhibiting the miRNA levels before tumor formation.

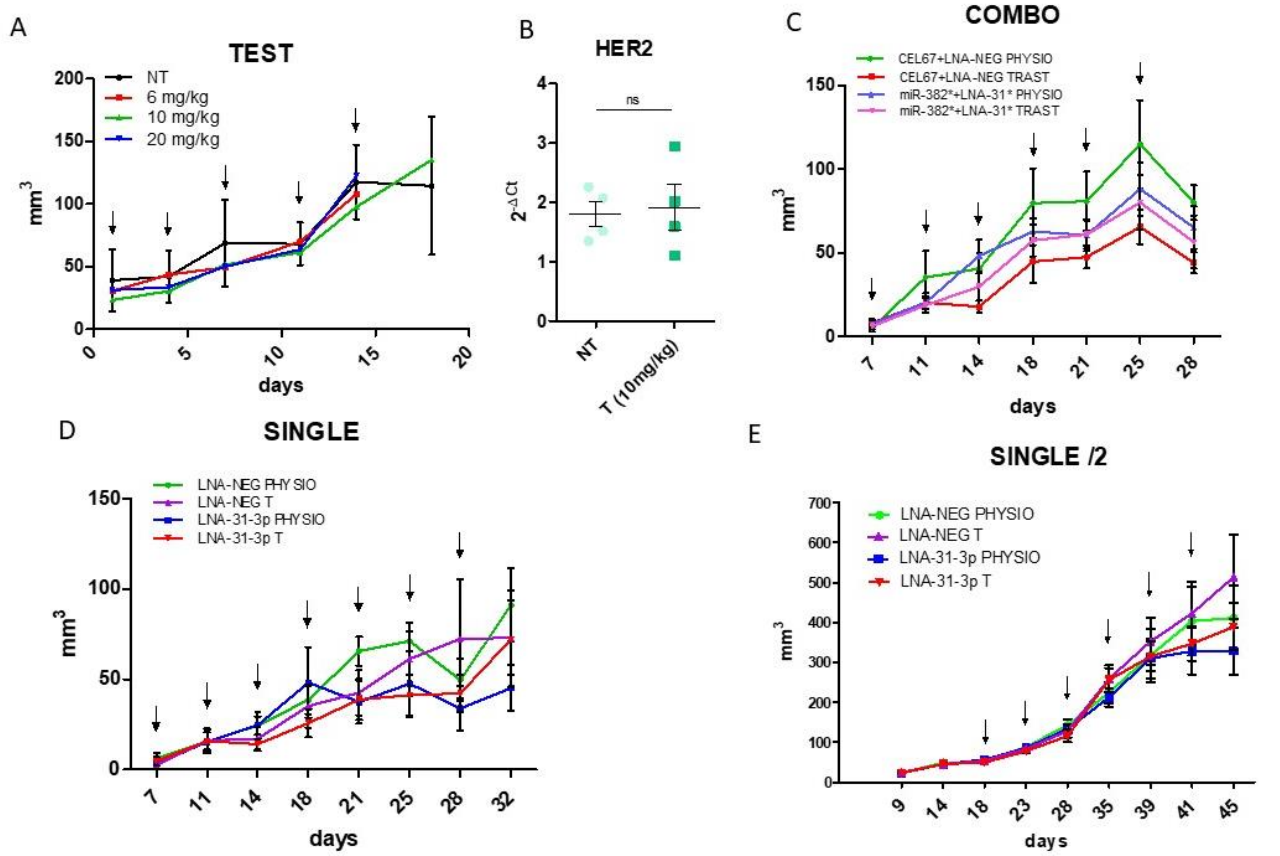


***Figure 4.10.*** *TEST in vivo experiment evaluating tumor growth of HCC1954 cell upon treatment (or not) with 6, 10 or 20 mg/kg of trastuzumab (A). qRT-PCR analysis evaluating HER2 expression in non-treated or trastuzumab-treated (only 10mg/kg-group) tumors at the end of the experiment (ns= non significative) (B). COMBO in vivo experiment evaluating tumor growth of HCC1954 cell upon concomitant delivery of LNA-31-3p and miR-382-3p and treatment or not with trastuzumab, compared to controls (C). SINGLE in vivo experiment evaluating tumor growth of HCC1954 cell upon delivery of LNA-31-3p or control (5 injections) and treatment or not with trastuzumab (D). SINGLE/2 in vivo experiment evaluating tumor growth of HCC1954 cell upon delivery of LNA-31-3p or control (7 injections) and treatment or not with trastuzumab. Treatment started after 2 oligo injections (E). Trastuzumab treatments are indicated with a black arrow.*

Thus, we decided to transfect HCC1954 cells with LNA-31-3p or control *in vitro* and inject them in SCID mice, then started again the usual schedule of alternated LNA and trastuzumab delivery once the tumors were palpable. This time, we detected a statistically significant difference between the groups LNA-31-3p + trastuzumab and the untreated LNA-NEG in terms of tumor volume (**Figure 4.11A**). **Figure 4.11B** shows images of the

tumors collected at the sacrifice. Moreover, we weighted the tumors at the sacrifice, and we obtained statistically significant differences between all the experimental conditions: LNA-31-3p tumors, both untreated and treated, had a reduced weight compared to their controls (**Figure 4.11C**). **Figure 4.11D** shows the successful inhibition of miR-31-3p in LNA-31-3p transfected tumors, checked at the end of the experiment by qRT-PCR analysis.

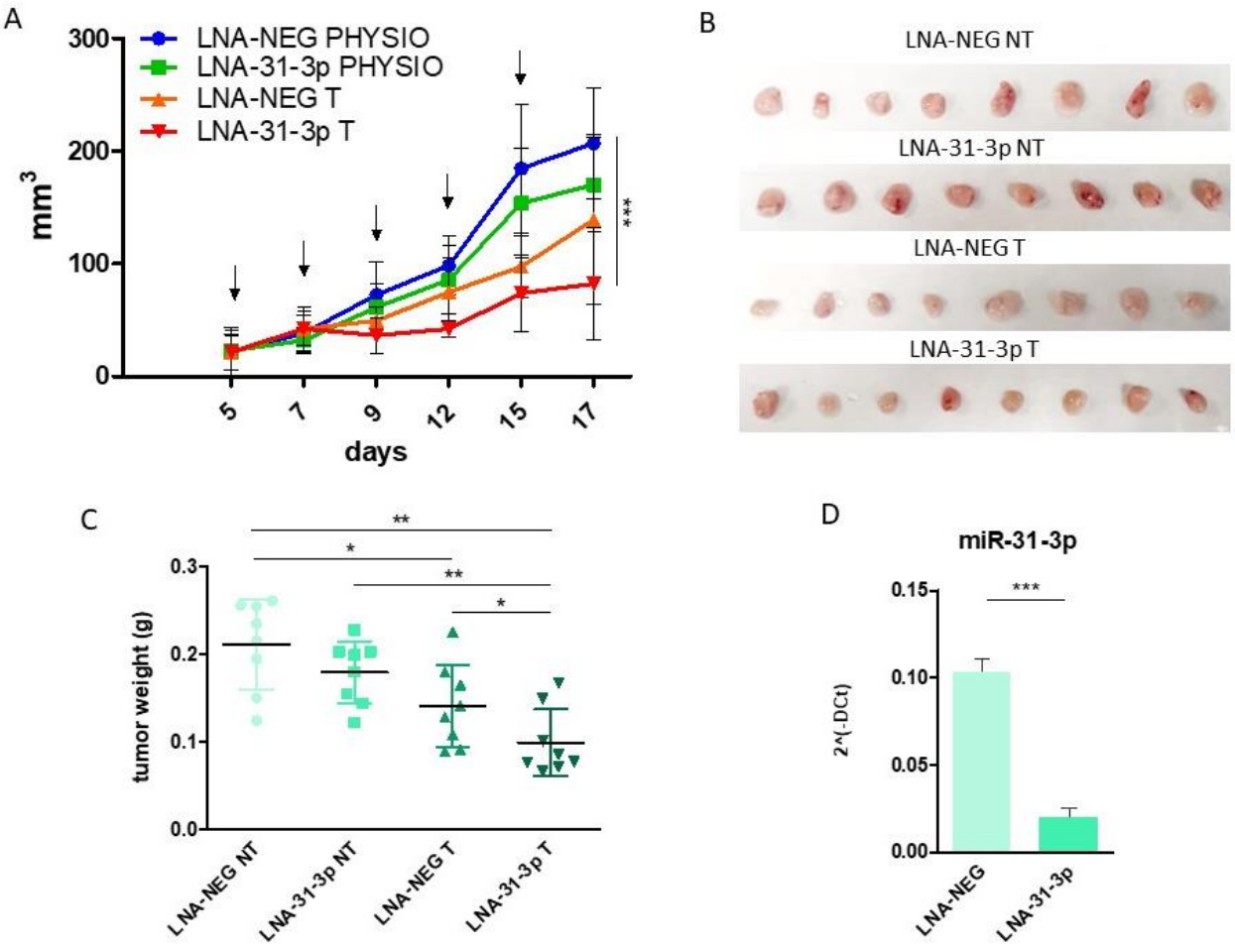


***Figure 4.11****. Mean tumor volumes after peritumoral injection of LNA-31-3p or control plus trastuzumab or saline (PHYSIO) treatment evaluated across different time points (n = 8/group; *** p≤0.001); trastuzumab treatments are indicated with a black arrow. (A). Images of the tumors collected at the sacrifice (B). Tumor weights at the sacrifice (*p≤0.05, **p≤0.01) (C). qRT-PCR evaluating miR-31-3p levels in HCC1954 tumors which received LNA-31-3p compared to control (±SEM, ***p<0.001) (D).*

### 4.5.3 Exploring miRNA mechanism of action: identification of targets

In order to better explore the molecular interactions that are responsible for the biological effects described above, I decided to identify possible miRNA direct targets by using four approaches (**Figure 4.12**):

A) Correlation analysis between the predictive signature composed of the two miRNAs and the expression levels of genes obtained from the gene profile of the NeoALTTO series. The resulting list of genes correlated with the signature was, consequently, matched with the lists of miR-31-3p and miR-382-3p putative targets predicted by at least three online tools. Next, a second correlation analysis was performed between the selected putative targets and the expression of the two miRNAs in the NeoALTTO series. The most promising genes, in terms of statistical significance of the correlation and biological role, were analyzed by qRT-PCR in miRNA-overexpressing cell line models.

B) Correlation analysis between the expression levels of the two miRNAs, independently considered, and the gene expression performed on the NeoALTTO series. In this case, the resulting list was not previously filtered for the correlation with the signature and was directly matched with the lists of putative targets.

C) Starting from the lists of miRNA putative targets, candidates were selected depending on the pathway they are involved in, considering the context of the study, and information found in the literature.

D) RNA-seq analysis on SKBr3 and HCC1954 cells modulated for miR-31-3p expression

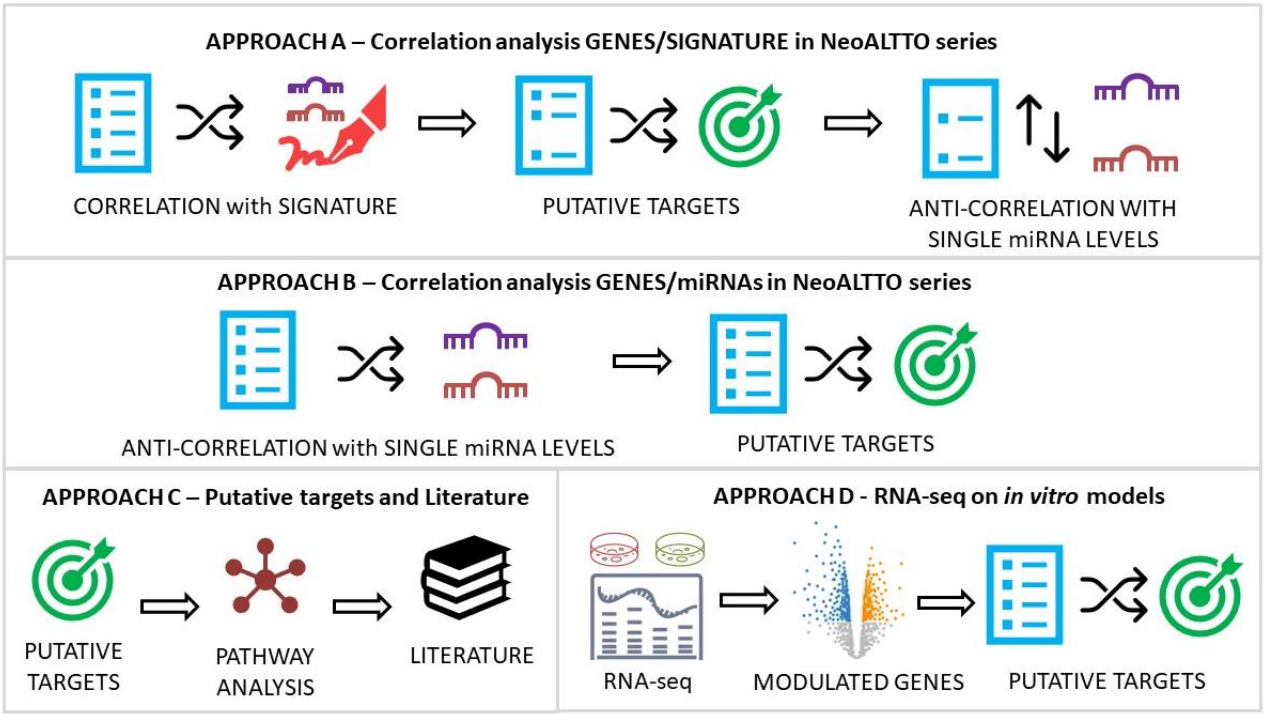


***Figure 4.12.*** *Schematic representation of the four approaches for miRNA target identification*

### 4.5.4 Approach A

Starting from the results of approach A, 70 genes resulted significantly correlated with the signature (Spearman correlation coefficient ≥0.40 in absolute value, **Figure 4.13A**), 20 of which are predicted to be direct targets of either miR-31-3p or miR-382-3p. Among the genes that resulted anti-correlated with the corresponding miRNA, *PDPK1*, *PRDM10*, *ASXL2*, *SLC25A17*, *RAB10* and *LPIN1* for miR-31-3p, and *TFAP2C* for miR-382-3p, were analyzed by qRT-PCR in *in vitro* models. These genes were selected based on either highest anti-correlation score, as *SLC25A17* (r=-0.39), *PRDM10* (r=-0.38), *ASXL2* (r=-0.37) and *RAB10* (r=-0.33), or relevant biological function like *PDPK1*, *LPIN1* and *TFAP2C*. In particular, PDPK1 is directly involved in the PI3K/Akt pathway, phosphorylating and activating protein kinases, including AKT, and it has been already linked to trastuzumab resistance mechanisms [218]. *LPIN1* encodes for phosphatidic acid phosphatase (PAP)

lipin-1, which is directly phosphorylated by the oncogene src, a close interactor of HER2 pathway, and it is linked to breast cancer malignancy [219]. Lastly, *TFAP2C* encodes for the transcription factor AP-2γ, which regulates a set of genes that constitute a signature that predicts outcome in HER2+ breast cancer [220]. Unfortunately, most of the predicted targets resulted upmodulated rather than downmodulated upon overexpression of the putative targeting miRNA (**Figure 4.13B-C**). To exclude that this increase was the result of a feedback loop to restore gene expression upon inhibition, I checked PDPK1 protein level, both phosphorylated and total forms as example, in miR-31-3p overexpressing SKBr3 cells. The western blot analysis confirmed the qRT-PCR data (**Figure 4.13D**).

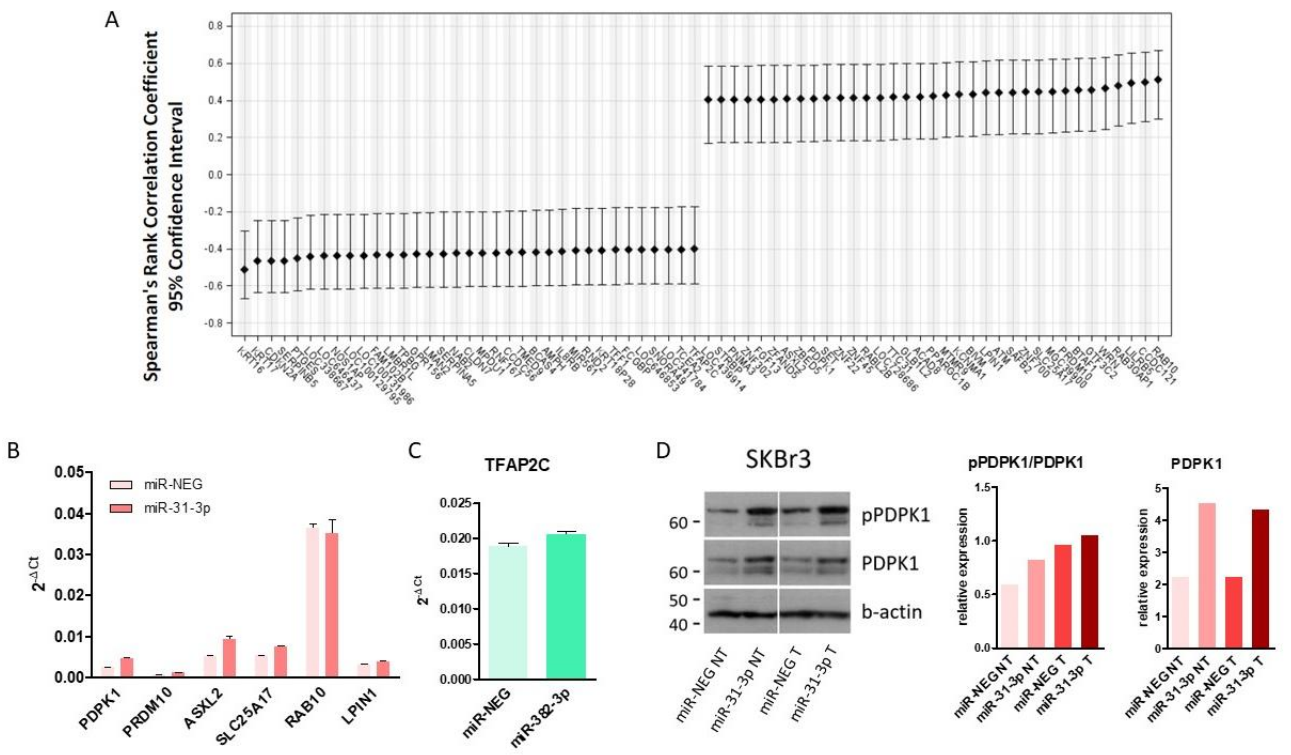


***Figure 4.13**. Correlation coefficients of the 70 genes significantly correlated with the miRNA-based predictive signature in the NeoALTTO study (A). qRT-PCR evaluating PDPK1, PRDM10, ASXL2, SLC25A17, RAB10 and LPIN1 mRNA levels in miR-31-3p overexpressing SKBr3 compared to control at 24h after miRNA transfection (B). qRT-PCR evaluating TFAP2C mRNA levels in miR-382-3p overexpressing HCC1954 at 24h after miRNA transfection (C). Western blot analysis showing pPDPK1 and PDPK1 protein levels in SKBr3 cells transfected or not with miR-31-3p and treated or not with*

*trastuzumab. Images and quantification are representative of three biological replicates and the expression of the activated form is normalized on the total protein and quantified in the bar plot on the right, while PDPK1 levels are normalized on the expression of b-actin (D).*

### 4.5.5 Approach B

Approach B led to a list of 127 genes correlated with miR-31-3p, 83 of which anti-correlated (Spearman Corr. Coeff. ≤-0.40). 8 of 83 genes were putative targets and are listed in **Table 4.1**. 111 genes instead correlated with miR-382-3p expression. Among the 58 anti-correlated genes, 7 were predicted as targets (**Table 4.1**). Validation of these genes is still ongoing.

***Table 4.1*** *List of miR-31-3p and miR-382-3p putative targets resulting from the intersection between in silico predicted targets and anti-correlated genes in the NeoALTTO study*

| PUTATIVE TARGETS of miR-31-3p | | | |
|---|---|---|---|
| ***Symbol*** | ***Complete name*** | ***Function*** | ***Corr.*** |
| **MFAP3** | Microfibril Associated Protein 3 | ECM | **-0.46** |
| **CDC42SE2** | CDC42 Small Effector 2 | Cytoskeleton | **-0.45** |
| **EIF4EBP2** | Translation Initiation Factor binding protein | Repressor of translation | **-0.45** |
| **PRDM10** | PR/SET Domain 10 | Transcription Factor | **-0.45** |
| **RCAN3** | RCAN Family member 3 | Calcium-mediated signalling | **-0.44** |
| **ABLIM1** | Actin binding LIM protein 1 | Scaffold protein - Cytoskeleton | **-0.43** |
| **GUF1** | GTP Binding Elongation Factor | GTPase (mitochondria) | **-0.41** |
| **MCOLN2** | Mucolipin TRP Cation Channel 2 | Cation (Ca2+) channel | **-0.40** |
| **PUTATIVE TARGETS of miR-382-3p** | | | |
| ***Symbol*** | ***Complete name*** | ***Function*** | ***Corr.*** |
| **COIL** | Coilin | Post-transcription modification | **-0.47** |
| **RB1CC1** | RB1 Inducible Coiled-Coil 1 | Cell growth, prolif, autophagy | **-0.44** |
| **ANKRD28** | Ankyrin repeat domain 28 | phosphatase | **-0.44** |
| **TP53INP1** | P53 inducible nuclear protein 1 | Autophagy, antioxidant | **-0.43** |
| **SHOC2** | Leucin Rich Repeat Scaffold protein | Scaffold x RAS/MAPK signalling | **-0.41** |
| **UBXN6** | UBX domain protein 6 | Endo- to lysosome transport | **-0.41** |
| **NTN4** | Netrin 4 | ECM | **-0.40** |

### 4.5.6 Approach C

Approach C, instead, led to the investigation of ERBIN, namely ERBB2 interactive protein, a putative target of miR-31-3p and described as HER2 stabilizer at the membrane level

[221]. ERBIN levels, analyzed by western blot assay, resulted downmodulated by miR-31-3p only in HCC1954 cells and not in SKBr3 (**Figure 4.14A**). Luciferase assay performed in HEK293 cells demonstrated that miR-31-3p binds ERBIN 3'UTR (**Figure 4.14B**).

Given ERBIN biological role, I performed flow cytometry analysis to check whether HER2 stability increased upon miR-31-3p inhibition with LNA-31-3p, thus justifying the increase of response to trastuzumab of HCC1954 cells due to an increase of target availability on cell membranes. I performed the analysis using a limiting dilution of the antibody to overcome the possibility of a saturated reaction between anti-HER2 antibody and HER2, a situation that would have masked differences between my experimental conditions. Starting from a concentration of 0.625 ug/mL, I reached an antibody concentration of 0.05 ug/mL. However, no significant changes in HER2 expression at membrane level were observed (**Figure 4.14C**). Thus, to investigate ERBIN possible implication in resistance to trastuzumab, I decided to silence it in concomitance with trastuzumab treatment both in 2D and 3D setting. Unfortunately, I obtained no significant changes between the different experimental conditions, neither in terms of HER2 pathway modulation nor in 3D cell growth and response to trastuzumab (**Figure 4.14D-E**). Thus, the results obtained do not support a direct involvement of ERBIN in the biological effects described in the previous paragraphs.

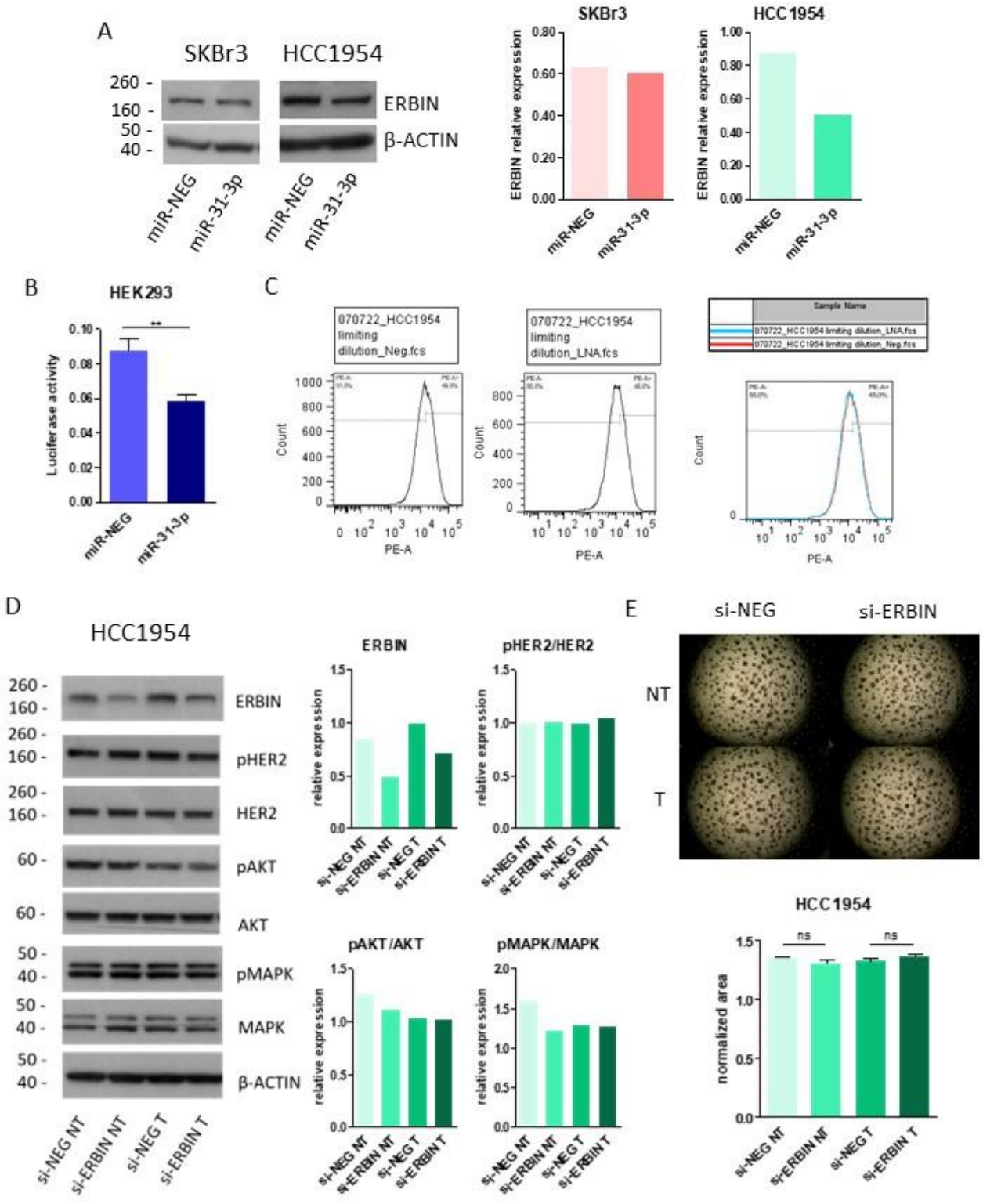


***Figure 4.14.*** *Western blot analysis evaluating ERBIN expression in miR-31-3p overexpressing SKBr3 and HCC1954 cells compared to control. Protein levels were quantified in the bar plot on the right normalizing on b-actin signal; images and quantifications are representative of three biological replicates (A). Luciferase reporter assay assessing miR-31-3p direct targeting of ERBIN performed in HEK293 cells. The bar plot shows mean values of luciferase activity of three biological replicates (±SEM, **p<0.01) (B). Representative*

*flow cytometry analysis assessing HER2 expression on HCC1954 cell membranes upon miR-31-3p inhibition (second graph), compared to control (first graph). The third graph shows the overlay of the two samples (C). Western blot analysis evaluating ERBIN, pHER2, pAKT and pMAPK levels in non-treated or trastuzumab-treated HCC1954 cells silenced (or not, si-NEG) for ERBIN expression (si-ERBIN). Images and quantifications are representative of three biological replicates; ERBIN signal was normalized on b-actin signal while pHER2, pAKT and pMAPK levels were normalized on their respective total protein signals (D). 3D assay evaluating cell growth and viability of HCC1954 silenced (or not) for ERBIN expression and treated or not with trastuzumab, compared to controls. Images are representative of three biological replicates. The bar plots show the mean normalized area occupied by cell colonies at day 5 of treatment (± SEM, ns=not significative).*

### 4.5.7 Approach D

Approaches A and C described in the previous paragraphs were not successful in giving insight into miR-31-3p mechanism of action, while approach B is still ongoing. Thus, in parallel, I decided to perform an RNA-seq analysis on my *in vitro* models, SKBr3 and HCC1954, modulated for miRNA expression and treated or not the day after with trastuzumab for 24h.

*RNAseq analysis on SKBr3 cells*

For what concerns SKBr3 cells, a total of 155 genes resulted significantly modulated between miR-31-3p NT and miR-NEG NT conditions (94 down, 61 up) and 196 genes between miR-31-3p T and miR-NEG T (101 down, 95 up). Trastuzumab treatment alone modulated 308 genes in the control condition (miR-NEG T vs miR-NEG NT), while the number is reduced to 8 in the presence of miRNA overexpression (miR-31-3p T vs miR-31-3p NT). This result suggests that miRNA upmodulation dampens the effect of the anti-HER2 agent on SKBr3 cells.

Among the downmodulated genes in miR-31-3p overexpressing cells, 31 were predicted as direct targets by at least 2 online tools (**Table 4.2**). Surprisingly, *ERBB3*, HER3 coding

gene, is included in this list even though its upmodulation has been demonstrated to reduce response to trastuzumab [222].

***Table 4.2*** *List of genes downmodulated by miR-31-3p in in both non-treated and treated SKBr3 cells, which are predicted as miRNA direct targets by at least two online prediction tools*

| GENE | FULL NAME | LogFC | FDR | PREDICTION TOOLS |
|---|---|---|---|---|
| **CA12** | Carbonic Anhydrase 12 | -0.64 | 0.0022 | miRwalk, TargetScan |
| **CCNY** | Cyclin Y | -0.62 | 0.0048 | miRwalk, TargetScan |
| **CDK6** | Cyclin Dependent Kinase 6 | -0.45 | 0.0442 | miRwalk, TargetScan |
| **CYB5R1** | Cytochrome B5 Reductase 1 | -0.66 | 0.0047 | miRwalk, TargetScan |
| **EHBP1** | EH Domain Binding Protein 1 | -0.51 | 0.0141 | miRwalk, TargetScan |
| **ERBB3** | Erb-B2 Receptor Tyrosine Kinase 3 | -0.62 | 0.0024 | miRwalk, TargetScan |
| **GUCD1** | Guanylyl Cyclase Domain Containing 1 | -0.72 | 0.0080 | miRwalk, TargetScan |
| **ITPRIPL2** | Inositol 1,4,5-Trisphosphate Receptor Interacting Protein Like 2 | -0.40 | 0.0360 | miRwalk, TargetScan |
| **LPGAT1** | Lysophosphatidylglycerol Acyltransferase 1 | -0.41 | 0.0229 | miRwalk, TargetScan |
| **LSM14B** | LSM Family Member 14B | -0.72 | 0.0061 | miRwalk, TargetScan |
| **MLEC** | Malectin | -0.61 | 0.0012 | miRwalk, TargetScan |
| **NEDD9** | Neural Precursor Cell Expressed, Developmentally Down-Regulated 9 | -0.57 | 0.0163 | miRwalk, TargetScan |
| **PTBP3** | Polypyrimidine Tract Binding Protein 3 | -0.44 | 0.0121 | miRwalk, TargetScan |
| **PTPRF** | Protein Tyrosine Phosphatase Receptor Type F | -0.39 | 0.0190 | miRwalk, TargetScan |
| **SEC31A** | SEC31 Homolog A, COPII Coat Complex Component | -0.50 | 0.0047 | miRwalk, TargetScan |
| **SNX27** | Sorting Nexin 27 | -0.34 | 0.0395 | miRwalk, TargetScan |
| **CYB5RL** | Cytochrome B5 Reductase Like | -0.80 | 0.0163 | miRwalk, TargetScan |
| **LNPEP** | Leucyl And Cystinyl Aminopeptidase | -0.35 | 0.0409 | miRwalk, TargetScan |
| **LRRC8B** | Leucine Rich Repeat Containing 8 VRAC Subunit B | -0.77 | 0.0229 | miRwalk, TargetScan |
| **MAP3K7** | Mitogen-Activated Protein Kinase Kinase Kinase 7 | -0.37 | 0.0448 | miRwalk, TargetScan |
| **NEBL** | Nebulette | -0.36 | 0.0239 | miRwalk, TargetScan |
| **PDPR** | Pyruvate Dehydrogenase Phosphatase Regulatory Subunit | -0.81 | 0.0129 | miRwalk, TargetScan |
| **SCAMP5** | Secretory Carrier Membrane Protein 5 | -1.02 | 0.0338 | miRwalk, TargetScan |
| **USP12** | Ubiquitin Specific Peptidase 12 | -0.56 | 0.0353 | miRwalk, TargetScan |
| **UBE2H** | Ubiquitin Conjugating Enzyme E2 H | -0.36 | 0.0363 | miRwalk, TargetScan |
| **XPNPEP3** | X-Prolyl Aminopeptidase 3 | -0.78 | 0.0129 | miRwalk, TargetScan |
| **ZBTB5** | Zinc Finger And BTB Domain Containing 5 | -0.52 | 0.0382 | miRwalk, TargetScan |
| **PPP2R5C** | Protein Phosphatase 2 Regulatory Subunit B'Gamma | -0.34 | 0.0238 | miRwalk, miRTarBase |
| **CHMP4B** | Charged Multivesicular Body Protein 4B | -0.47 | 0.0061 | TargetScan, miRTarBase |
| **EPB41L4B** | Erythrocyte Membrane Protein Band 4.1 Like 4B | -0.60 | 0.0186 | TargetScan, miRTarBase |
| **PLEKHB2** | Pleckstrin Homology Domain Containing B2 | -0.96 | 0.0002 | TargetScan, miRTarBase |

In order to better understand miR-31-3p mechanism of action, I performed a pathway enrichment analysis using the Enrichr software (https://maayanlab.cloud/Enrichr/) and considering the pathway enriched based on The Molecular Signatures Database (MSigDB)

hallmark gene set collection [207]. In **Table 4.3** are listed the significant enriched pathways in miR-31-3p NT vs miR-NEG NT, miR-31-3p T vs miR-NEG T and miR-NEG T vs miR-NEG NT comparisons.

***Table 4.3*** *Significant enriched pathways in treated or not miR-31-3p overexpressing SKBr3 cells, compared to controls*

| **miR-31-3p NT vs miR-NEG NT** | | | |
|---|---|---|---|
| **Term** | **Overlap** | **P-value** | **Adjusted P-value** |
| TGF-beta Signaling | 4/54 | 8.1E-04 | 2.2E-02 |
| UV Response Up | 6/158 | 1.5E-03 | 2.2E-02 |
| Apoptosis | 6/161 | 1.6E-03 | 2.2E-02 |
| mTORC1 Signaling | 6/200 | 4.7E-03 | 4.7E-02 |
| **miR-31-3p T vs miR-NEG T** | | | |
| mTORC1 Signaling | 12/200 | 6.9E-07 | 2.9E-05 |
| TGF-beta Signaling | 4/54 | 1.9E-03 | 2.6E-02 |
| Protein Secretion | 5/96 | 2.6E-03 | 2.6E-02 |
| Androgen Response | 5/100 | 3.1E-03 | 2.6E-02 |
| Myc Targets V1 | 7/200 | 3.6E-03 | 2.6E-02 |
| Oxidative Phosphorylation | 7/200 | 3.6E-03 | 2.6E-02 |
| **miR-NEG T vs miR-NEG NT** | | | |
| G2-M Checkpoint | 33/200 | 1.4E-24 | 5.5E-23 |
| E2F Targets | 31/200 | 2.6E-22 | 5.2E-21 |
| Myc Targets V1 | 25/200 | 6.4E-16 | 8.5E-15 |
| mTORC1 Signaling | 22/200 | 5.3E-13 | 5.3E-12 |
| Cholesterol Homeostasis | 8/74 | 1.7E-05 | 1.4E-04 |
| Androgen Response | 9/100 | 2.3E-05 | 1.5E-04 |
| Fatty Acid Metabolism | 11/158 | 3.3E-05 | 1.9E-04 |
| Myc Targets V2 | 6/58 | 2.5E-04 | 1.3E-03 |
| Glycolysis | 10/200 | 1.1E-03 | 4.7E-03 |
| Mitotic Spindle | 9/199 | 3.7E-03 | 1.5E-02 |
| Spermatogenesis | 7/135 | 4.8E-03 | 1.7E-02 |
| DNA Repair | 7/150 | 8.4E-03 | 2.8E-02 |
| Oxidative Phosphorylation | 8/200 | 1.2E-02 | 3.7E-02 |

**Figure 4.15** is, instead, a schematic representation showing the enriched pathways shared between the different comparisons. *mTORC1 Signaling* resulted enriched in all groups, while *TGF-beta Signaling* was enriched only in the presence of miR-31-3p, both in non-treated and treated condition. *Androgen Response*, *Myc Targets V1* and *Oxidative*

*Phosphoriylation* were, instead, the pathways shared by miR-31-3p T vs miR-NEG T and miR-NEG T vs miR-NEG NT, which could suggest that those gene sets are modulated by the miRNAs only in response to trastuzumab treatment. Indeed, all the genes included in the three pathways, that are also in common between the two comparisons, are modulated in opposite way by the miRNA and the treatment alone. I then performed Ingenuity Pathway Analysis (IPA) to predict activation (z-score ≥ 2) or inhibition (z-score ≤ -2) of pathways based on the amplitude of negative or positive fold change of the enriched genes included in those pathways, upon miR-31-3p overexpression in SKBr3 cells. For example, the most activated pathway in non-treated miR-31-3p overexpressing SKBr3 is *Protein kinase A (PKA) signaling* (z-score=2.24), which includes *CTNNB1* (Catenin beta-1) and *TGFBR1* (Transforming Growth Factor Beta Receptor 1) genes, already present also in the MSigDB hallmark gene set *TGF-Beta Signaling.* In accordance with my data, PKA activation has been demonstrated to confer resistance to trastuzumab in human breast cancer cell lines [223]. In trastuzumab-treated miR-31-3p overexpressing cells, instead, among the activated IPA pathways stand out *Mitotic G2-G2/M phases* (z-score=2.65) and *PI3K/AKT Signaling* (z-score=2), a clear indication that the drug is not efficiently exerting its anti-tumoral effect. These results support the *in vitro* data demonstrating that miR-31-3p overexpression is able to counteract trastuzumab activity in SKBr3 cells.

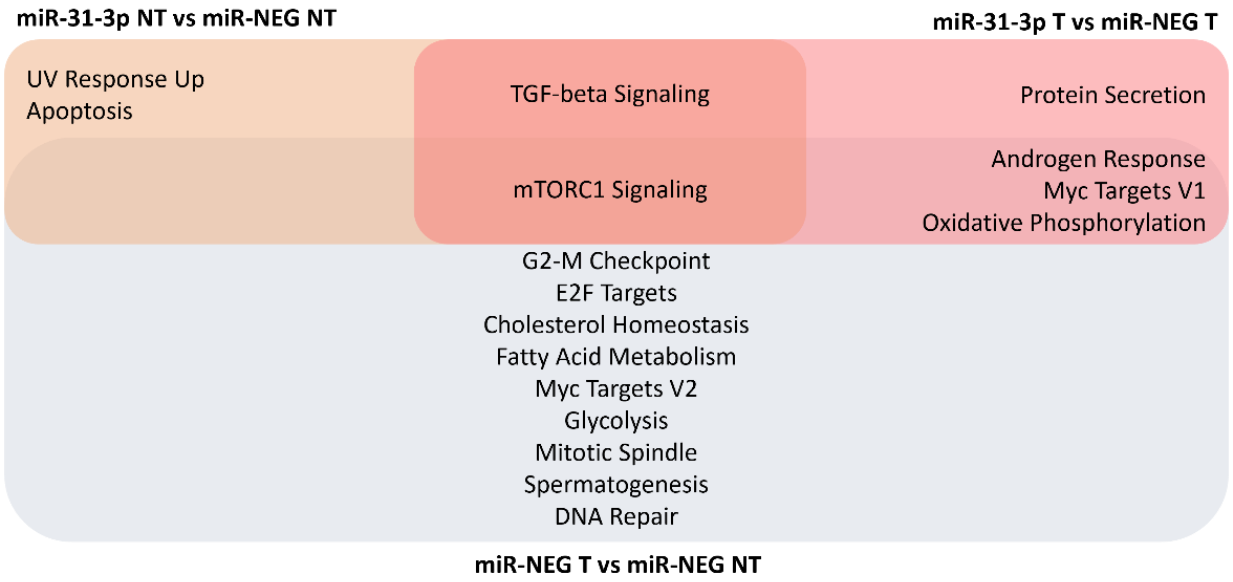


***Figure 4.15***. *Schematic representation showing the significant enriched MSigDB Hallmarks gene sets that are shared between miR-31-3p NT vs miR-NEG NT, miR-31-3p T vs miR-NEG T and miR-NEG T vs miR-NEG NT comparisons in SKBr3 cells.*

A preliminary western blot analysis was performed to validate gene modulation at protein level in the miR-31-3p NT vs miR-NEG NT comparison group. Based on their function, I selected as downmodulated genes *ERBB3* (logFC -0.62, FDR 0.0024), and *FOXO3* (or *FOXO3A*, logFC -0.39, 0.024), a transcription factor that mainly acts as tumor suppressor, inhibiting cell proliferation and inducing transcription of apoptosis genes [224]. *CTNNB1* and *CREB1* (CAMP Responsive Element Binding Protein 1) are the upmodulated genes I chose to study. *CTNNB1* (logFC 0.37, FDR 0.014) encodes for β-catenin, which is part of a complex of proteins that constitute adherens junctions, and it is known to be involved in trastuzumab resistance mechanisms with its partner WNT [225,226]. *CREB1* (logFC 0.34, FDR 0.038) encodes for a transcription factor downstream the PI3K/AKT pathway, modulating different cellular processes like cell growth and proliferation, differentiation, apoptosis, and survival, and it was found overexpressed in solid tumors [227,228]. Moreover, FOXO3 and CREB1 were selected for protein analysis also because they are

included in the IPA activated pathway *ERK5 Signaling* (z-score=2), which has also been linked to trastuzumab resistance mechanisms [229].

**Figure 4.16** shows images and quantification of the western blot analysis. Despite what expected from RNAseq data, where HER3 was among the genes downmodulated also in miR-31-3p NT vs miR-NEG NT group, protein levels of both total and phosphorylated HER3 resulted downmodulated by miR-31-3p only in treated cells. FOXO3A protein levels also decreased only in the combination group. As for β-catenin, it increased upon miR-31-3p overexpression both in non-treated and treated cells. Finally, CREB1 activity only did increase in non-treated miR-31-3p overexpressing cells; on the contrary, in treated samples, the increase in total protein did not result in a higher activation. Considering that the western blot analysis is not completely overlapping with the RNAseq analysis, I checked pHER2 and HER2 expression and validated the usual upmodulation of HER2 by miR-31-3p only in the treated condition. Replicates of this analysis are needed to verify putative miRNA target modulation.

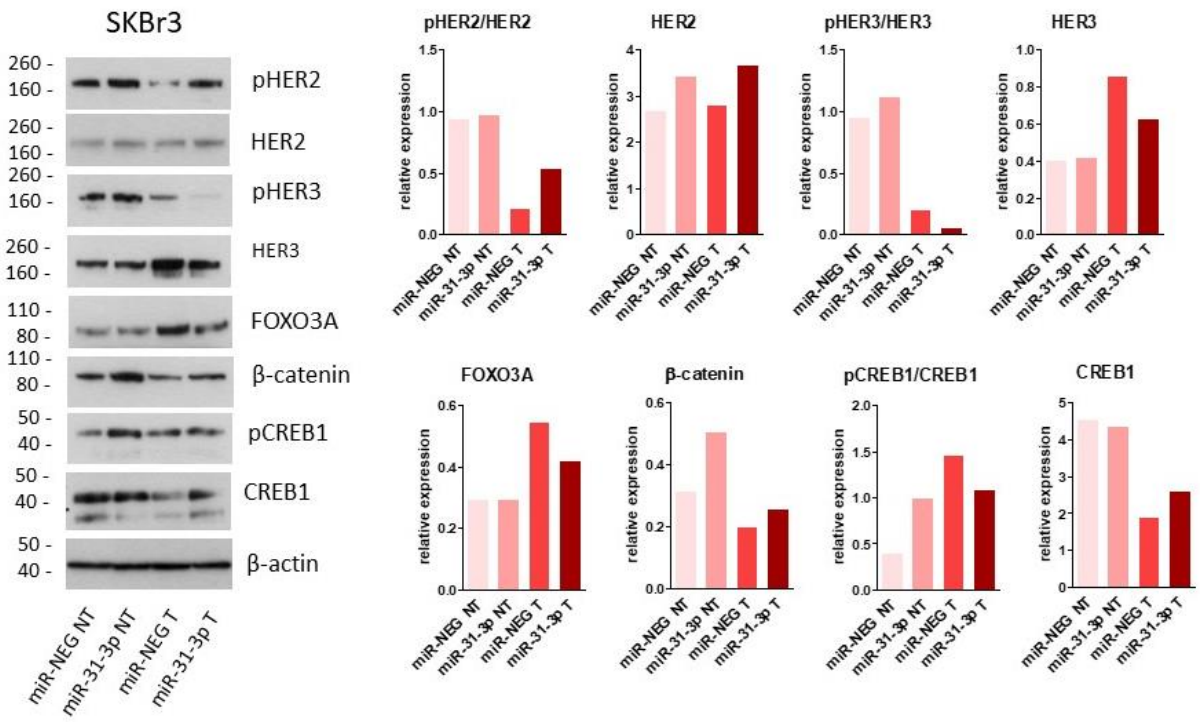


***Figure 4.16***. *Western blot analysis assessing pHER2, HER2, pHER3, HER3, FOXO3A, β-catenin, pCREB1 and CREB1 protein levels in SKBr3 cells transfected or not with miR-31-3p and treated or not with trastuzumab. Bar plots show quantification of the bands, total protein levels were normalized on β-actin signal, while phosphorylated form levels were normalized on total protein levels.*

*RNAseq analysis on HCC1954 cells*

The RNA-seq performed on HCC1954 cells aimed at evaluating the effect of both miR-31-3p upmodulation and downmodulation to better recapitulate miRNA mechanism of action in concomitance or not with trastuzumab treatment. The analysis was carried out on cells treated for 24h and not 72h considering that at 24h HCC1954 cell viability was already affected by miR-31-3p inhibition, as described in Chapter 4.2. These are the numbers of significant modulated genes in the different comparisons:

- miR-31-3p NT vs NEG NT: 1041 significant modulated genes, 529 down and 512 up;
- miR-31-3p T vs NEG T: 1170 significant modulated genes, 622 down and 548 up;

- miR-NEG T vs miR-NEG NT: 137 significant modulated genes, 87 down and 50 up;
- LNA-31-3p NT vs LNA-NEG NT: 877 significant modulated genes, 472 down and 405 up.
- LNA-31-3p T vs LNA-NEG T: 741 significant modulated genes, 318 down and 423 up.
- LNA-NEG T vs LNA-NEG NT: 35 significant modulated genes, 26 down e 9 up.

Is it immediately clear that the number of significantly modulated genes found in HCC1954 comparisons are quite higher than in SKBr3 cells, except for miR-NEG T vs miR-NEG NT (n=137) and LNA-NEG T vs LNA-NEG NT (n=35). In SKBr3 cells the modulated genes by the treatment alone were 308. It could be speculated that these results mirrors the different responsiveness of the cell lines to trastuzumab.

Among the downmodulated genes in miR-31-3p overexpressing cells, 137 were predicted as direct targets by at least 2 online tools. Since the number is high, in **Table 4.4** are reported only the 21 genes that are putatively targeted by miR-31-3p in both SKBr3 and HCC1954.

***Table 4.4*** *List of genes downmodulated by miR-31-3p in both non-treated and treated SKBr3 and HCC1954, which are predicted as miRNA direct targets by at least two online prediction tools*

| GENE | FULL NAME | LogFC | FDR | PREDICTION TOOLS |
|---|---|---|---|---|
| **CCNY** | Cyclin Y | -0.62 | 1.1E-09 | miRwalk, TargetScan |
| **CYB5R1** | Cytochrome B5 Reductase 1 | -0.75 | 8.0E-08 | miRwalk, TargetScan |
| **EHBP1** | EH Domain Binding Protein 1 | -0.45 | 2.9E-03 | miRwalk, TargetScan |
| **ERBB3** | Erb-B2 Receptor Tyrosine Kinase 3 | -0.76 | 8.9E-08 | miRwalk, TargetScan |
| **GUCD1** | Guanylyl Cyclase Domain Containing 1 | -1.02 | 6.6E-08 | miRwalk, TargetScan |
| **ITPRIPL2** | Inositol 1,4,5-Trisphosphate Receptor Interacting Protein Like 2 | -0.66 | 7.0E-08 | miRwalk, TargetScan |
| **LPGAT1** | Lysophosphatidylglycerol Acyltransferase 1 | -0.69 | 6.7E-06 | miRwalk, TargetScan |
| **LSM14B** | LSM Family Member 14B | -0.98 | 6.6E-08 | miRwalk, TargetScan |
| **MLEC** | Malectin | -0.92 | 6.6E-08 | miRwalk, TargetScan |
| **PTBP3** | Polypyrimidine Tract Binding Protein 3 | -0.42 | 7.8E-08 | miRwalk, TargetScan |
| **PTPRF** | Protein Tyrosine Phosphatase Receptor Type F | -0.39 | 8.7E-08 | miRwalk, TargetScan |
| **SEC31A** | SEC31 Homolog A, COPII Coat Complex Component | -0.48 | 1.3E-09 | miRwalk, TargetScan |
| **LRRC8B** | Leucine Rich Repeat Containing 8 VRAC Subunit B | -0.45 | 1.0E-03 | miRwalk, TargetScan |
| **NEBL** | Nebulette | -0.40 | 4.9E-03 | miRwalk, TargetScan |
| **PDPR** | Pyruvate Dehydrogenase Phosphatase Regulatory Subunit | -0.70 | 1.3E-09 | miRwalk, TargetScan |
| **SCAMP5** | Secretory Carrier Membrane Protein 5 | -1.94 | 3.3E-04 | miRwalk, TargetScan |
| **UBE2H** | Ubiquitin Conjugating Enzyme E2 H | -0.39 | 9.1E-08 | miRwalk, TargetScan |
| **XPNPEP3** | X-Prolyl Aminopeptidase 3 | -0.70 | 8.6E-04 | miRwalk, TargetScan |
| **PPP2R5C** | Protein Phosphatase 2 Regulatory Subunit B'Gamma | -0.52 | 7.0E-0.8 | miRwalk, miRTarBase |
| **CHMP4B** | Charged Multivesicular Body Protein 4B | -0.64 | 6.7E-06 | TargetScan, miRTarBase |
| **PLEKHB2** | Pleckstrin Homology Domain Containing B2 | -0.81 | 6.6E-08 | TargetScan, miRTarBase |

Pathway enrichment analysis performed on the miRNA-related comparisons resulted in the list of gene sets included in **Table 4.5**.

***Table 4.5*** *Significant enriched pathways in treated or not miR-31-3p overexpressing HCC1954 cells, compared to controls*

| **miR-31-3p NT vs miR-NEG NT** | | | |
|---|---|---|---|
| **Term** | **Overlap** | **P-value** | **Adjusted P-value** |
| Estrogen Response Early | 31/200 | 4.9E-08 | 2.4E-06 |
| TGF-beta Signaling | 13/54 | 2.9E-06 | 7.1E-05 |
| Hypoxia | 27/200 | 5.4E-06 | 8.9E-05 |
| p53 Pathway | 26/200 | 1.6E-05 | 2.0E-04 |
| UV Response Dn | 20/144 | 5.8E-05 | 5.7E-04 |
| IL-2/STAT5 Signaling | 24/199 | 1.1E-04 | 8.4E-04 |
| TNF-alpha Signaling via NF-kB | 24/200 | 1.2E-04 | 8.4E-04 |
| Estrogen Response Late | 23/200 | 3.1E-04 | 1.9E-03 |
| Interferon Gamma Response | 22/200 | 7.6E-04 | 3.4E-03 |
| mTORC1 Signaling | 22/200 | 7.6E-04 | 3.4E-03 |
| Glycolysis | 22/200 | 7.6E-04 | 3.4E-03 |
| Wnt-beta Catenin Signaling | 8/42 | 1.3E-03 | 5.2E-03 |
| Unfolded Protein Response | 14/113 | 2.2E-03 | 7.9E-03 |
| Angiogenesis | 7/36 | 2.2E-03 | 7.9E-03 |
| KRAS Signaling Up | 20/200 | 4.0E-03 | 1.3E-02 |
| E2F Targets | 19/200 | 8.4E-03 | 2.4E-02 |
| heme Metabolism | 19/200 | 8.4E-03 | 2.4E-02 |
| **miR-31-3p T vs miR-NEG T** | | | |
| Estrogen Response Early | 36/200 | 1.2E-09 | 5.8E-08 |
| p53 Pathway | 31/200 | 5.5E-07 | 1.4E-05 |
| mTORC1 Signaling | 27/200 | 3.8E-05 | 4.7E-04 |
| KRAS Signaling Up | 27/200 | 3.8E-05 | 4.7E-04 |
| TGF-beta Signaling | 12/54 | 4.9E-05 | 4.8E-04 |
| TNF-alpha Signaling via NF-kB | 26/200 | 1.0E-04 | 8.2E-04 |
| IL-2/STAT5 Signaling | 25/199 | 2.3E-04 | 1.6E-03 |
| Estrogen Response Late | 24/200 | 6.0E-04 | 3.7E-03 |
| PI3K/AKT/mTOR Signaling | 15/105 | 1.1E-03 | 5.9E-03 |
| Protein Secretion | 14/96 | 1.3E-03 | 6.2E-03 |
| Glycolysis | 23/200 | 1.4E-03 | 6.2E-03 |
| Fatty Acid Metabolism | 19/158 | 2.1E-03 | 8.5E-03 |
| Apoptosis | 19/161 | 2.6E-03 | 9.8E-03 |
| Hypoxia | 22/200 | 3.0E-03 | 1.1E-02 |
| Angiogenesis | 7/36 | 4.2E-03 | 1.4E-02 |
| Epithelial Mesenchymal Transition | 21/200 | 6.4E-03 | 1.8E-02 |
| Inflammatory Response | 21/200 | 6.4E-03 | 1.8E-02 |
| Wnt-beta Catenin Signaling | 7/42 | 9.9E-03 | 2.7E-02 |
| **miR-NEG T vs miR-NEG NT** | | | |
| Estrogen Response Early | 7/200 | 4.6E-04 | 1.5E-02 |
| Estrogen Response Late | 6/200 | 2.6E-03 | 4.1E-02 |

**Figure 4.17** is the schematic representation showing the shared pathways. *Estrogen Response Early* and *Estrogen Response Late* gene sets resulted significantly modulated in all the three comparisons, but no genes are shared. 10 gene sets were, instead, significantly modulated only upon miR-31-3p overexpression, including *TGF-beta Signaling* and *mTORC1 Signaling*, already found in the SKBr3-related analysis.

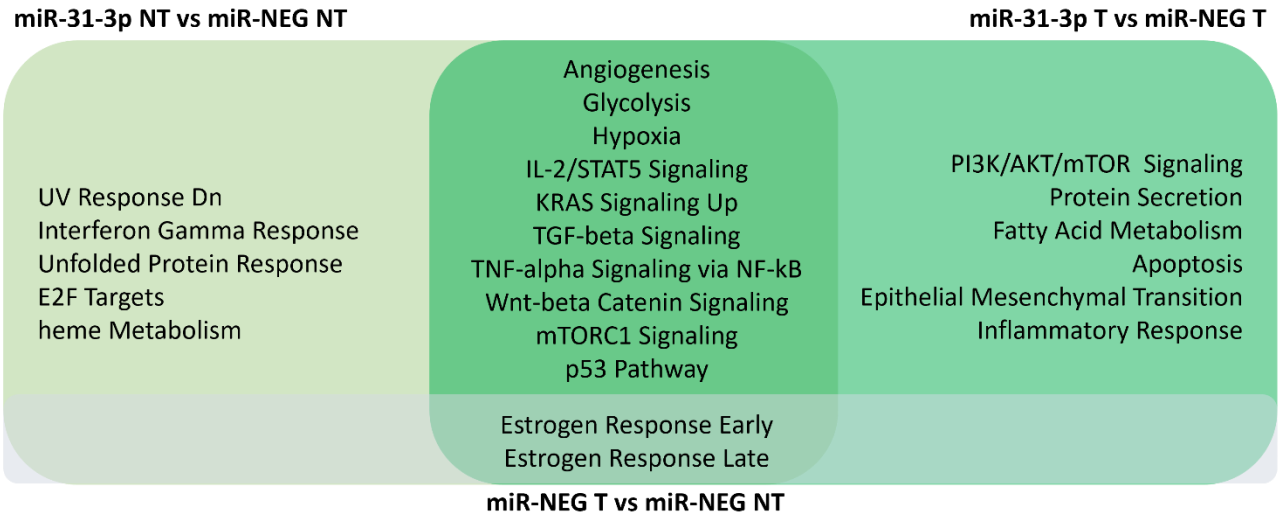


***Figure 4.17****. Schematic representation showing the significant enriched MSigDB Hallmarks gene sets that are shared between miR-31-3p NT vs miR-NEG NT, miR-31-3p T vs miR-NEG T and miR-NEG T vs miR-NEG NT comparisons in HCC1954 cells.*

In **Figure 4.18** I merged the results of enrichment pathway analysis performed in miRNA-related comparisons in the two cell lines, followed by a schematic representation of the main molecular interactions in *TGF-beta Signaling* and *mTORC1 Signaling* pathways (**Figure 4.19**).

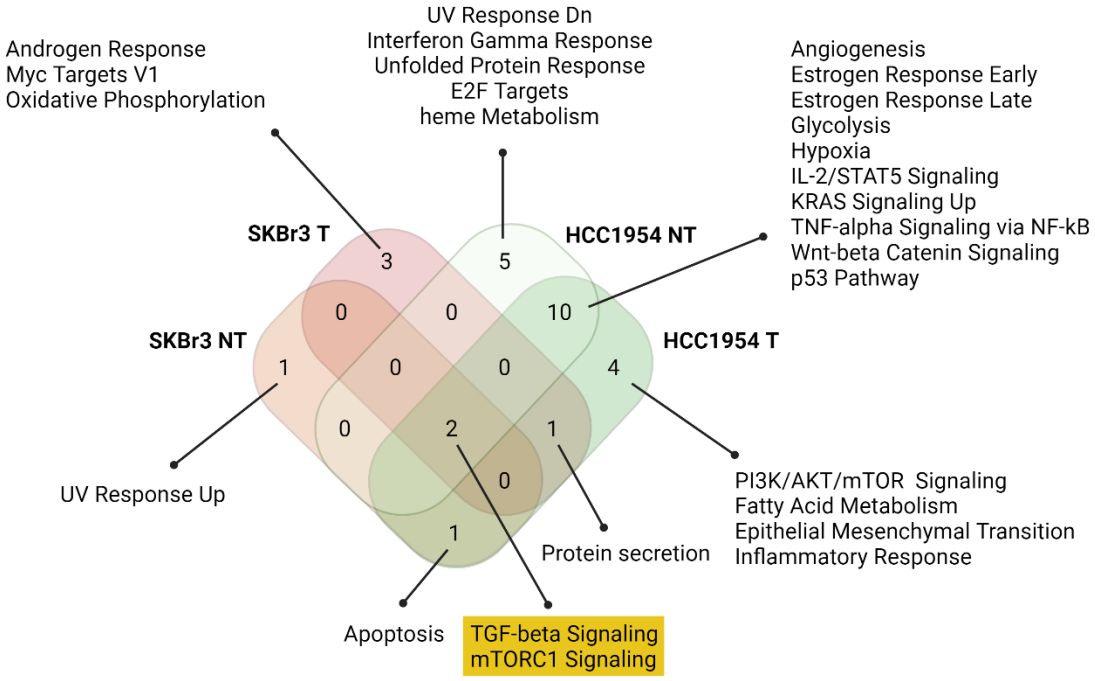


***Figure 4.18***. *Significant enriched pathways in miRNA-related comparisons (miR-31-3p vs miR-NEG) in treated and non-treated SKBr3 and HCC1954. Highlighted in yellow are TGF-beta Signaling and mTORC1 Signaling gene sets, which are shared between all the comparisons. Created with BioRender.com*

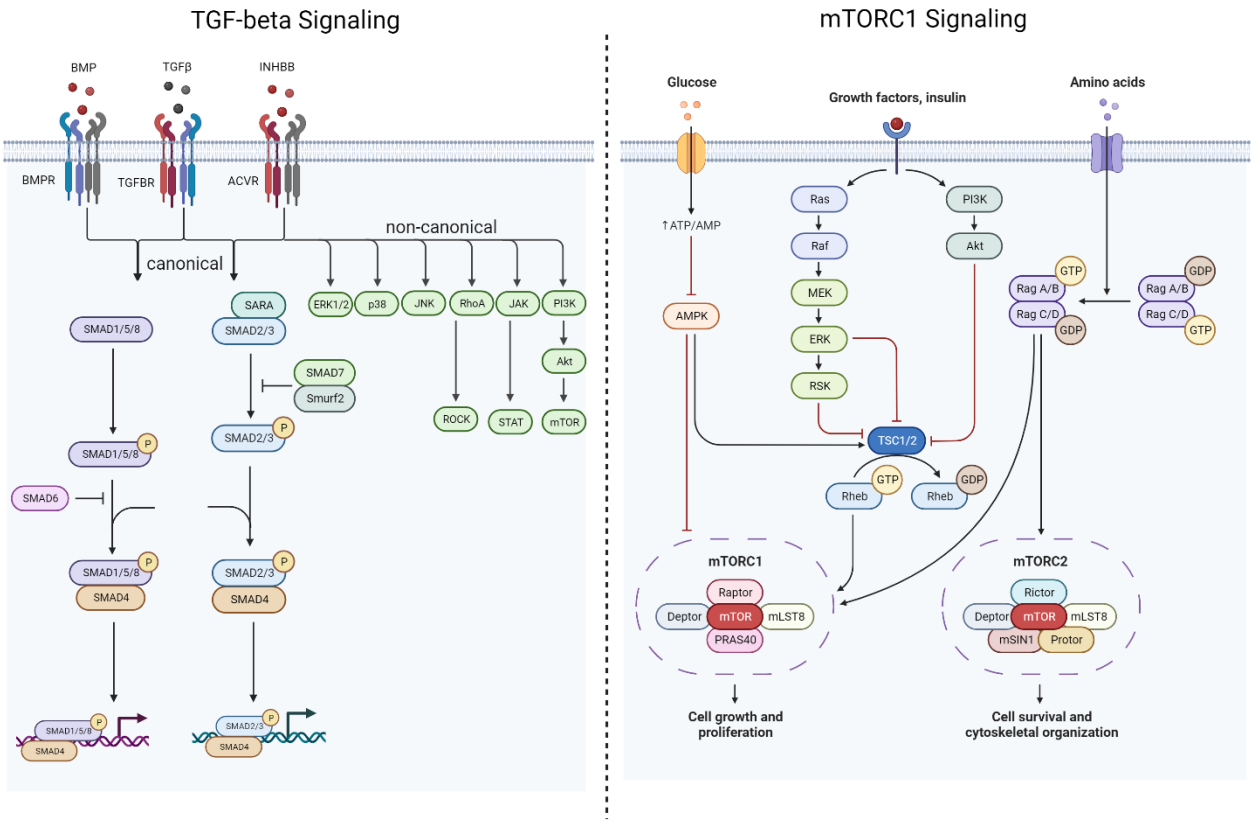


***Figure 4.19*** *Schematic representation of the main molecular interactions in TGF-beta Signaling and mTORC1 Signaling pathways (Created with BioRender.com).*

Pathway enrichment analysis performed on the LNA-related comparisons resulted in the list of gene sets included in **Table 4.6**. No significant enriched gene set was found in the comparison LNA-NEG T vs LNA-NEG NT.

***Table 4.6*** *Significant enriched pathways in treated or not LNA-31-3p transfected HCC1954 cells, compared to controls*

| **LNA-31-3p NT vs LNA-NEG NT** | | | |
|---|---|---|---|
| **Term** | **Overlap** | **P-value** | **Adjusted P-value** |
| Interferon Alpha Response | 20/97 | 6.2E-09 | 3.0E-07 |
| Interferon Gamma Response | 28/200 | 5.6E-08 | 1.4E-06 |
| Cholesterol Homeostasis | 14/74 | 3.4E-06 | 5.5E-05 |
| mTORC1 Signaling | 24/200 | 7.8E-06 | 9.4E-05 |
| TNF-alpha Signaling via NF-kB | 22/200 | 7.1E-05 | 6.8E-04 |
| Hypoxia | 21/200 | 2.0E-04 | 1.6E-03 |
| Unfolded Protein Response | 14/113 | 4.3E-04 | 2.9E-03 |
| Myc Targets V1 | 17/200 | 7.1E-03 | 3.8E-02 |
| Inflammatory Response | 17/200 | 7.1E-03 | 3.8E-02 |
| **LNA-31-3p T vs LNA-NEG T** | | | |
| Interferon Alpha Response | 18/97 | 1.5E-08 | 5.2E-07 |
| Interferon Gamma Response | 26/200 | 2.7E-08 | 5.2E-07 |
| Unfolded Protein Response | 19/113 | 3.3E-08 | 5.2E-07 |
| TNF-alpha Signaling via NF-kB | 25/200 | 1.1E-07 | 1.3E-06 |
| p53 Pathway | 22/200 | 5.4E-06 | 5.2E-05 |
| Hypoxia | 19/200 | 1.7E-04 | 1.4E-03 |
| UV Response Up | 13/158 | 6.0E-03 | 4.1E-02 |
| Apoptosis | 13/161 | 7.0E-03 | 4.2E-02 |

**Figure 4.20** is the schematic representation showing the shared pathways between the two comparisons.

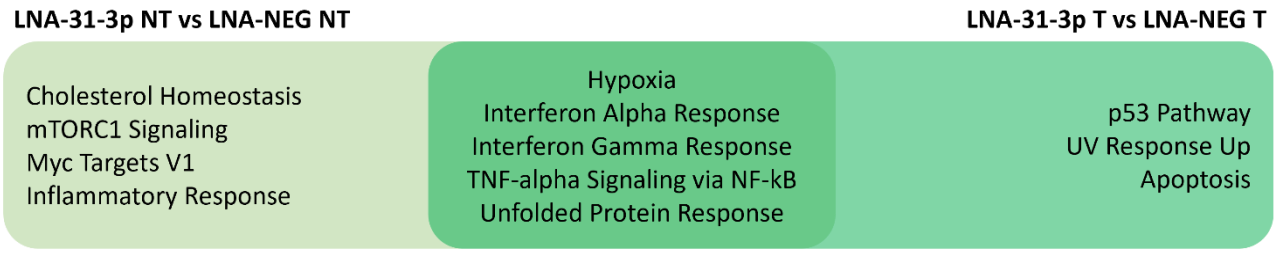


***Figure 4.20**. Schematic representation showing the significant enriched MSigDB Hallmarks gene sets that are shared between LNA-31-3p NT vs LNA-NEG NT and LNA-31-3p T vs LNA-NEG T comparisons in HCC1954 cells.*

In order to exploit results from both the upmodulation and the downmodulation of miR-31-3p in the same cell line, I also checked which pathways were enriched when only the downmodulated genes by the miRNA (miR-31-3p NT vs miR-NEG NT_down) and the upmodulated genes by its inhibitor LNA-31-3p (LNA-31-3p NT vs LNA-NEG NT_up) were considered for the enrichment analysis, highlighting the commonalities (**Figure 4.21**). It is interesting to note that *mTORC1 Signaling* comes out as a core modulated pathway even in this context. Many of the other recurrent gene sets, like *TGF-beta Signaling*, *TNF-alpha Signaling via NF-kB* and *p53 Pathway* are all functionally interconnected with each other, with *mTORC1 signaling* and with HER2 signaling pathway.

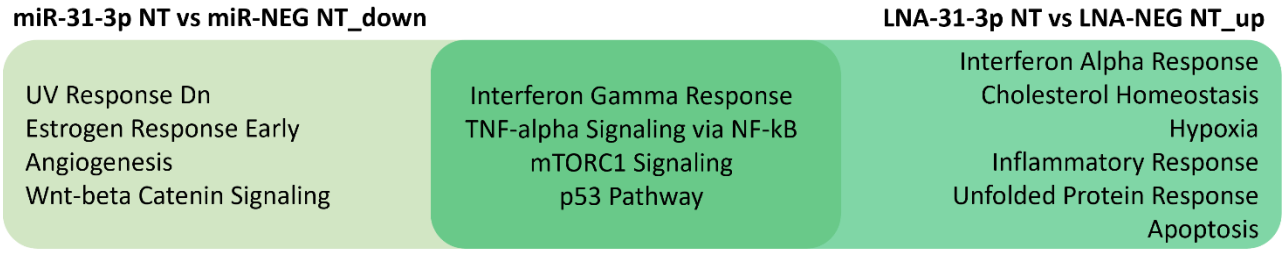


***Figure 4.21***. *Schematic representation showing the significant enriched MsigDB Hallmarks gene sets that are shared between miR-31-3p NT vs miR-NEG NT and LNA-31-3p T vs LNA-NEG T comparisons in HCC1954 cells.*

Finally, I performed IPA analysis also in HCC1954-related comparisons and it revealed, for example, that the most predicted activated pathway in non-treated miR-31-3p overexpressing HCC1954 cells was *PI3K/AKT Signaling* (z-score 3.27). Since the significant activated and inhibited pathways in the different comparisons were numerous, I decided to see which cellular functions were positively or negatively enriched, so that single interacting pathways were grouped together in higher functional categories. In miR-31-3p NT vs miR-NEG NT comparison, the most significantly activated functional category was *cell proliferation of tumor cell lines* (z-score=3.36). *Cell proliferation of breast cancer cell line* (z-score=2.36) was the most significant among the top 10 activated functional categories in miR-31-3p T vs miR-NEG T comparison. In the same group, *Apoptosis of epithelial cell line* (z-score=-2.78) was, instead, the most significantly inhibited category. On the contrary, in both LNA-31-3p vs LNA-NEG comparisons, regardless of the presence of the treatment, *cell death of tumor cells* (z-score=3.14 in the non-treated group and z-score=4.65 in trastuzumab-treated group) had the highest significance among the top 5 activated functional categories, while, coherently, *cell viability of carcinoma cell lines* (z-score=-2.68)

was included in the top 5 inhibited functional categories. These results are in line with what I observed in *in vitro* experiments in 2D and 3D settings.

Thus, taking into consideration the results obtained from *in vitro* and *in vivo* experiments described in the previous chapters, together with the RNAseq analyses, it can be concluded that miR-31-3p modulation in the two HER2+ breast cancer cell lines SKBr3 and HCC1954 considerably affects cell proliferation and viability upon trastuzumab treatment. Future experiments will unveil more details on the precise mechanism of action and direct molecular interactions of the miRNA.

### 4.6 MiR-31-3p negatively correlates with an activation of immune cell subsets in the NeoALTTO study

The experiments described so far suggest that miR-31-3p exerts an active role in HER2+ breast cancer cells. On the contrary, the modulation of miR-382-3p led to minor changes in in tumor behavior. The immune system, as described in the introduction, plays an important role in the context of trastuzumab response. Thus, I hypothesized that miR-382-3p could be effective in the immune compartment. In collaboration with the Bioinformatics and Biostatistics Unit, a correlation analysis between miRNA expression and both the immune infiltrate in the NeoALTTO study and 60 immune-related metagenes was performed (28 immuno signature by Charoentong et al., 13 by Safonov et al., 14 tumor-infiltrating immune cells population by CIBERSORT and immune-related metagenes 5 by Rody et al) [212–215]. Both predictive miRNAs were included in this analysis. No correlation was found between miRNA expression and distribution of TILs in

terms of number of infiltrating lymphocytes detected by IHC in patient biopsies. Correlation analysis of the expression of each miRNA and different immune-related metagenes are reported in **Table 4.7**, considering a Spearman correlation coefficient >0.30 in absolute value.

***Table 4.7**. Summary of the results of the correlation analysis between miRNA expression in the NeoALTTO study and immune metagenes.*

| Signature with Spearman Correlation coeff. >0.30 in absolute value | miR | Spearman Correlation coeff. | 95% CI | | N |
|---|---|---|---|---|---|
| S2C - Activated CD4 T cell[a] | miR_31_3p | -0.30 | -0.51 | -0.05 | 61 |
| S3C- Activated CD8 T cell [a] | miR_31_3p | -0.37 | -0.56 | -0.12 | 61 |
| S7C -Central memory CD4 T cell[a] | miR_31_3p | -0.38 | -0.57 | -0.14 | 61 |
| S13C - Immature B cell[a] | miR_31_3p | -0.35 | -0.55 | -0.10 | 61 |
| S25C -T follicular helper cell[a] | miR_31_3p | -0.32 | -0.53 | -0.07 | 61 |
| S3S - Cytolytic[b] | miR_31_3p | -0.31 | -0.52 | -0.06 | 61 |
| S6S - LCK[b] | miR_31_3p | -0.37 | -0.56 | -0.12 | 61 |
| S10S -NK[b] | miR_31_3p | -0.30 | -0.51 | -0.05 | 61 |
| Plasma_cells[c] | miR_31_3p | -0.39 | -0.58 | -0.15 | 61 |
| Mast_cells_activated[c] | miR_31_3p | 0.31 | 0.07 | 0.52 | 61 |
| LCK [d] | miR_31_3p | -0.38 | -0.57 | -0.13 | 61 |
| MHC II[d] | miR_31_3p | -0.34 | -0.54 | -0.10 | 61 |
| | | | | | |
| S3C Activated CD8 T cell [a] | miR_382_3p | -0.39 | -0.58 | -0.14 | 60 |
| S3S Cytolytic [b] | miR_382_3p | -0.30 | -0.51 | -0.05 | 60 |
| Plasma_cells [c] | miR_382_3p | -0.32 | -0.53 | -0.07 | 60 |

*a Charoentong et al. Cell Reports 18, 248–262, January 3, 2017; b Safonov et al Cancer Res (2017) 77 (12): 3317–3324., c tumor-infiltrating immune cells (TIICs) population generated by CIBERSORT; d Pizzamiglio et al. Clin Cancer Res (2021) 27 (23): 6307–6313 7. Rody et al . Breast Cancer Res 2009; 11 :R15.*

These analyses suggested that miR-31-3p, in particular, negatively correlated with the presence of activated immune cell subsets, except for mast cells, which however still have a controversial role in breast cancer responsiveness to anti-HER2 therapies [230]. As for miR-382-3p, despite its opposite correlation with pCR to miR-31-3p, it showed a similar pattern of correlation but with fewer signatures. Further analyses and experiments are

needed to explore miRNA-immune system relationship in the context of trastuzumab treatment.

In conclusion, the results described in this PhD thesis demonstrate that overexpression of miR-31-3p was able to increase HER2 activity and cell number of non-treated and trastuzumab-treated HER2-addicted SKBr3 cells. On the contrary, HER2 non-addicted HCC1954 cells transfected with miR-31-3p inhibitor (LNA-31-3p) alone or in combination with miR-382-3p showed an increased response to trastuzumab *in vitro*, but the effect on cell viability was mainly due to miR-31-3p inhibition. Moreover, LNA-31-3p alone was able to reduce HCC1954 cell viability also in a 3D setting, regardless of trastuzumab treatment. According to the RNAseq analyses, these biological effects could be mediated by miR-31-3p modulation of TGF-β and mTOR signaling pathways. Functional studies will better explore the molecular mechanisms involved and will help identifying direct miRNA targets.

The results obtained with LNA-31-3p were then validated also *in vivo* in SCID mice: combination of LNA-31-3p administration and trastuzumab treatment led to the most significant tumor weight reduction in comparison with control group.

Finally, correlation analyses between the expression of the miRNAs of interest in the neoALTTO series and available immune signatures and metagenes revealed that miR-31-3p expression in patients negatively correlated with the activation of immune cell subsets. Future experiments will assess the effect of miRNA modulation on the immune compartment, which plays a crucial role in tumor response to trastuzumab.

# 5 DISCUSSION

At present, overcoming resistance to treatment is one of the biggest challenges of cancer research. Enormous achievements have been made in drug development in the past decades; however, intrinsic or acquired resistance mechanisms are responsible for most events of relapse, a major cause of cancer-related death. HER2+ breast cancer patient's resistance to trastuzumab treatment is, unfortunately, a crucial example. Alternative anti-HER2 agents have been already proposed and tested alone or in combination with trastuzumab. One of the best performing strategies at present is double blocking of HER2 by administration of trastuzumab and pertuzumab. Pertuzumab synergizes with trastuzumab by interfering with HER2 dimerization with other HER receptors and blocking ligand-activated signaling from HER2/EGFR and HER2/HER3 heterodimers [231]. The tyrosine-kinase inhibitor lapatinib was proposed, instead, to overcome resistance to trastuzumab mediated by IGF1R upregulation or by the presence of HER2 truncated forms. The NeoALTTO clinical study was conducted to compare trastuzumab and lapatinib combination (plus chemotherapy) against single agents (plus chemotherapy) in a neoadjuvant setting for HER2+ early breast cancer patients. Although higher pCR rates were achieved upon combination administration, lapatinib-containing treatment arms were linked to higher percentages of adverse events [232]. Moreover, many HER2 overexpressing breast malignancies also escape the combinatorial approaches. With the intent to avoid patient's overtreatment and unnecessary side effects, our group have recently identified a two tumor miRNA-based signature comprising miR-31-3p (Odds Ratio (OR) 0.70, 95% Confidence Interval (CI): 0.53–0.92) and miR-382-3p (OR 1.39, 95% CI:

1.01–1.91), that predicts response in the trastuzumab arm of the NeoALTTO study, helping the identification of patients who would benefit more from the single agent regiment.

In this PhD thesis, I demonstrated that miR-31-3p, besides being a powerful biomarker, also plays an active role in reducing cell response to trastuzumab *in vitro* and *in vivo*. I started the investigation of the two miRNAs by analysing their basal expression in different HER2+ breast cancer cell lines. Both miRNAs displayed a varied range of expression: HCC1954 cells express miR-31-3p 10 times more than SKBr3 cells, around 30 times more than MDAMB361 and 100 times more than BT474. It was interesting to note that miR-31-5p, the other mature miRNA encoded by MIR31, is 10 times more expressed than miR-31-3p in all cell lines, consequently showing a comparable trend of expression between the different models to its complementary strand. This result suggests that each cell line differently regulates the expression of the precursor miRNA, but the strand selection always favours the 5p over the 3p mature miRNA in all cases and with the same ratio. Nevertheless, in the predictive signature it was miR-31-3p that statistically "weighted" more, since miR-31-5p removal from the model did not sensibly affect the power of the signature predictivity. It is conceivable that even a slight perturbation of the basal lower levels of miR-31-3p causes a more significant biological effect then what would occur with miR-31-5p expression fluctuations. MiR-382-3p is expressed 15 times more in MDAMB361 than in SKBr3, 30 times more than in HCC1954 and 100 times more than in BT474. It could be interesting to address these findings because the peculiar high peaks of expression of miR-31-3p in HCC1954 cells, and miR-382-3p in MDAMB361 cell,

could be related to cell line specific mechanisms that might give insights on miRNA biological role.

A limitation of the present work is that I performed all the experiments on SKBr3 and HCC1954 cells, which, differently from BT474 and MDAMB361, are both ER negative. Half of the enrolled patients in the NeoALTTO study were HER2+/ER+, and ER upmodulation is one of the escape mechanisms tumors cells use to compensate HER2 blockade. Future studies will have to address the effect of miR-31-3p and miR-382-3p in ER+ breast cancer cells, even though it is important to keep in mind that the predictive capability of the miRNA signature composed by the two miRNAs is independent from ER status. SKBr3 and HCC1954 cell lines are HER2+/ER-/PR-, and both present a loss-of-function mutation in *TP53*. HCC1954 cells also present a gain-of-function mutation in *PIK3CA*, gene coding for PI3K, which has been linked to resistance to trastuzumab, even in the NeoALTTO study, because it sustains the activation of HER2 signaling cascade upon HER2 blocking [232–234]. This is supported by the results of the western blot analysis assessing HER2 phosphorylation status upon 1h, 9h and 24h of trastuzumab treatment of HCC1954 cells in the 2D assay. Indeed, 1h after drug administration, despite pHER2 downmodulation, pAKT and pMAPK levels not only are not downmodulated, but they are even higher than in non-treated cells.

Considering the non-treated conditions, a decrease in pHER2 expression over time is evident in both SKBr3 and HCC1954 cells. This phenomenon may be attributed to the medium change occurring at the time of trastuzumab treatment, which can give a rapid

boost of HER2 activation in all experimental conditions, which fades overtime upon nutrient consumption. Moreover, a rise in proliferation rate results in a higher cellular confluence, which, in turn, elicits a negative feedback effect on HER2 activity.

MiR-31-3p overexpression increased pHER2 levels in both trastuzumab-treated and non-treated SKBr3 cells, paralleled by a higher activation of MAPK only and solely in the treated condition, while AKT activity always diminished. This result is puzzling considering the increase in cell number upon miR-31-3p upmodulation in both non-treated and trastuzumab-treated SKBr3 cells grown in 3D for five days. One possible explanation can be found in the wide range of molecular interactions established by AKT and MAPK in multiple key pathways like angiogenesis, metabolism, growth, proliferation, survival, protein synthesis, transcription, and apoptosis, and miR-31-3p could target at the same time positive and negative regulators of the two kinases. For example, according to the results of the RNAseq performed on non-treated and trastuzumab treated (for 24h) SKBr3 cells, miR-31-3p upmodulation reduces both PPP2R5C, regulatory subunit of AKT negative regulator Protein Phosphatase 2A (PP2A), and Integrin Subunit Beta 6 (ITGB6), which is known to promote AKT activation [235,236]. Thus, the biological effect elicited by miR-31-3p upregulation is the result of the sum of different and sometimes contrasting molecular modulations. However, one must also consider that the molecular interactions engaged in 2D at 24h may not be the same established in 3D and maintained over a period of 5 days. Moreover, RNAseq analysis gives insight into gene expression regulations that may not be mirrored at protein level due to post-transcriptional regulatory events. Indeed,

the result of my preliminary western blot analysis assessing HER3, FOXO3, β-catenin and CREB1 levels, was not completely consistent with the output of SKBr3 RNAseq.

As mentioned before, HCC1954 cell line expresses much higher basal levels of miR-31-3p than all the other HER2+ cell lines analysed, and it is also not responsive to trastuzumab. Thus, this cell line was the perfect model to evaluate the effect of miR-31-3p inhibition on cell sensitiveness to treatment with the anti-HER2 agent. The initial experiments testing the combination of miR-382-3p overexpression and miR-31-3p inhibition with LNA-31-3p, suggested that the latter had a greater impact on HCC1954 cell viability, which I was even able to appreciate in the 2D assay. Indeed, LNA-31-3p transfection plus trastuzumab treatment is able to significantly reduce HCC1954 cell number compared to the treated-only control. Considering the 3D assay, inhibition of miR-31-3p significantly reduced cell number in non-treated and trastuzumab-treated conditions.

Taking into account both 2D and 3D assay results, it is evident that it is only LNA-31-3p that reduces cell viability, and trastuzumab never exerted any effect. On the contrary, trastuzumab alone did significantly reduce tumor weight *in vivo*, and its combination with LNA-31-3p was even more powerful. One important difference between all the settings is that SCID mice, although lacking functional lymphocytes, retain elements of the innate immune system including natural killer cells and macrophages. As already mentioned, the ability of trastuzumab to trigger ADCC is a major contributor to treatment efficacy. Indeed, it has been demonstrated that patients who have pre-existing high levels of immune cells or immune-related genes in their tumour microenvironment respond best to

HER2-targeted therapies [237]. Thus, it could be hypothesized that the significant reduction in tumor weight given by trastuzumab, is mediated by the drug-dependent activation of the innate immune system. The combination with the anti-proliferative activity of LNA-31-3p then led to an even greater reduction in tumor weights. This hypothesis is supported by the correlation analysis performed between miRNA expression and both the immune infiltrate in the NeoALTTO study and 60 immune-related metagenes. These analyses suggest that miR-31-3p could negatively impact on the immune system activity. The only positively correlated feature with miR-31-3p expression was *"mast_cell_activated"* metagene. Interestingly, in 2020, Majorini MT *et al* from our Institute demonstrated that mast cell infiltration is predictive of an increased risk of relapse in patients with HER2+ breast cancer treated with adjuvant trastuzumab [238]. RNAseq analysis conducted on HCC1954 cells revealed that miR-31-3p modulation, both in non-treated and treated cells, altered the expression of immune-related genes. Indeed, among the pathways significantly modulated in the different comparisons were included *Inflammatory Response*, *Interferon Gamma Response*, *Interferon Alpha Response* and *TNF-alpha Signaling via NF-kB*. Interferon proteins are a family of cytokines typically released by the host cells in the presence of a pathogen and modulate the immune response. There are two main classes of interferons (INFs): type I IFNs (13 isoforms of IFN-$\alpha$, IFN-$\beta$, IFN-$\varepsilon$, IFN-$\kappa$ and IFN-$\omega$) and type II IFN (IFN-$\gamma$). In cancer, they can exert both anti- and pro-tumor effects. In 2011, Stagg J et al demonstrated that trastuzumab efficacy depends on both type I and type II IFNs release [239]. Genes belonging to *Interferon alpha response* pathway resulted enriched in LNA-related comparisons and retained this significant enrichment

even considering only the upmodulated (and not the downmodulated) genes upon LNA-31-3p transfection. This result suggests that miR-31-3p inhibition in HCC1954 cells induced an upmodulation of molecules involved in the IFN-$\alpha$ response pathway that could explain the additive antitumor effect of LNA-31-3p and trastuzumab in SCID mice. This is particularly interesting because the entire family of type I interferons is encoded by genes located right beside *MIR31* coding sequence on chromosome 9p21.3. It could be speculated that miR-31-3p plays a role as a locally transcriptional regulator of type I interferons. Functional studies are necessary to investigate such intriguing mechanism.

The *in vivo* study demonstrated that the combination of trastuzumab and miR-31-3p inhibition significantly reduced HCC1954 tumors. However, having obtained a statistically significant result only upon injection of HCC1954 cells transfected *in vitro* with LNA-31-3p, and not after direct intratumor injection of LNA-31-3p in mice, we still do not have a proof-of-concept experiment that would support LNA-31-3p as a miRNA-based therapy. A deeper understanding of miR-31-3p mechanism of action is needed and the RNAseq performed on SKBr3 cells and HCC1954 is a huge source of information that will have to be summed up, for example, with immunohistochemistry analyses on the tumors of the *in vivo* experiment to characterize the immune compartment response to miRNA modulation in tumor cells. Identifying which are the other possible miRNA expressing cells in the tumor microenvironment besides the tumor could also help adding pieces to the puzzle we are trying to delineate. Indeed, we planned to perform an in situ hybridization (ISH) on HER2+ breast cancer tissue sections in order to visualize miRNA expressing cells. It is also conceivable that miR-31-3p could be exchanged between tumor

cells and stromal cells, incapsulated in exosomes. The ISH assay will be a starting point for future additional evaluations. The literature already provides hits on this matter: miR-31-5p, miR-31-3p brother miRNA mature strand, was demonstrated to have an active role in inducing an exhausted phenotype in T cells. Since MIR31 mature miRNAs seem to be closely transcriptionally connected, we could hypothesize a role also for miR-31-3p [240]. Moreover, miR-31-5p was identified as biomarker of $CD56^{bright}$ NK cells, which are immature NK cells that exert limited cytotoxic capacity [241]. It is interesting to note that in the same work, even though the authors focus only on the 5p strand, also miR-31-3p appears in the list of significantly upregulated miRNAs in $CD56^{bright}$ NK cells when compared to the mature counterpart $CD56^{dim}$ NK cells. These data support an immune-modulating role of miR-31 that, in the context of trastuzumab treatment, could result detrimental for an efficient anti-tumor activity of the drug.

Finally, correlation analyses performed on the NeoALTTO study between gene and miRNA expression and the RNAseq analyses on HER2+ breast cancer cell lines will help identify direct miR-31-3p targets, which could potentially serve as additional therapeutic options to be explored for the clinic.

In conclusion, the results presented in this PhD thesis demonstrate that miR-31-3p, besides being a powerful biomarker of response to trastuzumab together with miR-382-3p, has an active role in modulating HER2+ breast cancer cell viability and proliferation, both *in vitro* and *in vivo*, possibly by affecting major signaling pathways like TGF-β Signaling and mTOR Signaling. Moreover, evidence of miR-31-3p involvement in moulding the activity

of the immune system provided both by the literature and by correlation analysis performed on the NeoALTTO study, supports once more miR-31-3p (and possibly miR-31-5p) inhibition as a possible winning strategy to restore response to trastuzumab in resistant HER2+ breast cancer patients (**Figure 5.1**).

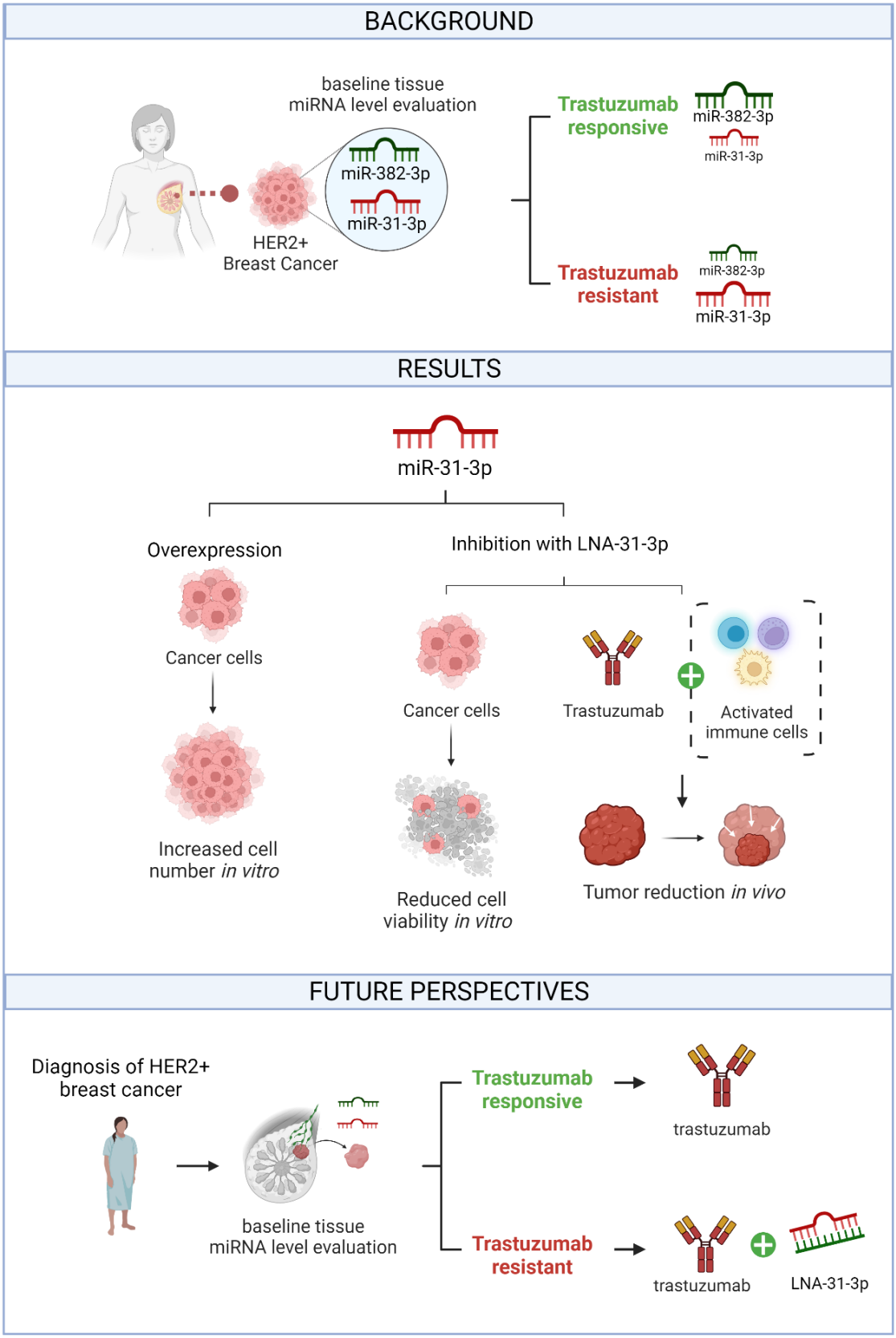


***Figure 5.1*** *Thesis graphical summary (Created with BioRender.com).*

# 6 REFERENCES


1. McGhee, D.E.; Steele, J.R. Breast Biomechanics: What Do We Really Know? *Physiology (Bethesda)* **2020**, *35*, 144–156, doi:10.1152/physiol.00024.2019.
2. Gaskin, K.M.; Peoples, G.E.; McGhee, D.E. The Fibro-Adipose Structure of the Female Breast: A Dissection Study. *Clin Anat* **2020**, *33*, 146–155, doi:10.1002/ca.23505.
3. Alipour, S. Physical Breast Examination in Pregnancy and Lactation. *Adv Exp Med Biol* **2020**, *1252*, 9–16, doi:10.1007/978-3-030-41596-9_2.
4. Tiede, B.; Kang, Y. From Milk to Malignancy: The Role of Mammary Stem Cells in Development, Pregnancy and Breast Cancer. *Cell Res* **2011**, *21*, 245–257, doi:10.1038/cr.2011.11.
5. Watson, C.J.; Khaled, W.T. Mammary Development in the Embryo and Adult: A Journey of Morphogenesis and Commitment. *Development* **2008**, *135*, 995–1003, doi:10.1242/dev.005439.
6. Hilton, H.N.; Clarke, C.L.; Graham, J.D. Estrogen and Progesterone Signalling in the Normal Breast and Its Implications for Cancer Development. *Mol Cell Endocrinol* **2018**, *466*, 2–14, doi:10.1016/j.mce.2017.08.011.
7. Arnold, M.; Morgan, E.; Rumgay, H.; Mafra, A.; Singh, D.; Laversanne, M.; Vignat, J.; Gralow, J.R.; Cardoso, F.; Siesling, S.; et al. Current and Future Burden of Breast Cancer: Global Statistics for 2020 and 2040. *Breast* **2022**, *66*, 15–23, doi:10.1016/j.breast.2022.08.010.
8. Sung, H.; Ferlay, J.; Siegel, R.L.; Laversanne, M.; Soerjomataram, I.; Jemal, A.; Bray, F. Global Cancer Statistics 2020: GLOBOCAN Estimates of Incidence and Mortality

Worldwide for 36 Cancers in 185 Countries. *CA Cancer J Clin* **2021**, *71*, 209–249, doi:10.3322/caac.21660.

9. Anderson, B.O.; Ilbawi, A.M.; Fidarova, E.; Weiderpass, E.; Stevens, L.; Abdel-Wahab, M.; Mikkelsen, B. The Global Breast Cancer Initiative: A Strategic Collaboration to Strengthen Health Care for Non-Communicable Diseases. *Lancet Oncol* **2021**, *22*, 578–581, doi:10.1016/S1470-2045(21)00071-1.
10. Maajani, K.; Jalali, A.; Alipour, S.; Khodadost, M.; Tohidinik, H.R.; Yazdani, K. The Global and Regional Survival Rate of Women With Breast Cancer: A Systematic Review and Meta-Analysis. *Clin Breast Cancer* **2019**, *19*, 165–177, doi:10.1016/j.clbc.2019.01.006.
11. Sun, Y.-S.; Zhao, Z.; Yang, Z.-N.; Xu, F.; Lu, H.-J.; Zhu, Z.-Y.; Shi, W.; Jiang, J.; Yao, P.-P.; Zhu, H.-P. Risk Factors and Preventions of Breast Cancer. *Int J Biol Sci* **2017**, *13*, 1387–1397, doi:10.7150/ijbs.21635.
12. Eriksson, M.; Czene, K.; Pawitan, Y.; Leifland, K.; Darabi, H.; Hall, P. A Clinical Model for Identifying the Short-Term Risk of Breast Cancer. *Breast Cancer Res* **2017**, *19*, 29, doi:10.1186/s13058-017-0820-y.
13. Kim, S.; Tran, T.X.M.; Song, H.; Park, B. Microcalcifications, Mammographic Breast Density, and Risk of Breast Cancer: A Cohort Study. *Breast Cancer Res* **2022**, *24*, 96, doi:10.1186/s13058-022-01594-0.
14. Román, M.; Louro, J.; Posso, M.; Alcántara, R.; Peñalva, L.; Sala, M.; Del Riego, J.; Prieto, M.; Vidal, C.; Sánchez, M.; et al. Breast Density, Benign Breast Disease, and Risk

of Breast Cancer over Time. *Eur Radiol* **2021**, *31*, 4839–4847, doi:10.1007/s00330-020-07490-5.

15. Giaquinto, A.N.; Sung, H.; Miller, K.D.; Kramer, J.L.; Newman, L.A.; Minihan, A.; Jemal, A.; Siegel, R.L. Breast Cancer Statistics, 2022. *CA Cancer J Clin* **2022**, *72*, 524–541, doi:10.3322/caac.21754.
16. Munsell, M.F.; Sprague, B.L.; Berry, D.A.; Chisholm, G.; Trentham-Dietz, A. Body Mass Index and Breast Cancer Risk According to Postmenopausal Estrogen-Progestin Use and Hormone Receptor Status. *Epidemiol Rev* **2014**, *36*, 114–136, doi:10.1093/epirev/mxt010.
17. Picon-Ruiz, M.; Morata-Tarifa, C.; Valle-Goffin, J.J.; Friedman, E.R.; Slingerland, J.M. Obesity and Adverse Breast Cancer Risk and Outcome: Mechanistic Insights and Strategies for Intervention. *CA Cancer J Clin* **2017**, *67*, 378–397, doi:10.3322/caac.21405.
18. Agresti, R.; Meneghini, E.; Baili, P.; Minicozzi, P.; Turco, A.; Cavallo, I.; Funaro, F.; Amash, H.; Berrino, F.; Tagliabue, E.; et al. Association of Adiposity, Dysmetabolisms, and Inflammation with Aggressive Breast Cancer Subtypes: A Cross-Sectional Study. *Breast Cancer Res Treat* **2016**, *157*, 179–189, doi:10.1007/s10549-016-3802-3.
19. Ren, W.; Chen, M.; Qiao, Y.; Zhao, F. Global Guidelines for Breast Cancer Screening: A Systematic Review. *Breast* **2022**, *64*, 85–99, doi:10.1016/j.breast.2022.04.003.
20. Autier, P.; Boniol, M. Mammography Screening: A Major Issue in Medicine. *Eur J Cancer* **2018**, *90*, 34–62, doi:10.1016/j.ejca.2017.11.002.

21. Beňačka, R.; Szabóová, D.; Guľašová, Z.; Hertelyová, Z.; Radoňák, J. Classic and New Markers in Diagnostics and Classification of Breast Cancer. *Cancers (Basel)* **2022**, *14*, 5444, doi:10.3390/cancers14215444.
22. Mamouch, F.; Berrada, N.; Aoullay, Z.; El Khanoussi, B.; Errihani, H. Inflammatory Breast Cancer: A Literature Review. *World J Oncol* **2018**, *9*, 129–135, doi:10.14740/wjon1161.
23. Giuliano, A.E.; Edge, S.B.; Hortobagyi, G.N. Eighth Edition of the AJCC Cancer Staging Manual: Breast Cancer. *Ann Surg Oncol* **2018**, *25*, 1783–1785, doi:10.1245/s10434-018-6486-6.
24. Perou, C.M.; Sørlie, T.; Eisen, M.B.; van de Rijn, M.; Jeffrey, S.S.; Rees, C.A.; Pollack, J.R.; Ross, D.T.; Johnsen, H.; Akslen, L.A.; et al. Molecular Portraits of Human Breast Tumours. *Nature* **2000**, *406*, 747–752, doi:10.1038/35021093.
25. Parker, J.S.; Mullins, M.; Cheang, M.C.U.; Leung, S.; Voduc, D.; Vickery, T.; Davies, S.; Fauron, C.; He, X.; Hu, Z.; et al. Supervised Risk Predictor of Breast Cancer Based on Intrinsic Subtypes. *J Clin Oncol* **2009**, *27*, 1160–1167, doi:0.1200/JCO.2008.18.1370.
26. Orrantia-Borunda, E.; Anchondo-Nuñez, P.; Acuña-Aguilar, L.E.; Gómez-Valles, F.O.; Ramírez-Valdespino, C.A. Subtypes of Breast Cancer. In *Breast Cancer*; Mayrovitz, H.N., Ed.; Exon Publications: Brisbane (AU), 2022 ISBN 978-0-645-33203-2.
27. Gao, J.J.; Swain, S.M. Luminal A Breast Cancer and Molecular Assays: A Review. *Oncologist* **2018**, *23*, 556–565, doi:10.1634/theoncologist.2017-0535.
28. Ades, F.; Zardavas, D.; Bozovic-Spasojevic, I.; Pugliano, L.; Fumagalli, D.; de Azambuja, E.; Viale, G.; Sotiriou, C.; Piccart, M. Luminal B Breast Cancer: Molecular

Characterization, Clinical Management, and Future Perspectives. *J Clin Oncol* **2014**, *32*, 2794–2803, doi:10.1200/JCO.2013.54.1870.

29. Li, Z.-H.; Hu, P.-H.; Tu, J.-H.; Yu, N.-S. Luminal B Breast Cancer: Patterns of Recurrence and Clinical Outcome. *Oncotarget* **2016**, *7*, 65024–65033, doi:10.18632/oncotarget.11344.
30. Loibl, S.; Gianni, L. HER2-Positive Breast Cancer. *Lancet* **2017**, *389*, 2415–2429, doi:10.1016/S0140-6736(16)32417-5.
31. Goutsouliak, K.; Veeraraghavan, J.; Sethunath, V.; De Angelis, C.; Osborne, C.K.; Rimawi, M.F.; Schiff, R. Towards Personalized Treatment for Early Stage HER2-Positive Breast Cancer. *Nat Rev Clin Oncol* **2020**, *17*, 233–250, doi:10.1038/s41571-019-0299-9.
32. Bianchini, G.; De Angelis, C.; Licata, L.; Gianni, L. Treatment Landscape of Triple-Negative Breast Cancer - Expanded Options, Evolving Needs. *Nat Rev Clin Oncol* **2022**, *19*, 91–113, doi:10.1038/s41571-021-00565-2.
33. Turner, K.M.; Yeo, S.K.; Holm, T.M.; Shaughnessy, E.; Guan, J.-L. Heterogeneity within Molecular Subtypes of Breast Cancer. *Am J Physiol Cell Physiol* **2021**, *321*, C343–C354, doi:10.1152/ajpcell.00109.2021.
34. Mohamed, G.A.; Mahmood, S.; Ognjenovic, N.B.; Lee, M.K.; Wilkins, O.M.; Christensen, B.C.; Muller, K.E.; Pattabiraman, D.R. Lineage Plasticity Enables Low-ER Luminal Tumors to Evolve and Gain Basal-like Traits. *Breast Cancer Research* **2023**, *25*, 23, doi:10.1186/s13058-023-01621-8.

35. LeVee, A.; Spector, K.; Larkin, B.; Dezem, F.; Plummer, J.; Dadmanesh, F.; Patil, S.; McArthur, H.L. Incidence and Prognostic Impact of HER2-positivity Loss after Dual HER2-directed Neoadjuvant Therapy for HER2+ Breast Cancer. *Cancer Med* **2023**, *12*, 10647–10659, doi:10.1002/cam4.5817.
36. Niikura, N.; Liu, J.; Hayashi, N.; Mittendorf, E.A.; Gong, Y.; Palla, S.L.; Tokuda, Y.; Gonzalez-Angulo, A.M.; Hortobagyi, G.N.; Ueno, N.T. Loss of Human Epidermal Growth Factor Receptor 2 (HER2) Expression in Metastatic Sites of HER2-Overexpressing Primary Breast Tumors. *J Clin Oncol* **2012**, *30*, 593–599, doi:10.1200/JCO.2010.33.8889.
37. Gote, V.; Nookala, A.R.; Bolla, P.K.; Pal, D. Drug Resistance in Metastatic Breast Cancer: Tumor Targeted Nanomedicine to the Rescue. *Int J Mol Sci* **2021**, *22*, 4673, doi:10.3390/ijms22094673.
38. Amin, D.N.; Sergina, N.; Ahuja, D.; McMahon, M.; Blair, J.A.; Wang, D.; Hann, B.; Koch, K.M.; Shokat, K.M.; Moasser, M.M. Resiliency and Vulnerability in the HER2-HER3 Tumorigenic Driver. *Sci Transl Med* **2010**, *2*, 16ra7, doi:10.1126/scitranslmed.3000389.
39. Miricescu, D.; Totan, A.; Stanescu-Spinu, I.-I.; Badoiu, S.C.; Stefani, C.; Greabu, M. PI3K/AKT/MTOR Signaling Pathway in Breast Cancer: From Molecular Landscape to Clinical Aspects. *Int J Mol Sci* **2020**, *22*, 173, doi:10.3390/ijms22010173.
40. Parsons, R.; Simpson, L. PTEN and Cancer. *Methods Mol Biol* **2003**, *222*, 147–166, doi:10.1385/1-59259-328-3:147.

41. Manning, B.D.; Toker, A. AKT/PKB Signaling: Navigating the Network. *Cell* **2017**, *169*, 381–405, doi:10.1016/j.cell.2017.04.001.

42. Ullah, R.; Yin, Q.; Snell, A.H.; Wan, L. RAF-MEK-ERK Pathway in Cancer Evolution and Treatment. *Semin Cancer Biol* **2022**, *85*, 123–154, doi:10.1016/j.semcancer.2021.05.010.

43. Moasser, M.M. The Oncogene HER2: Its Signaling and Transforming Functions and Its Role in Human Cancer Pathogenesis. *Oncogene* **2007**, *26*, 6469–6487, doi:10.1038/sj.onc.1210477.

44. Nami, B.; Wang, Z. HER2 in Breast Cancer Stemness: A Negative Feedback Loop towards Trastuzumab Resistance. *Cancers* **2017**, *9*, 40, doi:10.3390/cancers9050040.

45. Nahta, R.; Yuan, L.X.H.; Zhang, B.; Kobayashi, R.; Esteva, F.J. Insulin-like Growth Factor-I Receptor/Human Epidermal Growth Factor Receptor 2 Heterodimerization Contributes to Trastuzumab Resistance of Breast Cancer Cells. *Cancer Res* **2005**, *65*, 11118–11128, doi:10.1158/0008-5472.CAN-04-3841.

46. Moasser, M.M. The Oncogene HER2: Its Signaling and Transforming Functions and Its Role in Human Cancer Pathogenesis. *Oncogene* **2007**, *26*, 6469–6487, doi:10.1038/sj.onc.1210477.

47. Triulzi, T.; Forte, L.; Regondi, V.; Di Modica, M.; Ghirelli, C.; Carcangiu, M.L.; Sfondrini, L.; Balsari, A.; Tagliabue, E. HER2 Signaling Regulates the Tumor Immune Microenvironment and Trastuzumab Efficacy. *Oncoimmunology* **2019**, *8*, e1512942, doi:10.1080/2162402X.2018.1512942.

48. Galogre, M.; Rodin, D.; Pyatnitskiy, M.; Mackelprang, M.; Koman, I. A Review of HER2 Overexpression and Somatic Mutations in Cancers. *Crit Rev Oncol Hematol* **2023**, *186*, 103997, doi:10.1016/j.critrevonc.2023.103997.
49. Hendriks, B.S.; Wiley, H.S.; Lauffenburger, D. HER2-Mediated Effects on EGFR Endosomal Sorting: Analysis of Biophysical Mechanisms. *Biophys J* **2003**, *85*, 2732–2745, doi:10.1016/S0006-3495(03)74696-7.
50. Hellyer, N.J.; Kim, M.S.; Koland, J.G. Heregulin-Dependent Activation of Phosphoinositide 3-Kinase and Akt via the ErbB2/ErbB3 Co-Receptor. *J Biol Chem* **2001**, *276*, 42153–42161, doi:10.1074/jbc.M102079200.
51. Wolff, A.C.; Hammond, M.E.H.; Allison, K.H.; Harvey, B.E.; Mangu, P.B.; Bartlett, J.M.S.; Bilous, M.; Ellis, I.O.; Fitzgibbons, P.; Hanna, W.; et al. Human Epidermal Growth Factor Receptor 2 Testing in Breast Cancer: American Society of Clinical Oncology/College of American Pathologists Clinical Practice Guideline Focused Update. *Arch Pathol Lab Med* **2018**, *142*, 1364–1382, doi:10.5858/arpa.2018-0902-SA.
52. Ji, H.; Xuan, Q.; Nanding, A.; Zhang, H.; Zhang, Q. The Clinicopathologic and Prognostic Value of Altered Chromosome 17 Centromere Copy Number in HER2 Fish Equivocal Breast Carcinomas. *PLoS One* **2015**, *10*, e0132824, doi:10.1371/journal.pone.0132824.
53. Slamon, D.J.; Clark, G.M.; Wong, S.G.; Levin, W.J.; Ullrich, A.; McGuire, W.L. Human Breast Cancer: Correlation of Relapse and Survival with Amplification of the HER-2/Neu Oncogene. *Science* **1987**, *235*, 177–182, doi:10.1126/science.3798106.

54. Moja, L.; Tagliabue, L.; Balduzzi, S.; Parmelli, E.; Pistotti, V.; Guarneri, V.; D'Amico, R. Trastuzumab Containing Regimens for Early Breast Cancer. *Cochrane Database Syst Rev* **2012**, *2012*, CD006243, doi:10.1002/14651858.CD006243.pub2.

55. Metzger-Filho, O.; Winer, E.P.; Krop, I. Pertuzumab: Optimizing HER2 Blockade. *Clin Cancer Res* **2013**, *19*, 5552–5556, doi:10.1158/1078-0432.CCR-13-0518.

56. Konecny, G.E.; Pegram, M.D.; Venkatesan, N.; Finn, R.; Yang, G.; Rahmeh, M.; Untch, M.; Rusnak, D.W.; Spehar, G.; Mullin, R.J.; et al. Activity of the Dual Kinase Inhibitor Lapatinib (GW572016) against HER-2-Overexpressing and Trastuzumab-Treated Breast Cancer Cells. *Cancer Res* **2006**, *66*, 1630–1639, doi:10.1158/0008-5472.CAN-05-1182.

57. Collins, D.M.; Conlon, N.T.; Kannan, S.; Verma, C.S.; Eli, L.D.; Lalani, A.S.; Crown, J. Preclinical Characteristics of the Irreversible Pan-HER Kinase Inhibitor Neratinib Compared with Lapatinib: Implications for the Treatment of HER2-Positive and HER2-Mutated Breast Cancer. *Cancers (Basel)* **2019**, *11*, 737, doi:10.3390/cancers11060737.

58. Kulukian, A.; Lee, P.; Taylor, J.; Rosler, R.; de Vries, P.; Watson, D.; Forero-Torres, A.; Peterson, S. Preclinical Activity of HER2-Selective Tyrosine Kinase Inhibitor Tucatinib as a Single Agent or in Combination with Trastuzumab or Docetaxel in Solid Tumor Models. *Mol Cancer Ther* **2020**, *19*, 976–987, doi:10.1158/1535-7163.MCT-19-0873.

59. Lewis Phillips, G.D.; Li, G.; Dugger, D.L.; Crocker, L.M.; Parsons, K.L.; Mai, E.; Blättler, W.A.; Lambert, J.M.; Chari, R.V.J.; Lutz, R.J.; et al. Targeting HER2-Positive Breast Cancer with Trastuzumab-DM1, an Antibody-Cytotoxic Drug Conjugate. *Cancer Res* **2008**, *68*, 9280–9290, doi:10.1158/0008-5472.CAN-08-1776.

60. Yver, A.; Agatsuma, T.; Soria, J.-C. The Art of Innovation: Clinical Development of Trastuzumab Deruxtecan and Redefining How Antibody-Drug Conjugates Target HER2-Positive Cancers. *Ann Oncol* **2020**, *31*, 430–434, doi:10.1016/j.annonc.2019.11.019.
61. Makhlin, I.; DeMichele, A. Trastuzumab Deruxtecan: An Antibody-Drug Conjugate Embracing Its Destiny in Breast Cancer. *Cell Rep Med* **2022**, *3*, 100668, doi:10.1016/j.xcrm.2022.100668.
62. Pegram, M.; Hsu, S.; Lewis, G.; Pietras, R.; Beryt, M.; Sliwkowski, M.; Coombs, D.; Baly, D.; Kabbinavar, F.; Slamon, D. Inhibitory Effects of Combinations of HER-2/Neu Antibody and Chemotherapeutic Agents Used for Treatment of Human Breast Cancers. *Oncogene* **1999**, *18*, 2241–2251, doi:10.1038/sj.onc.1202526.
63. Hamirani, Y.; Fanous, I.; Kramer, C.M.; Wong, A.; Salerno, M.; Dillon, P. Anthracycline- and Trastuzumab-Induced Cardiotoxicity: A Retrospective Study. *Med Oncol* **2016**, *33*, 82, doi:10.1007/s12032-016-0797-x.
64. Slamon, D.; Eiermann, W.; Robert, N.; Pienkowski, T.; Martin, M.; Press, M.; Mackey, J.; Glaspy, J.; Chan, A.; Pawlicki, M.; et al. Adjuvant Trastuzumab in HER2-Positive Breast Cancer. *N Engl J Med* **2011**, *365*, 1273–1283, doi:10.1056/NEJMoa0910383.
65. Hua, X.; Bi, X.-W.; Zhao, J.-L.; Shi, Y.-X.; Lin, Y.; Wu, Z.-Y.; Zhang, Y.-Q.; Zhang, L.-H.; Zhang, A.-Q.; Huang, H.; et al. Trastuzumab Plus Endocrine Therapy or Chemotherapy as First-Line Treatment for Patients with Hormone Receptor-Positive and HER2-Positive Metastatic Breast Cancer (SYSUCC-002). *Clin Cancer Res* **2022**, *28*, 637–645, doi:10.1158/1078-0432.CCR-21-3435.

66. Yang, H.; Qiu, M.; Feng, Y.; Wen, N.; Zhou, J.; Qin, X.; Li, J.; Liu, X.; Wang, X.; Du, Z. The Role of Radiotherapy in HER2+ Early-Stage Breast Cancer Patients after Breast-Conserving Surgery. *Front Oncol* **2022**, *12*, 903001, doi:10.3389/fonc.2022.903001.

67. Giordano, S.H.; Franzoi, M.A.B.; Temin, S.; Anders, C.K.; Chandarlapaty, S.; Crews, J.R.; Kirshner, J.J.; Krop, I.E.; Lin, N.U.; Morikawa, A.; et al. Systemic Therapy for Advanced Human Epidermal Growth Factor Receptor 2-Positive Breast Cancer: ASCO Guideline Update. *J Clin Oncol* **2022**, *40*, 2612–2635, doi:10.1200/JCO.22.00519.

68. Cortés, J.; Kim, S.-B.; Chung, W.-P.; Im, S.-A.; Park, Y.H.; Hegg, R.; Kim, M.H.; Tseng, L.-M.; Petry, V.; Chung, C.-F.; et al. Trastuzumab Deruxtecan versus Trastuzumab Emtansine for Breast Cancer. *N Engl J Med* **2022**, *386*, 1143–1154, doi:10.1056/NEJMoa2115022.

69. Modi, S.; Jacot, W.; Yamashita, T.; Sohn, J.; Vidal, M.; Tokunaga, E.; Tsurutani, J.; Ueno, N.T.; Prat, A.; Chae, Y.S.; et al. Trastuzumab Deruxtecan in Previously Treated HER2-Low Advanced Breast Cancer. *N Engl J Med* **2022**, *387*, 9–20, doi:10.1056/NEJMoa2203690.

70. Sidaway, P. T-DXd Active in HER2-Low Disease. *Nat Rev Clin Oncol* **2022**, *19*, 493, doi:10.1038/s41571-022-00663-9.

71. Li, Y.; Tsang, J.Y.; Tam, F.; Loong, T.; Tse, G.M. Comprehensive Characterization of HER2-Low Breast Cancers: Implications in Prognosis and Treatment. *EBioMedicine* **2023**, *91*, 104571, doi:10.1016/j.ebiom.2023.104571.

72. Giordano, S.H.; Franzoi, M.A.B.; Temin, S.; Anders, C.K.; Chandarlapaty, S.; Crews, J.R.; Kirshner, J.J.; Krop, I.E.; Lin, N.U.; Morikawa, A.; et al. Systemic Therapy for

Advanced Human Epidermal Growth Factor Receptor 2-Positive Breast Cancer: ASCO Guideline Update. *J Clin Oncol* **2022**, *40*, 2612–2635, doi:10.1200/JCO.22.00519.

73. Drebin, J.A.; Link, V.C.; Weinberg, R.A.; Greene, M.I. Inhibition of Tumor Growth by a Monoclonal Antibody Reactive with an Oncogene-Encoded Tumor Antigen. *Proc Natl Acad Sci U S A* **1986**, *83*, 9129–9133, doi:10.1073/pnas.83.23.9129.
74. Carter, P.; Presta, L.; Gorman, C.M.; Ridgway, J.B.; Henner, D.; Wong, W.L.; Rowland, A.M.; Kotts, C.; Carver, M.E.; Shepard, H.M. Humanization of an Anti-P185HER2 Antibody for Human Cancer Therapy. *Proc Natl Acad Sci U S A* **1992**, *89*, 4285–4289, doi:10.1073/pnas.89.10.4285.
75. Sawyers, C.L. Herceptin: A First Assault on Oncogenes That Launched a Revolution. *Cell* **2019**, *179*, 8–12, doi:10.1016/j.cell.2019.08.027.
76. Piccart-Gebhart, M.J.; Procter, M.; Leyland-Jones, B.; Goldhirsch, A.; Untch, M.; Smith, I.; Gianni, L.; Baselga, J.; Bell, R.; Jackisch, C.; et al. Trastuzumab after Adjuvant Chemotherapy in HER2-Positive Breast Cancer. *N Engl J Med* **2005**, *353*, 1659–1672, doi:10.1056/NEJMoa052306.
77. Romond, E.H.; Perez, E.A.; Bryant, J.; Suman, V.J.; Geyer, C.E.; Davidson, N.E.; Tan-Chiu, E.; Martino, S.; Paik, S.; Kaufman, P.A.; et al. Trastuzumab plus Adjuvant Chemotherapy for Operable HER2-Positive Breast Cancer. *N Engl J Med* **2005**, *353*, 1673–1684, doi:10.1056/NEJMoa052122.
78. Gianni, L.; Eiermann, W.; Semiglazov, V.; Manikhas, A.; Lluch, A.; Tjulandin, S.; Zambetti, M.; Vazquez, F.; Byakhow, M.; Lichinitser, M.; et al. Neoadjuvant Chemotherapy with Trastuzumab Followed by Adjuvant Trastuzumab versus

Neoadjuvant Chemotherapy Alone, in Patients with HER2-Positive Locally Advanced Breast Cancer (the NOAH Trial): A Randomised Controlled Superiority Trial with a Parallel HER2-Negative Cohort. *Lancet* **2010**, *375*, 377–384, doi:10.1016/S0140-6736(09)61964-4.

79. Pohlmann, P.R.; Mayer, I.A.; Mernaugh, R. Resistance to Trastuzumab in Breast Cancer. *Clin Cancer Res* **2009**, *15*, 7479–7491, doi:10.1158/1078-0432.CCR-09-0636.
80. Christianson, T.A.; Doherty, J.K.; Lin, Y.J.; Ramsey, E.E.; Holmes, R.; Keenan, E.J.; Clinton, G.M. NH2-Terminally Truncated HER-2/Neu Protein: Relationship with Shedding of the Extracellular Domain and with Prognostic Factors in Breast Cancer. *Cancer Res* **1998**, *58*, 5123–5129.
81. Molina, M.A.; Codony-Servat, J.; Albanell, J.; Rojo, F.; Arribas, J.; Baselga, J. Trastuzumab (Herceptin), a Humanized Anti-Her2 Receptor Monoclonal Antibody, Inhibits Basal and Activated Her2 Ectodomain Cleavage in Breast Cancer Cells. *Cancer Res* **2001**, *61*, 4744–4749.
82. Valabrega, G.; Montemurro, F.; Aglietta, M. Trastuzumab: Mechanism of Action, Resistance and Future Perspectives in HER2-Overexpressing Breast Cancer. *Ann Oncol* **2007**, *18*, 977–984, doi:10.1093/annonc/mdl475.
83. Austin, C.D.; De Mazière, A.M.; Pisacane, P.I.; van Dijk, S.M.; Eigenbrot, C.; Sliwkowski, M.X.; Klumperman, J.; Scheller, R.H. Endocytosis and Sorting of ErbB2 and the Site of Action of Cancer Therapeutics Trastuzumab and Geldanamycin. *Mol Biol Cell* **2004**, *15*, 5268–5282, doi:10.1091/mbc.e04-07-0591.

84. Hudis, C.A. Trastuzumab--Mechanism of Action and Use in Clinical Practice. *N Engl J Med* **2007**, *357*, 39–51, doi:10.1056/NEJMra043186.

85. Bianchini, G.; Gianni, L. The Immune System and Response to HER2-Targeted Treatment in Breast Cancer. *Lancet Oncol* **2014**, *15*, e58-68, doi:10.1016/S1470-2045(13)70477-7.

86. Di Modica, M.; Tagliabue, E.; Triulzi, T. Predicting the Efficacy of HER2-Targeted Therapies: A Look at the Host. *Dis Markers* **2017**, *2017*, 7849108, doi:10.1155/2017/7849108.

87. Izumi, Y.; Xu, L.; di Tomaso, E.; Fukumura, D.; Jain, R.K. Tumour Biology: Herceptin Acts as an Anti-Angiogenic Cocktail. *Nature* **2002**, *416*, 279–280, doi:10.1038/416279b.

88. Scaltriti, M.; Rojo, F.; Ocaña, A.; Anido, J.; Guzman, M.; Cortes, J.; Di Cosimo, S.; Matias-Guiu, X.; Ramon y Cajal, S.; Arribas, J.; et al. Expression of P95HER2, a Truncated Form of the HER2 Receptor, and Response to Anti-HER2 Therapies in Breast Cancer. *J Natl Cancer Inst* **2007**, *99*, 628–638, doi:10.1093/jnci/djk134.

89. Anido, J.; Scaltriti, M.; Bech Serra, J.J.; Santiago Josefat, B.; Todo, F.R.; Baselga, J.; Arribas, J. Biosynthesis of Tumorigenic HER2 C-Terminal Fragments by Alternative Initiation of Translation. *EMBO J* **2006**, *25*, 3234–3244, doi:10.1038/sj.emboj.7601191.

90. Nagy, P.; Friedländer, E.; Tanner, M.; Kapanen, A.I.; Carraway, K.L.; Isola, J.; Jovin, T.M. Decreased Accessibility and Lack of Activation of ErbB2 in JIMT-1, a Herceptin-Resistant, MUC4-Expressing Breast Cancer Cell Line. *Cancer Res* **2005**, *65*, 473–482.

91. Scerri, J.; Scerri, C.; Schäfer-Ruoff, F.; Fink, S.; Templin, M.; Grech, G. PKC-Mediated Phosphorylation and Activation of the MEK/ERK Pathway as a Mechanism of

Acquired Trastuzumab Resistance in HER2-Positive Breast Cancer. *Front Endocrinol (Lausanne)* **2022**, *13*, 1010092, doi:10.3389/fendo.2022.1010092.

92. Berns, K.; Horlings, H.M.; Hennessy, B.T.; Madiredjo, M.; Hijmans, E.M.; Beelen, K.; Linn, S.C.; Gonzalez-Angulo, A.M.; Stemke-Hale, K.; Hauptmann, M.; et al. A Functional Genetic Approach Identifies the PI3K Pathway as a Major Determinant of Trastuzumab Resistance in Breast Cancer. *Cancer Cell* **2007**, *12*, 395–402, doi:10.1016/j.ccr.2007.08.030.
93. Goel, S.; Krop, I.E. PIK3CA Mutations in HER2-Positive Breast Cancer: An Ongoing Conundrum. *Ann Oncol* **2016**, *27*, 1368–1372, doi:10.1093/annonc/mdw246.
94. Nagata, Y.; Lan, K.-H.; Zhou, X.; Tan, M.; Esteva, F.J.; Sahin, A.A.; Klos, K.S.; Li, P.; Monia, B.P.; Nguyen, N.T.; et al. PTEN Activation Contributes to Tumor Inhibition by Trastuzumab, and Loss of PTEN Predicts Trastuzumab Resistance in Patients. *Cancer Cell* **2004**, *6*, 117–127, doi:10.1016/j.ccr.2004.06.022.
95. Lu, Y.; Zi, X.; Zhao, Y.; Mascarenhas, D.; Pollak, M. Insulin-like Growth Factor-I Receptor Signaling and Resistance to Trastuzumab (Herceptin). *J Natl Cancer Inst* **2001**, *93*, 1852–1857, doi:10.1093/jnci/93.24.1852.
96. Shattuck, D.L.; Miller, J.K.; Carraway, K.L.; Sweeney, C. Met Receptor Contributes to Trastuzumab Resistance of Her2-Overexpressing Breast Cancer Cells. *Cancer Res* **2008**, *68*, 1471–1477, doi:10.1158/0008-5472.CAN-07-5962.
97. Dua, R.; Zhang, J.; Nhonthachit, P.; Penuel, E.; Petropoulos, C.; Parry, G. EGFR Over-Expression and Activation in High HER2, ER Negative Breast Cancer Cell Line

Induces Trastuzumab Resistance. *Breast Cancer Res Treat* **2010**, *122*, 685–697, doi:10.1007/s10549-009-0592-x.

98. Gallardo, A.; Lerma, E.; Escuin, D.; Tibau, A.; Muñoz, J.; Ojeda, B.; Barnadas, A.; Adrover, E.; Sánchez-Tejada, L.; Giner, D.; et al. Increased Signalling of EGFR and IGF1R, and Deregulation of PTEN/PI3K/Akt Pathway Are Related with Trastuzumab Resistance in HER2 Breast Carcinomas. *Br J Cancer* **2012**, *106*, 1367–1373, doi:10.1038/bjc.2012.85.
99. Pegram, M.; Jackisch, C.; Johnston, S.R.D. Estrogen/HER2 Receptor Crosstalk in Breast Cancer: Combination Therapies to Improve Outcomes for Patients with Hormone Receptor-Positive/HER2-Positive Breast Cancer. *NPJ Breast Cancer* **2023**, *9*, 45, doi:10.1038/s41523-023-00533-2.
100. Boero, S.; Morabito, A.; Banelli, B.; Cardinali, B.; Dozin, B.; Lunardi, G.; Piccioli, P.; Lastraioli, S.; Carosio, R.; Salvi, S.; et al. Analysis of in Vitro ADCC and Clinical Response to Trastuzumab: Possible Relevance of FcγRIIIA/FcγRIIA Gene Polymorphisms and HER-2 Expression Levels on Breast Cancer Cell Lines. *J Transl Med* **2015**, *13*, 324, doi:10.1186/s12967-015-0680-0.
101. Gavin, P.G.; Song, N.; Kim, S.R.; Lipchik, C.; Johnson, N.L.; Bandos, H.; Finnigan, M.; Rastogi, P.; Fehrenbacher, L.; Mamounas, E.P.; et al. Association of Polymorphisms in FCGR2A and FCGR3A With Degree of Trastuzumab Benefit in the Adjuvant Treatment of ERBB2/HER2-Positive Breast Cancer: Analysis of the NSABP B-31 Trial. *JAMA Oncol* **2017**, *3*, 335–341, doi:10.1001/jamaoncol.2016.4884.

102. Varchetta, S.; Gibelli, N.; Oliviero, B.; Nardini, E.; Gennari, R.; Gatti, G.; Silva, L.S.; Villani, L.; Tagliabue, E.; Ménard, S.; et al. Elements Related to Heterogeneity of Antibody-Dependent Cell Cytotoxicity in Patients under Trastuzumab Therapy for Primary Operable Breast Cancer Overexpressing Her2. *Cancer Res* **2007**, *67*, 11991–11999, doi:10.1158/0008-5472.CAN-07-2068.

103. Beano, A.; Signorino, E.; Evangelista, A.; Brusa, D.; Mistrangelo, M.; Polimeni, M.A.; Spadi, R.; Donadio, M.; Ciuffreda, L.; Matera, L. Correlation between NK Function and Response to Trastuzumab in Metastatic Breast Cancer Patients. *J Transl Med* **2008**, *6*, 25, doi:10.1186/1479-5876-6-25.

104. Mozaffari, F.; Lindemalm, C.; Choudhury, A.; Granstam-Björneklett, H.; Helander, I.; Lekander, M.; Mikaelsson, E.; Nilsson, B.; Ojutkangas, M.-L.; Osterborg, A.; et al. NK-Cell and T-Cell Functions in Patients with Breast Cancer: Effects of Surgery and Adjuvant Chemo- and Radiotherapy. *Br J Cancer* **2007**, *97*, 105–111, doi:10.1038/sj.bjc.6603840.

105. Tagliabue, E.; Campiglio, M.; Pupa, S.M.; Ménard, S.; Balsari, A. Activity and Resistance of Trastuzumab According to Different Clinical Settings. *Cancer Treat Rev* **2012**, *38*, 212–217, doi:10.1016/j.ctrv.2011.06.002.

106. Souza-Fonseca-Guimaraes, F.; Rossi, G.R.; Dagley, L.F.; Foroutan, M.; McCulloch, T.R.; Yousef, J.; Park, H.-Y.; Gunter, J.H.; Beavis, P.A.; Lin, C.-Y.; et al. TGFβ and CIS Inhibition Overcomes NK-Cell Suppression to Restore Antitumor Immunity. *Cancer Immunol Res* **2022**, *10*, 1047–1054, doi:10.1158/2326-6066.CIR-21-1052.

107. Witalisz-Siepracka, A.; Klein, K.; Zdársky, B.; Stoiber, D. The Multifaceted Role of STAT3 in NK-Cell Tumor Surveillance. *Front Immunol* **2022**, *13*, 947568, doi:10.3389/fimmu.2022.947568.

108. Rye, I.H.; Trinh, A.; Saetersdal, A.B.; Nebdal, D.; Lingjaerde, O.C.; Almendro, V.; Polyak, K.; Børresen-Dale, A.-L.; Helland, Å.; Markowetz, F.; et al. Intratumor Heterogeneity Defines Treatment-Resistant HER2+ Breast Tumors. *Mol Oncol* **2018**, *12*, 1838–1855, doi:10.1002/1878-0261.12375.

109. Fernandez-Martinez, A.; Krop, I.E.; Hillman, D.W.; Polley, M.-Y.; Parker, J.S.; Huebner, L.; Hoadley, K.A.; Shepherd, J.; Tolaney, S.; Henry, N.L.; et al. Survival, Pathologic Response, and Genomics in CALGB 40601 (Alliance), a Neoadjuvant Phase III Trial of Paclitaxel-Trastuzumab With or Without Lapatinib in HER2-Positive Breast Cancer. *J Clin Oncol* **2020**, *38*, 4184–4193, doi:10.1200/JCO.20.01276.

110. Fumagalli, D.; Venet, D.; Ignatiadis, M.; Azim, H.A.; Maetens, M.; Rothé, F.; Salgado, R.; Bradbury, I.; Pusztai, L.; Harbeck, N.; et al. RNA Sequencing to Predict Response to Neoadjuvant Anti-HER2 Therapy: A Secondary Analysis of the NeoALTTO Randomized Clinical Trial. *JAMA Oncol* **2017**, *3*, 227–234, doi:10.1001/jamaoncol.2016.3824.

111. Denkert, C.; Huober, J.; Loibl, S.; Prinzler, J.; Kronenwett, R.; Darb-Esfahani, S.; Brase, J.C.; Solbach, C.; Mehta, K.; Fasching, P.A.; et al. HER2 and ESR1 MRNA Expression Levels and Response to Neoadjuvant Trastuzumab plus Chemotherapy in Patients with Primary Breast Cancer. *Breast Cancer Res* **2013**, *15*, R11, doi:10.1186/bcr3384.

112. Schneeweiss, A.; Chia, S.; Hickish, T.; Harvey, V.; Eniu, A.; Hegg, R.; Tausch, C.; Seo, J.H.; Tsai, Y.-F.; Ratnayake, J.; et al. Pertuzumab plus Trastuzumab in Combination with Standard Neoadjuvant Anthracycline-Containing and Anthracycline-Free Chemotherapy Regimens in Patients with HER2-Positive Early Breast Cancer: A Randomized Phase II Cardiac Safety Study (TRYPHAENA). *Ann Oncol* **2013**, *24*, 2278–2284, doi:10.1093/annonc/mdt182.

113. Perez, E.A.; Thompson, E.A.; Ballman, K.V.; Anderson, S.K.; Asmann, Y.W.; Kalari, K.R.; Eckel-Passow, J.E.; Dueck, A.C.; Tenner, K.S.; Jen, J.; et al. Genomic Analysis Reveals That Immune Function Genes Are Strongly Linked to Clinical Outcome in the North Central Cancer Treatment Group N9831 Adjuvant Trastuzumab Trial. *J Clin Oncol* **2015**, *33*, 701–708, doi:10.1200/JCO.2014.57.6298.

114. Bianchini, G.; Pusztai, L.; Pienkowski, T.; Im, Y.-H.; Bianchi, G.V.; Tseng, L.-M.; Liu, M.-C.; Lluch, A.; Galeota, E.; Magazzù, D.; et al. Immune Modulation of Pathologic Complete Response after Neoadjuvant HER2-Directed Therapies in the NeoSphere Trial. *Ann Oncol* **2015**, *26*, 2429–2436, doi:10.1093/annonc/mdv395.

115. Salgado, R.; Denkert, C.; Campbell, C.; Savas, P.; Nuciforo, P.; Aura, C.; de Azambuja, E.; Eidtmann, H.; Ellis, C.E.; Baselga, J.; et al. Tumor-Infiltrating Lymphocytes and Associations With Pathological Complete Response and Event-Free Survival in HER2-Positive Early-Stage Breast Cancer Treated With Lapatinib and Trastuzumab: A Secondary Analysis of the NeoALTTO Trial. *JAMA Oncol* **2015**, *1*, 448–454, doi:10.1001/jamaoncol.2015.0830.

116. Triulzi, T.; De Cecco, L.; Sandri, M.; Prat, A.; Giussani, M.; Paolini, B.; Carcangiu, M.L.; Canevari, S.; Bottini, A.; Balsari, A.; et al. Whole-Transcriptome Analysis Links Trastuzumab Sensitivity of Breast Tumors to Both HER2 Dependence and Immune Cell Infiltration. *Oncotarget* **2015**, *6*, 28173–28182, doi:10.18632/oncotarget.4405.

117. Triulzi, T.; Bianchini, G.; Di Cosimo, S.; Pienkowski, T.; Im, Y.-H.; Bianchi, G.V.; Galbardi, B.; Dugo, M.; De Cecco, L.; Tseng, L.-M.; et al. The TRAR Gene Classifier to Predict Response to Neoadjuvant Therapy in HER2-Positive and ER-Positive Breast Cancer Patients: An Explorative Analysis from the NeoSphere Trial. *Mol Oncol* **2022**, *16*, 2355–2366, doi:10.1002/1878-0261.13141.

118. Lee, R.C.; Feinbaum, R.L.; Ambros, V. The C. Elegans Heterochronic Gene Lin-4 Encodes Small RNAs with Antisense Complementarity to Lin-14. *Cell* **1993**, *75*, 843–854, doi:10.1016/0092-8674(93)90529-y.

119. Reinhart, B.J.; Slack, F.J.; Basson, M.; Pasquinelli, A.E.; Bettinger, J.C.; Rougvie, A.E.; Horvitz, H.R.; Ruvkun, G. The 21-Nucleotide Let-7 RNA Regulates Developmental Timing in Caenorhabditis Elegans. *Nature* **2000**, *403*, 901–906, doi:10.1038/35002607.

120. Ambros, V. The Functions of Animal MicroRNAs. *Nature* **2004**, *431*, 350–355, doi:10.1038/nature02871.

121. Bartel, D.P. MicroRNAs: Genomics, Biogenesis, Mechanism, and Function. *Cell* **2004**, *116*, 281–297, doi:10.1016/s0092-8674(04)00045-5.

122. Dexheimer, P.J.; Cochella, L. MicroRNAs: From Mechanism to Organism. *Front Cell Dev Biol* **2020**, *8*, 409, doi:10.3389/fcell.2020.00409.

123. Lee, Y.; Kim, M.; Han, J.; Yeom, K.-H.; Lee, S.; Baek, S.H.; Kim, V.N. MicroRNA Genes Are Transcribed by RNA Polymerase II. *EMBO J* **2004**, *23*, 4051–4060, doi:10.1038/sj.emboj.7600385.

124. Gregory, R.I.; Yan, K.-P.; Amuthan, G.; Chendrimada, T.; Doratotaj, B.; Cooch, N.; Shiekhattar, R. The Microprocessor Complex Mediates the Genesis of MicroRNAs. *Nature* **2004**, *432*, 235–240, doi:10.1038/nature03120.

125. Chendrimada, T.P.; Gregory, R.I.; Kumaraswamy, E.; Norman, J.; Cooch, N.; Nishikura, K.; Shiekhattar, R. TRBP Recruits the Dicer Complex to Ago2 for MicroRNA Processing and Gene Silencing. *Nature* **2005**, *436*, 740–744, doi:10.1038/nature03868.

126. Krol, J.; Loedige, I.; Filipowicz, W. The Widespread Regulation of MicroRNA Biogenesis, Function and Decay. *Nat Rev Genet* **2010**, *11*, 597–610, doi:10.1038/nrg2843.

127. Moretti, F.; Thermann, R.; Hentze, M.W. Mechanism of Translational Regulation by MiR-2 from Sites in the 5′ Untranslated Region or the Open Reading Frame. *RNA* **2010**, *16*, 2493–2502, doi:10.1261/rna.2384610.

128. Hausser, J.; Syed, A.P.; Bilen, B.; Zavolan, M. Analysis of CDS-Located MiRNA Target Sites Suggests That They Can Effectively Inhibit Translation. *Genome Res* **2013**, *23*, 604–615, doi:10.1101/gr.139758.112.

129. Fukao, A.; Aoyama, T.; Fujiwara, T. The Molecular Mechanism of Translational Control via the Communication between the MicroRNA Pathway and RNA-Binding Proteins. *RNA Biol* **2015**, *12*, 922–926, doi:10.1080/15476286.2015.1073436.

130. Fukaya, T.; Iwakawa, H.-O.; Tomari, Y. MicroRNAs Block Assembly of EIF4F Translation Initiation Complex in Drosophila. *Mol Cell* **2014**, *56*, 67–78, doi:10.1016/j.molcel.2014.09.004.

131. Vasudevan, S.; Tong, Y.; Steitz, J.A. Switching from Repression to Activation: MicroRNAs Can up-Regulate Translation. *Science* **2007**, *318*, 1931–1934, doi:10.1126/science.1149460.

132. Place, R.F.; Li, L.-C.; Pookot, D.; Noonan, E.J.; Dahiya, R. MicroRNA-373 Induces Expression of Genes with Complementary Promoter Sequences. *Proc Natl Acad Sci U S A* **2008**, *105*, 1608–1613, doi:10.1073/pnas.0707594105.

133. Kim, H.; Kim, J.; Yu, S.; Lee, Y.-Y.; Park, J.; Choi, R.J.; Yoon, S.-J.; Kang, S.-G.; Kim, V.N. A Mechanism for MicroRNA Arm Switching Regulated by Uridylation. *Mol Cell* **2020**, *78*, 1224-1236.e5, doi:10.1016/j.molcel.2020.04.030.

134. Ro, S.; Park, C.; Young, D.; Sanders, K.M.; Yan, W. Tissue-Dependent Paired Expression of MiRNAs. *Nucleic Acids Res* **2007**, *35*, 5944–5953, doi:10.1093/nar/gkm641.

135. Mitra, R.; Adams, C.M.; Jiang, W.; Greenawalt, E.; Eischen, C.M. Pan-Cancer Analysis Reveals Cooperativity of Both Strands of MicroRNA That Regulate Tumorigenesis and Patient Survival. *Nat Commun* **2020**, *11*, 968, doi:10.1038/s41467-020-14713-2.

136. Medley, J.C.; Panzade, G.; Zinovyeva, A.Y. MicroRNA Strand Selection: Unwinding the Rules. *Wiley Interdiscip Rev RNA* **2021**, *12*, e1627, doi:10.1002/wrna.1627.

137. Srinivasan, G.; Williamson, E.A.; Kong, K.; Jaiswal, A.S.; Huang, G.; Kim, H.-S.; Schärer, O.; Zhao, W.; Burma, S.; Sung, P.; et al. MiR223-3p Promotes Synthetic

Lethality in BRCA1-Deficient Cancers. *Proceedings of the National Academy of Sciences* **2019**, *116*, 17438–17443, doi:10.1073/pnas.1903150116.

138. Calin, G.A.; Dumitru, C.D.; Shimizu, M.; Bichi, R.; Zupo, S.; Noch, E.; Aldler, H.; Rattan, S.; Keating, M.; Rai, K.; et al. Frequent Deletions and Down-Regulation of Micro- RNA Genes MiR15 and MiR16 at 13q14 in Chronic Lymphocytic Leukemia. *Proc Natl Acad Sci U S A* **2002**, *99*, 15524–15529, doi:10.1073/pnas.242606799.

139. Calin, G.A.; Sevignani, C.; Dumitru, C.D.; Hyslop, T.; Noch, E.; Yendamuri, S.; Shimizu, M.; Rattan, S.; Bullrich, F.; Negrini, M.; et al. Human MicroRNA Genes Are Frequently Located at Fragile Sites and Genomic Regions Involved in Cancers. *Proc Natl Acad Sci U S A* **2004**, *101*, 2999–3004, doi:10.1073/pnas.0307323101.

140. Anglesio, M.S.; Wang, Y.; Yang, W.; Senz, J.; Wan, A.; Heravi-Moussavi, A.; Salamanca, C.; Maines-Bandiera, S.; Huntsman, D.G.; Morin, G.B. Cancer-Associated Somatic DICER1 Hotspot Mutations Cause Defective MiRNA Processing and Reverse-Strand Expression Bias to Predominantly Mature 3p Strands through Loss of 5p Strand Cleavage. *J Pathol* **2013**, *229*, 400–409, doi:10.1002/path.4135.

141. Saito, Y.; Liang, G.; Egger, G.; Friedman, J.M.; Chuang, J.C.; Coetzee, G.A.; Jones, P.A. Specific Activation of MicroRNA-127 with Downregulation of the Proto-Oncogene BCL6 by Chromatin-Modifying Drugs in Human Cancer Cells. *Cancer Cell* **2006**, *9*, 435–443, doi:10.1016/j.ccr.2006.04.020.

142. Lim, Y.-Y.; Wright, J.A.; Attema, J.L.; Gregory, P.A.; Bert, A.G.; Smith, E.; Thomas, D.; Lopez, A.F.; Drew, P.A.; Khew-Goodall, Y.; et al. Epigenetic Modulation of the

MiR-200 Family Is Associated with Transition to a Breast Cancer Stem-Cell-like State. *J Cell Sci* **2013**, *126*, 2256–2266, doi:10.1242/jcs.122275.

143. Lin, S.; Gregory, R.I. MicroRNA Biogenesis Pathways in Cancer. *Nat Rev Cancer* **2015**, *15*, 321–333, doi:10.1038/nrc3932.

144. Baer, C.; Claus, R.; Plass, C. Genome-Wide Epigenetic Regulation of MiRNAs in Cancer. *Cancer Res* **2013**, *73*, 473–477, doi:10.1158/0008-5472.CAN-12-3731.

145. Iorio, M.V.; Croce, C.M. MicroRNA Dysregulation in Cancer: Diagnostics, Monitoring and Therapeutics. A Comprehensive Review. *EMBO Mol Med* **2012**, *4*, 143–159, doi:10.1002/emmm.201100209.

146. Dhawan, A.; Scott, J.G.; Harris, A.L.; Buffa, F.M. Pan-Cancer Characterisation of MicroRNA across Cancer Hallmarks Reveals MicroRNA-Mediated Downregulation of Tumour Suppressors. *Nat Commun* **2018**, *9*, 5228, doi:10.1038/s41467-018-07657-1.

147. Ma, L.; Teruya-Feldstein, J.; Weinberg, R.A. Tumour Invasion and Metastasis Initiated by MicroRNA-10b in Breast Cancer. *Nature* **2007**, *449*, 682–688, doi:10.1038/nature06174.

148. Li, N.; Fu, H.; Tie, Y.; Hu, Z.; Kong, W.; Wu, Y.; Zheng, X. MiR-34a Inhibits Migration and Invasion by down-Regulation of c-Met Expression in Human Hepatocellular Carcinoma Cells. *Cancer Lett* **2009**, *275*, 44–53, doi:10.1016/j.canlet.2008.09.035.

149. Lu, J.; Getz, G.; Miska, E.A.; Alvarez-Saavedra, E.; Lamb, J.; Peck, D.; Sweet-Cordero, A.; Ebert, B.L.; Mak, R.H.; Ferrando, A.A.; et al. MicroRNA Expression Profiles Classify Human Cancers. *Nature* **2005**, *435*, 834–838, doi:10.1038/nature03702.

150. Murakami, Y.; Yasuda, T.; Saigo, K.; Urashima, T.; Toyoda, H.; Okanoue, T.; Shimotohno, K. Comprehensive Analysis of MicroRNA Expression Patterns in Hepatocellular Carcinoma and Non-Tumorous Tissues. *Oncogene* **2006**, *25*, 2537–2545, doi:10.1038/sj.onc.1209283.

151. Yanaihara, N.; Caplen, N.; Bowman, E.; Seike, M.; Kumamoto, K.; Yi, M.; Stephens, R.M.; Okamoto, A.; Yokota, J.; Tanaka, T.; et al. Unique MicroRNA Molecular Profiles in Lung Cancer Diagnosis and Prognosis. *Cancer Cell* **2006**, *9*, 189–198, doi:10.1016/j.ccr.2006.01.025.

152. Ferracin, M.; Negrini, M. Micromarkers 2.0: An Update on the Role of MicroRNAs in Cancer Diagnosis and Prognosis. *Expert Rev Mol Diagn* **2015**, *15*, 1369–1381, doi:10.1586/14737159.2015.1081058.

153. Giussani, M.; Ciniselli, C.M.; De Cecco, L.; Lecchi, M.; Dugo, M.; Gargiuli, C.; Mariancini, A.; Mancinelli, E.; Cosentino, G.; Veneroni, S.; et al. Circulating MiRNAs as Novel Non-Invasive Biomarkers to Aid the Early Diagnosis of Suspicious Breast Lesions for Which Biopsy Is Recommended. *Cancers (Basel)* **2021**, *13*, 4028, doi:10.3390/cancers13164028.

154. Iorio, M.V.; Ferracin, M.; Liu, C.-G.; Veronese, A.; Spizzo, R.; Sabbioni, S.; Magri, E.; Pedriali, M.; Fabbri, M.; Campiglio, M.; et al. MicroRNA Gene Expression Deregulation in Human Breast Cancer. *Cancer Research* **2005**, *65*, 7065–7070, doi:10.1158/0008-5472.CAN-05-1783.

155. Leivonen, S.-K.; Sahlberg, K.K.; Mäkelä, R.; Due, E.U.; Kallioniemi, O.; Børresen-Dale, A.-L.; Perälä, M. High-Throughput Screens Identify MicroRNAs Essential for

HER2 Positive Breast Cancer Cell Growth. *Mol Oncol* **2014**, *8*, 93–104, doi:10.1016/j.molonc.2013.10.001.

156. Pattanayak, B.; Garrido-Cano, I.; Adam-Artigues, A.; Tormo, E.; Pineda, B.; Cabello, P.; Alonso, E.; Bermejo, B.; Hernando, C.; Martínez, M.T.; et al. MicroRNA-33b Suppresses Epithelial-Mesenchymal Transition Repressing the MYC-EZH2 Pathway in HER2+ Breast Carcinoma. *Front Oncol* **2020**, *10*, 1661, doi:10.3389/fonc.2020.01661.

157. Gorbatenko, A.; Søkilde, R.; Sorensen, E.E.; Newie, I.; Persson, H.; Morancho, B.; Arribas, J.; Litman, T.; Rovira, C.; Pedersen, S.F. HER2 and P95HER2 Differentially Regulate MiRNA Expression in MCF-7 Breast Cancer Cells and Downregulate MYB Proteins through MiR-221/222 and MiR-503. *Sci Rep* **2019**, *9*, 3352, doi:10.1038/s41598-019-39733-x.

158. Shabaninejad, Z.; Mowla, S.J.; Yousefi, F.; Soltani, B.M. A Novel MiRNA Located in the HER2 Gene Shows an Inhibitory Effect on Wnt Signaling and Cell Cycle Progression. *Biomed Res Int* **2022**, *2022*, 7216758, doi:10.1155/2022/7216758.

159. Li, M.; Fu, S.; Xiao, H. Genome-Wide Analysis of MicroRNA and MRNA Expression Signatures in Cancer. *Acta Pharmacol Sin* **2015**, *36*, 1200–1211, doi:10.1038/aps.2015.67.

160. Duran-Sanchon, S.; Moreno, L.; Augé, J.M.; Serra-Burriel, M.; Cuatrecasas, M.; Moreira, L.; Martín, A.; Serradesanferm, A.; Pozo, À.; Costa, R.; et al. Identification and Validation of MicroRNA Profiles in Fecal Samples for Detection of Colorectal Cancer. *Gastroenterology* **2020**, *158*, 947-957.e4, doi:10.1053/j.gastro.2019.10.005.

161. Li, H.; Liu, J.; Chen, J.; Wang, H.; Yang, L.; Chen, F.; Fan, S.; Wang, J.; Shao, B.; Yin, D.; et al. A Serum MicroRNA Signature Predicts Trastuzumab Benefit in HER2-Positive Metastatic Breast Cancer Patients. *Nat Commun* **2018**, *9*, 1614, doi:10.1038/s41467-018-03537-w.

162. Di Cosimo, S.; Appierto, V.; Pizzamiglio, S.; Tiberio, P.; Iorio, M.V.; Hilbers, F.; de Azambuja, E.; de la Peña, L.; Izquierdo, M.; Huober, J.; et al. Plasma MiRNA Levels for Predicting Therapeutic Response to Neoadjuvant Treatment in HER2-Positive Breast Cancer: Results from the NeoALTTO Trial. *Clin Cancer Res* **2019**, *25*, 3887–3895, doi:10.1158/1078-0432.CCR-18-2507.

163. Di Cosimo, S.; Appierto, V.; Pizzamiglio, S.; Silvestri, M.; Baselga, J.; Piccart, M.; Huober, J.; Izquierdo, M.; de la Pena, L.; Hilbers, F.S.; et al. Early Modulation of Circulating MicroRNAs Levels in HER2-Positive Breast Cancer Patients Treated with Trastuzumab-Based Neoadjuvant Therapy. *Int J Mol Sci* **2020**, *21*, 1386, doi:10.3390/ijms21041386.

164. Stevic, I.; Müller, V.; Weber, K.; Fasching, P.A.; Karn, T.; Marmé, F.; Schem, C.; Stickeler, E.; Denkert, C.; van Mackelenbergh, M.; et al. Specific MicroRNA Signatures in Exosomes of Triple-Negative and HER2-Positive Breast Cancer Patients Undergoing Neoadjuvant Therapy within the GeparSixto Trial. *BMC Med* **2018**, *16*, 179, doi:10.1186/s12916-018-1163-y.

165. Liu, B.; Su, F.; Lv, X.; Zhang, W.; Shang, X.; Zhang, Y.; Zhang, J. Serum MicroRNA-21 Predicted Treatment Outcome and Survival in HER2-Positive Breast Cancer Patients

Receiving Neoadjuvant Chemotherapy Combined with Trastuzumab. *Cancer Chemother Pharmacol* **2019**, *84*, 1039–1049, doi:10.1007/s00280-019-03937-9.

166. Zhang, S.; Wang, Y.; Wang, Y.; Peng, J.; Yuan, C.; Zhou, L.; Xu, S.; Lin, Y.; Du, Y.; Yang, F.; et al. Serum MiR-222-3p as a Double-Edged Sword in Predicting Efficacy and Trastuzumab-Induced Cardiotoxicity for HER2-Positive Breast Cancer Patients Receiving Neoadjuvant Target Therapy. *Front Oncol* **2020**, *10*, 631, doi:10.3389/fonc.2020.00631.

167. Paraskevopoulou, M.D.; Hatzigeorgiou, A.G. Analyzing MiRNA-LncRNA Interactions. *Methods Mol Biol* **2016**, *1402*, 271–286, doi:10.1007/978-1-4939-3378-5_21.

168. Müller, V.; Oliveira-Ferrer, L.; Steinbach, B.; Pantel, K.; Schwarzenbach, H. Interplay of LncRNA H19/MiR-675 and LncRNA NEAT1/MiR-204 in Breast Cancer. *Mol Oncol* **2019**, *13*, 1137–1149, doi:10.1002/1878-0261.12472.

169. Ichikawa, T.; Sato, F.; Terasawa, K.; Tsuchiya, S.; Toi, M.; Tsujimoto, G.; Shimizu, K. Trastuzumab Produces Therapeutic Actions by Upregulating MiR-26a and MiR-30b in Breast Cancer Cells. *PLoS One* **2012**, *7*, e31422, doi:10.1371/journal.pone.0031422.

170. Tormo, E.; Adam-Artigues, A.; Ballester, S.; Pineda, B.; Zazo, S.; González-Alonso, P.; Albanell, J.; Rovira, A.; Rojo, F.; Lluch, A.; et al. The Role of MiR-26a and MiR-30b in HER2+ Breast Cancer Trastuzumab Resistance and Regulation of the CCNE2 Gene. *Sci Rep* **2017**, *7*, 41309, doi:10.1038/srep41309.

171. Rezaei, Z.; Sebzari, A.; Kordi-Tamandani, D.M.; Dastjerdi, K. Involvement of the Dysregulation of MiR-23b-3p, MiR-195-5p, MiR-656-5p, and MiR-340-5p in Trastuzumab Resistance of HER2-Positive Breast Cancer Cells and System Biology

Approach to Predict Their Targets Involved in Resistance. *DNA Cell Biol* **2019**, *38*, 184–192, doi:10.1089/dna.2018.4427.

172. Luo, L.; Zhang, Z.; Qiu, N.; Ling, L.; Jia, X.; Song, Y.; Li, H.; Li, J.; Lyu, H.; Liu, H.; et al. Disruption of FOXO3a-MiRNA Feedback Inhibition of IGF2/IGF-1R/IRS1 Signaling Confers Herceptin Resistance in HER2-Positive Breast Cancer. *Nat Commun* **2021**, *12*, 2699, doi:10.1038/s41467-021-23052-9.

173. Zhou, Y.; Yuan, Y.; Li, L.; Wang, X.; Quan, Y.; Liu, C.; Yu, M.; Hu, X.; Meng, X.; Zhou, Z.; et al. HER2-Intronic MiR-4728-5p Facilitates HER2 Expression and Accelerates Cell Proliferation and Migration by Targeting EBP1 in Breast Cancer. *PLoS One* **2021**, *16*, e0245832, doi:10.1371/journal.pone.0245832.

174. Normann, L.S.; Aure, M.R.; Leivonen, S.-K.; Haugen, M.H.; Hongisto, V.; Kristensen, V.N.; Mælandsmo, G.M.; Sahlberg, K.K. MicroRNA in Combination with HER2-Targeting Drugs Reduces Breast Cancer Cell Viability in Vitro. *Sci Rep* **2021**, *11*, 10893, doi:10.1038/s41598-021-90385-2.

175. Normann, L.S.; Haugen, M.H.; Aure, M.R.; Kristensen, V.N.; Mælandsmo, G.M.; Sahlberg, K.K. MiR-101-5p Acts as a Tumor Suppressor in HER2-Positive Breast Cancer Cells and Improves Targeted Therapy. *Breast Cancer (Dove Med Press)* **2022**, *14*, 25–39, doi:10.2147/BCTT.S338404.

176. Chakraborty, C.; Sharma, A.R.; Sharma, G.; Lee, S.-S. Therapeutic Advances of MiRNAs: A Preclinical and Clinical Update. *J Adv Res* **2021**, *28*, 127–138, doi:10.1016/j.jare.2020.08.012.

177. Segal, M.; Slack, F.J. Challenges Identifying Efficacious MiRNA Therapeutics for Cancer. *Expert Opin Drug Discov* **2020**, *15*, 987–992, doi:10.1080/17460441.2020.1765770.

178. Baroni, S.; Romero-Cordoba, S.; Plantamura, I.; Dugo, M.; D'Ippolito, E.; Cataldo, A.; Cosentino, G.; Angeloni, V.; Rossini, A.; Daidone, M.G.; et al. Exosome-Mediated Delivery of MiR-9 Induces Cancer-Associated Fibroblast-like Properties in Human Breast Fibroblasts. *Cell Death Dis* **2016**, *7*, e2312, doi:10.1038/cddis.2016.224.

179. Sohel, M.M. Extracellular/Circulating MicroRNAs: Release Mechanisms, Functions and Challenges. *Achievements in the Life Sciences* **2016**, *10*, doi:10.1016/j.als.2016.11.007.

180. Liu, Q.; Peng, F.; Chen, J. The Role of Exosomal MicroRNAs in the Tumor Microenvironment of Breast Cancer. *Int J Mol Sci* **2019**, *20*, 3884, doi:10.3390/ijms20163884.

181. Yu, X.; Odenthal, M.; Fries, J.W.U. Exosomes as MiRNA Carriers: Formation-Function-Future. *Int J Mol Sci* **2016**, *17*, 2028, doi:10.3390/ijms17122028.

182. Gibbings, D.J.; Ciaudo, C.; Erhardt, M.; Voinnet, O. Multivesicular Bodies Associate with Components of MiRNA Effector Complexes and Modulate MiRNA Activity. *Nat Cell Biol* **2009**, *11*, 1143–1149, doi:10.1038/ncb1929.

183. Seok, H.; Lee, H.; Jang, E.-S.; Chi, S.W. Evaluation and Control of MiRNA-like off-Target Repression for RNA Interference. *Cell Mol Life Sci* **2018**, *75*, 797–814, doi:10.1007/s00018-017-2656-0.

184. Lai, X.; Eberhardt, M.; Schmitz, U.; Vera, J. Systems Biology-Based Investigation of Cooperating MicroRNAs as Monotherapy or Adjuvant Therapy in Cancer. *Nucleic Acids Res* **2019**, *47*, 7753–7766, doi:10.1093/nar/gkz638.

185. Korangath, P.; Barnett, J.D.; Sharma, A.; Henderson, E.T.; Stewart, J.; Yu, S.-H.; Kandala, S.K.; Yang, C.-T.; Caserto, J.S.; Hedayati, M.; et al. Nanoparticle Interactions with Immune Cells Dominate Tumor Retention and Induce T Cell-Mediated Tumor Suppression in Models of Breast Cancer. *Sci Adv* **2020**, *6*, eaay1601, doi:10.1126/sciadv.aay1601.

186. Meng, Z.; Lu, M. RNA Interference-Induced Innate Immunity, Off-Target Effect, or Immune Adjuvant? *Front Immunol* **2017**, *8*, 331, doi:10.3389/fimmu.2017.00331.

187. Orellana, E.A.; Abdelaal, A.M.; Rangasamy, L.; Tenneti, S.; Myoung, S.; Low, P.S.; Kasinski, A.L. Enhancing MicroRNA Activity through Increased Endosomal Release Mediated by Nigericin. *Mol Ther Nucleic Acids* **2019**, *16*, 505–518, doi:10.1016/j.omtn.2019.04.003.

188. Park, J.; Choi, Y.; Chang, H.; Um, W.; Ryu, J.H.; Kwon, I.C. Alliance with EPR Effect: Combined Strategies to Improve the EPR Effect in the Tumor Microenvironment. *Theranostics* **2019**, *9*, 8073–8090, doi:10.7150/thno.37198.

189. Shi, Y.; van der Meel, R.; Chen, X.; Lammers, T. The EPR Effect and beyond: Strategies to Improve Tumor Targeting and Cancer Nanomedicine Treatment Efficacy. *Theranostics* **2020**, *10*, 7921–7924, doi:10.7150/thno.49577.

190. Silva-Cázares, M.B.; Saavedra-Leos, M.Z.; Jordan-Alejandre, E.; Nuñez-Olvera, S.I.; Cómpean-Martínez, I.; López-Camarillo, C. Lipid-based Nanoparticles for the Therapeutic Delivery of Non-coding RNAs in Breast Cancer (Review). *Oncol Rep* **2020**, *44*, 2353–2363, doi:10.3892/or.2020.7791.

191. Hayward, S.L.; Francis, D.M.; Kholmatov, P.; Kidambi, S. Targeted Delivery of MicroRNA125a-5p by Engineered Lipid Nanoparticles for the Treatment of HER2 Positive Metastatic Breast Cancer. *J Biomed Nanotechnol* **2016**, *12*, 554–568, doi:10.1166/jbn.2016.2194.

192. Pizzamiglio, S.; Cosentino, G.; Ciniselli, C.M.; De Cecco, L.; Cataldo, A.; Plantamura, I.; Triulzi, T.; El-Abed, S.; Wang, Y.; Bajji, M.; et al. What If the Future of HER2-Positive Breast Cancer Patients Was Written in MiRNAs? An Exploratory Analysis from NeoALTTO Study. *Cancer Med* **2022**, *11*, 332–339, doi:10.1002/cam4.4449.

193. Mosakhani, N.; Lahti, L.; Borze, I.; Karjalainen-Lindsberg, M.-L.; Sundström, J.; Ristamäki, R.; Osterlund, P.; Knuutila, S.; Sarhadi, V.K. MicroRNA Profiling Predicts Survival in Anti-EGFR Treated Chemorefractory Metastatic Colorectal Cancer Patients with Wild-Type KRAS and BRAF. *Cancer Genet* **2012**, *205*, 545–551, doi:10.1016/j.cancergen.2012.08.003.

194. Manceau, G.; Imbeaud, S.; Thiébaut, R.; Liébaert, F.; Fontaine, K.; Rousseau, F.; Génin, B.; Le Corre, D.; Didelot, A.; Vincent, M.; et al. Hsa-MiR-31-3p Expression Is Linked to Progression-Free Survival in Patients with KRAS Wild-Type Metastatic Colorectal Cancer Treated with Anti-EGFR Therapy. *Clin Cancer Res* **2014**, *20*, 3338–3347, doi:10.1158/1078-0432.CCR-13-2750.

195. Mlcochova, J.; Faltejskova-Vychytilova, P.; Ferracin, M.; Zagatti, B.; Radova, L.; Svoboda, M.; Nemecek, R.; John, S.; Kiss, I.; Vyzula, R.; et al. MicroRNA Expression Profiling Identifies MiR-31-5p/3p as Associated with Time to Progression in Wild-Type

RAS Metastatic Colorectal Cancer Treated with Cetuximab. *Oncotarget* **2015**, *6*, 38695–38704, doi:10.18632/oncotarget.5735.

196. Laurent-Puig, P.; Grisoni, M.-L.; Heinemann, V.; Liebaert, F.; Neureiter, D.; Jung, A.; Montestruc, F.; Gaston-Mathe, Y.; Thiébaut, R.; Stintzing, S. Validation of MiR-31-3p Expression to Predict Cetuximab Efficacy When Used as First-Line Treatment in RAS Wild-Type Metastatic Colorectal Cancer. *Clin Cancer Res* **2019**, *25*, 134–141, doi:10.1158/1078-0432.CCR-18-1324.

197. Anandappa, G.; Lampis, A.; Cunningham, D.; Khan, K.H.; Kouvelakis, K.; Vlachogiannis, G.; Hedayat, S.; Tunariu, N.; Rao, S.; Watkins, D.; et al. MiR-31-3p Expression and Benefit from Anti-EGFR Inhibitors in Metastatic Colorectal Cancer Patients Enrolled in the Prospective Phase II PROSPECT-C Trial. *Clin Cancer Res* **2019**, *25*, 3830–3838, doi:10.1158/1078-0432.CCR-18-3769.

198. Strippoli, A.; Cocomazzi, A.; Basso, M.; Cenci, T.; Ricci, R.; Pierconti, F.; Cassano, A.; Fiorentino, V.; Barone, C.; Bria, E.; et al. C-MYC Expression Is a Possible Keystone in the Colorectal Cancer Resistance to EGFR Inhibitors. *Cancers (Basel)* **2020**, *12*, 638, doi:10.3390/cancers12030638.

199. Liu, Y.; Wang, Y.; Fu, X.; Lu, Z. Long Non-Coding RNA NEAT1 Promoted Ovarian Cancer Cells' Metastasis through Regulation of MiR-382-3p/ROCK1 Axial. *Cancer Sci* **2018**, *109*, 2188–2198, doi:10.1111/cas.13647.

200. Zhang, H.; Zhu, C.; He, Z.; Chen, S.; Li, L.; Sun, C. LncRNA PSMB8-AS1 Contributes to Pancreatic Cancer Progression via Modulating MiR-382-3p/STAT1/PD-L1 Axis. *J Exp Clin Cancer Res* **2020**, *39*, 179, doi:10.1186/s13046-020-01687-8.

201. Zhang, D.-J.; Fu, Z.-M.; Guo, Y.-Y.; Guo, F.; Wan, Y.-N.; Guan, G.-F. Circ_0000052/MiR-382-3p Axis Induces PD-L1 Expression and Regulates Cell Proliferation and Immune Evasion in Head and Neck Squamous Cell Carcinoma. *J Cell Mol Med* **2023**, *27*, 113–126, doi:10.1111/jcmm.17643.

202. Fang, H.; Wu, W.; Wu, Z. MiR-382-3p Downregulation Contributes to the Carcinogenesis of Lung Adenocarcinoma by Promoting AKT SUMOylation and Phosphorylation. *Exp Ther Med* **2022**, *24*, 440, doi:10.3892/etm.2022.11367.

203. Fu, L.; Li, Z.; Zhu, J.; Wang, P.; Fan, G.; Dai, Y.; Zheng, Z.; Liu, Y. Serum Expression Levels of MicroRNA-382-3p, -598-3p, -1246 and -184 in Breast Cancer Patients. *Oncol Lett* **2016**, *12*, 269–274, doi:10.3892/ol.2016.4582.

204. Rovero, S.; Amici, A.; Di Carlo, E.; Bei, R.; Nanni, P.; Quaglino, E.; Porcedda, P.; Boggio, K.; Smorlesi, A.; Lollini, P.L.; et al. DNA Vaccination against Rat Her-2/Neu P185 More Effectively Inhibits Carcinogenesis than Transplantable Carcinomas in Transgenic BALB/c Mice. *J Immunol* **2000**, *165*, 5133–5142, doi:10.4049/jimmunol.165.9.5133.

205. Davoren, P.A.; McNeill, R.E.; Lowery, A.J.; Kerin, M.J.; Miller, N. Identification of Suitable Endogenous Control Genes for MicroRNA Gene Expression Analysis in Human Breast Cancer. *BMC Molecular Biol* **2008**, *9*, 76, doi:10.1186/1471-2199-9-76.

206. Barber, R.D.; Harmer, D.W.; Coleman, R.A.; Clark, B.J. GAPDH as a Housekeeping Gene: Analysis of GAPDH MRNA Expression in a Panel of 72 Human Tissues. *Physiological Genomics* **2005**, *21*, 389–395, doi:10.1152/physiolgenomics.00025.2005.

207. Liberzon, A.; Birger, C.; Thorvaldsdóttir, H.; Ghandi, M.; Mesirov, J.P.; Tamayo, P. The Molecular Signatures Database (MSigDB) Hallmark Gene Set Collection. *Cell Syst* **2015**, *1*, 417–425, doi:10.1016/j.cels.2015.12.004.

208. Khan, M.B.; Ruggieri, R.; Jamil, E.; Tran, N.L.; Gonzalez, C.; Mugridge, N.; Gao, S.; MacDiarmid, J.; Brahmbhatt, H.; Sarkaria, J.N.; et al. Nanocell-Mediated Delivery of MiR-34a Counteracts Temozolomide Resistance in Glioblastoma. *Mol Med* **2021**, *27*, 28, doi:10.1186/s10020-021-00293-4.

209. Sticht, C.; De La Torre, C.; Parveen, A.; Gretz, N. MiRWalk: An Online Resource for Prediction of MicroRNA Binding Sites. *PLoS One* **2018**, *13*, e0206239, doi:10.1371/journal.pone.0206239.

210. Agarwal, V.; Bell, G.W.; Nam, J.-W.; Bartel, D.P. Predicting Effective MicroRNA Target Sites in Mammalian MRNAs. *eLife* **2015**, *4*, e05005, doi:10.7554/eLife.05005.

211. Huang, H.-Y.; Lin, Y.-C.-D.; Cui, S.; Huang, Y.; Tang, Y.; Xu, J.; Bao, J.; Li, Y.; Wen, J.; Zuo, H.; et al. MiRTarBase Update 2022: An Informative Resource for Experimentally Validated MiRNA-Target Interactions. *Nucleic Acids Res* **2022**, *50*, D222–D230, doi:10.1093/nar/gkab1079.

212. Charoentong, P.; Finotello, F.; Angelova, M.; Mayer, C.; Efremova, M.; Rieder, D.; Hackl, H.; Trajanoski, Z. Pan-Cancer Immunogenomic Analyses Reveal Genotype-Immunophenotype Relationships and Predictors of Response to Checkpoint Blockade. *Cell Rep* **2017**, *18*, 248–262, doi:10.1016/j.celrep.2016.12.019.

213. Safonov, A.; Jiang, T.; Bianchini, G.; Győrffy, B.; Karn, T.; Hatzis, C.; Pusztai, L. Immune Gene Expression Is Associated with Genomic Aberrations in Breast Cancer. *Cancer Res* **2017**, *77*, 3317–3324, doi:10.1158/0008-5472.CAN-16-3478.

214. Pizzamiglio, S.; Ciniselli, C.M.; Triulzi, T.; Gargiuli, C.; De Cecco, L.; de Azambuja, E.; Fumagalli, D.; Sotiriou, C.; Harbeck, N.; Izquierdo, M.; et al. Integrated Molecular and Immune Phenotype of HER2-Positive Breast Cancer and Response to Neoadjuvant Therapy: A NeoALTTO Exploratory Analysis. *Clin Cancer Res* **2021**, *27*, 6307–6313, doi:10.1158/1078-0432.CCR-21-1600.

215. Rody, A.; Holtrich, U.; Pusztai, L.; Liedtke, C.; Gaetje, R.; Ruckhaeberle, E.; Solbach, C.; Hanker, L.; Ahr, A.; Metzler, D.; et al. T-Cell Metagene Predicts a Favorable Prognosis in Estrogen Receptor-Negative and HER2-Positive Breast Cancers. *Breast Cancer Res* **2009**, *11*, R15, doi:10.1186/bcr2234.

216. Shiu, K.-K.; Wetterskog, D.; Mackay, A.; Natrajan, R.; Lambros, M.; Sims, D.; Bajrami, I.; Brough, R.; Frankum, J.; Sharpe, R.; et al. Integrative Molecular and Functional Profiling of ERBB2-Amplified Breast Cancers Identifies New Genetic Dependencies. *Oncogene* **2014**, *33*, 619–631, doi:10.1038/onc.2012.625.

217. Tatara, T.; Mukohara, T.; Tanaka, R.; Shimono, Y.; Funakoshi, Y.; Imamura, Y.; Toyoda, M.; Kiyota, N.; Hirai, M.; Kakeji, Y.; et al. 3D Culture Represents Apoptosis Induced by Trastuzumab Better than 2D Monolayer Culture. *Anticancer Res* **2018**, *38*, 2831–2839, doi:10.21873/anticanres.12528.

218. Tseng, P.-H.; Wang, Y.-C.; Weng, S.-C.; Weng, J.-R.; Chen, C.-S.; Brueggemeier, R.W.; Shapiro, C.L.; Chen, C.-Y.; Dunn, S.E.; Pollak, M.; et al. Overcoming

Trastuzumab Resistance in HER2-Overexpressing Breast Cancer Cells by Using a Novel Celecoxib-Derived Phosphoinositide-Dependent Kinase-1 Inhibitor. *Mol Pharmacol* **2006**, *70*, 1534–1541, doi:10.1124/mol.106.023911.

219. Song, L.; Liu, Z.; Hu, H.-H.; Yang, Y.; Li, T.Y.; Lin, Z.-Z.; Ye, J.; Chen, J.; Huang, X.; Liu, D.-T.; et al. Proto-Oncogene Src Links Lipogenesis via Lipin-1 to Breast Cancer Malignancy. *Nat Commun* **2020**, *11*, 5842, doi:10.1038/s41467-020-19694-w.

220. Wu, V.T.; Kiriazov, B.; Koch, K.E.; Gu, V.W.; Beck, A.C.; Borcherding, N.; Li, T.; Addo, P.; Wehrspan, Z.J.; Zhang, W.; et al. A TFAP2C Gene Signature Is Predictive of Outcome in HER2-Positive Breast Cancer. *Mol Cancer Res* **2020**, *18*, 46–56, doi:10.1158/1541-7786.MCR-19-0359.

221. Mei, L.; Borg, J.-P. ERBB2 Oncogenicity: ERBIN Helps to Perform the Job. *Mol Cell Oncol* **2015**, *2*, e995033, doi:10.4161/23723556.2014.995033.

222. Gandullo-Sánchez, L.; Capone, E.; Ocaña, A.; Iacobelli, S.; Sala, G.; Pandiella, A. HER3 Targeting with an Antibody-Drug Conjugate Bypasses Resistance to Anti-HER2 Therapies. *EMBO Mol Med* **2020**, *12*, e11498, doi:10.15252/emmm.201911498.

223. Gu, L.; Lau, S.K.; Loera, S.; Somlo, G.; Kane, S.E. Protein Kinase A Activation Confers Resistance to Trastuzumab in Human Breast Cancer Cell Lines. *Clin Cancer Res* **2009**, *15*, 7196–7206, doi:10.1158/1078-0432.CCR-09-0585.

224. Liu, Y.; Ao, X.; Ding, W.; Ponnusamy, M.; Wu, W.; Hao, X.; Yu, W.; Wang, Y.; Li, P.; Wang, J. Critical Role of FOXO3a in Carcinogenesis. *Mol Cancer* **2018**, *17*, 104, doi:10.1186/s12943-018-0856-3.

225. Kim, Y.; Bae, Y.J.; Kim, J.-H.; Kim, H.; Shin, S.-J.; Jung, D.H.; Park, H. Wnt/β-Catenin Pathway Is a Key Signaling Pathway to Trastuzumab Resistance in Gastric Cancer Cells. *BMC Cancer* **2023**, *23*, 922, doi:10.1186/s12885-023-11447-4.

226. Hao, X.; Zheng, J.; Yu, X.; Li, Z.; Ren, G. β-Catenin Promotes Resistance to Trastuzumab in Breast Cancer Cells through Enhancing Interaction between HER2 and SRC. *Acta Biochim Pol* **2023**, *70*, 261–269, doi:10.18388/abp.2020_6357.

227. D'Auria, F.; Centurione, L.; Centurione, M.A.; Angelini, A.; Di Pietro, R. Regulation of Cancer Cell Responsiveness to Ionizing Radiation Treatment by Cyclic AMP Response Element Binding Nuclear Transcription Factor. *Front Oncol* **2017**, *7*, 76, doi:10.3389/fonc.2017.00076.

228. Stati, G.; Passaretta, F.; Gindraux, F.; Centurione, L.; Di Pietro, R. The Role of the CREB Protein Family Members and the Related Transcription Factors in Radioresistance Mechanisms. *Life (Basel)* **2021**, *11*, 1437, doi:10.3390/life11121437.

229. Zhang, J.; Pearson, A.J.; Sabherwal, N.; Telfer, B.A.; Ali, N.; Kan, K.; Xu, Q.; Zhang, W.; Chen, F.; Li, S.; et al. Inhibiting ERK5 Overcomes Breast Cancer Resistance to Anti-HER2 Therapy by Targeting the G1/S Cell Cycle Transition. *Cancer Res Commun* **2022**, *2*, 131–145, doi:10.1158/2767-9764.CRC-21-0089.

230. Majorini, M.T.; Colombo, M.P.; Lecis, D. Few, but Efficient: The Role of Mast Cells in Breast Cancer and Other Solid Tumors. *Cancer Res* **2022**, *82*, 1439–1447, doi:10.1158/0008-5472.CAN-21-3424.

231. Richard, S.; Selle, F.; Lotz, J.-P.; Khalil, A.; Gligorov, J.; Soares, D.G. Pertuzumab and Trastuzumab: The Rationale Way to Synergy. *An Acad Bras Cienc* **2016**, *88 Suppl 1*, 565–577, doi:10.1590/0001-3765201620150178.

232. de Azambuja, E.; Holmes, A.P.; Piccart-Gebhart, M.; Holmes, E.; Di Cosimo, S.; Swaby, R.F.; Untch, M.; Jackisch, C.; Lang, I.; Smith, I.; et al. Lapatinib with Trastuzumab for HER2-Positive Early Breast Cancer (NeoALTTO): Survival Outcomes of a Randomised, Open-Label, Multicentre, Phase 3 Trial and Their Association with Pathological Complete Response. *Lancet Oncol* **2014**, *15*, 1137–1146, doi:10.1016/S1470-2045(14)70320-1.

233. O'Brien, N.A.; Browne, B.C.; Chow, L.; Wang, Y.; Ginther, C.; Arboleda, J.; Duffy, M.J.; Crown, J.; O'Donovan, N.; Slamon, D.J. Activated Phosphoinositide 3-Kinase/AKT Signaling Confers Resistance to Trastuzumab but Not Lapatinib. *Mol Cancer Ther* **2010**, *9*, 1489–1502, doi:10.1158/1535-7163.MCT-09-1171.

234. Shi, W.; Jiang, T.; Nuciforo, P.; Hatzis, C.; Holmes, E.; Harbeck, N.; Sotiriou, C.; Peña, L.; Loi, S.; Rosa, D.D.; et al. Pathway Level Alterations Rather than Mutations in Single Genes Predict Response to HER2-Targeted Therapies in the Neo-ALTTO Trial. *Ann Oncol* **2017**, *28*, 128–135, doi:10.1093/annonc/mdw434.

235. Seshacharyulu, P.; Pandey, P.; Datta, K.; Batra, S.K. Phosphatase: PP2A Structural Importance, Regulation and Its Aberrant Expression in Cancer. *Cancer Lett* **2013**, *335*, 9–18, doi:10.1016/j.canlet.2013.02.036.

236. Bianconi, D.; Unseld, M.; Prager, G.W. Integrins in the Spotlight of Cancer. *Int J Mol Sci* **2016**, *17*, 2037, doi:10.3390/ijms17122037.

237. Di Modica, M.; Tagliabue, E.; Triulzi, T. Predicting the Efficacy of HER2-Targeted Therapies: A Look at the Host. *Dis Markers* **2017**, *2017*, 7849108, doi:10.1155/2017/7849108.

238. Majorini, M.T.; Cancila, V.; Rigoni, A.; Botti, L.; Dugo, M.; Triulzi, T.; De Cecco, L.; Fontanella, E.; Jachetti, E.; Tagliabue, E.; et al. Infiltrating Mast Cell-Mediated Stimulation of Estrogen Receptor Activity in Breast Cancer Cells Promotes the Luminal Phenotype. *Cancer Res* **2020**, *80*, 2311–2324, doi:10.1158/0008-5472.CAN-19-3596.

239. Stagg, J.; Loi, S.; Divisekera, U.; Ngiow, S.F.; Duret, H.; Yagita, H.; Teng, M.W.; Smyth, M.J. Anti-ErbB-2 MAb Therapy Requires Type I and II Interferons and Synergizes with Anti-PD-1 or Anti-CD137 MAb Therapy. *Proc Natl Acad Sci U S A* **2011**, *108*, 7142–7147, doi:10.1073/pnas.1016569108.

240. Moffett, H.F.; Cartwright, A.N.R.; Kim, H.-J.; Godec, J.; Pyrdol, J.; Äijö, T.; Martinez, G.J.; Rao, A.; Lu, J.; Golub, T.R.; et al. The MicroRNA MiR-31 Inhibits CD8+ T Cell Function in Chronic Viral Infection. *Nat Immunol* **2017**, *18*, 791–799, doi:10.1038/ni.3755.

241. Pesce, S.; Squillario, M.; Greppi, M.; Loiacono, F.; Moretta, L.; Moretta, A.; Sivori, S.; Castagnola, P.; Barla, A.; Candiani, S.; et al. New MiRNA Signature Heralds Human NK Cell Subsets at Different Maturation Steps: Involvement of MiR-146a-5p in the Regulation of KIR Expression. *Front Immunol* **2018**, *9*, 2360, doi:10.3389/fimmu.2018.02360.